2004

Effects of transcription on chromosome domain behavior and characterization of transcription-induced domain barriers to supercoil diffusion in the Salmonella typhimurium chromosome.

Shuang Deng
University of Alabama at Birmingham

EFFECTS OF TRANSCRIPTION ON CHROMOSOME DOMAIN BEHAVIOR AND CHARACTERIZATION OF TRANSCRIPTION-INDUCED DOMAIN BARRIERS TO SUPERCOIL DIFFUSION IN THE *SALMONELLA TYPHIMURIUM* CHROMOSOME

by

SHUANG DENG

A DISSERTATION

Submitted to the graduate faculty of The University of Alabama at Birmingham,
in partial fulfillment of the requirements for the degree of
Doctor of Philosophy

BIRMINGHAM, ALABAMA

2004

ABSTRACT OF DISSERTATION
GRADUATE SCHOOL, UNIVERSITY OF ALABAMA AT BIRMINGHAM

Degree Ph.D. Program Biochemistry and Molecular Genetics

Name of Candidate Shuang Deng

Committee Chair N. Patrick Higgins

Title Effects of Transcription on Chromosome Domain Behavior and Characterization of Transcription-induced Domain Barriers to Supercoil Diffusion in the *Salmonella typhimurium* Chromosome

Many studies demonstrate that bacterial chromosomes are composed of independent domains that limit supercoil diffusion. However, factors responsible for domain formation have remained unknown. Studies on small circular plasmids suggested that transcription could affect DNA topology.

Using the lambda Red recombination system, we constructed *Salmonella typhimurium* strains that carry transponson Tn*10*. Regulation of Tn*10*-derived tetracycline resistance involves a repressor, TetR, and a membrane-bound export pump, TetA. Because the *tetA* gene was previously demonstrated to cause a topological change in plamids, we tested the effect of the *tetA* gene upon chromosomal topology by using the γδ resolution assay, which is based on site-specific recombination. Strains deficient in TetR activity had 60-fold higher transcription levels (from the *tetA* promoter P_A) than the TetR-positive strains showed. High transcription of *tetA* caused a dramatic decrease in the γδ resolution efficiency for domains that include the *tetA* module. Replacing *tetA* with genes encoding cytosolic proteins LacZ and Kan also led to the appearance of similar barriers to supercoil diffusion. In strains containing a functional *tetR* located next to a regulated *lacZ* promoter (P_R*tetR*-P_A*lacZ*), induction of transcription from the *tetA* promoter with chlor-

tetracycline showed that transcription strength determines the impact on γδ resolution levels. Chromosomal genes such as the *atp* operon and the *nmpC* gene further proved this finding. The results clearly suggest that strong transcription causes a domain barrier. Transcription-driven barriers are dynamic, and a short half-life resolvase showed that barriers appeared and disappeared over a 10- to 20-min span. Further investigation of the *tetA*-driven domain barriers revealed, that when *tetA* was placed within the *res-res* interval, it always blocked the resolution. When *tetA* was put outside the *res-res* interval, it only affected the resolution within 1 kb of the end of the *tetA* gene. These results suggest that barriers to supercoil diffusion might be transient structures caused by highly transcribed regions and extending up to 1 kb beyond the sequence being transcribed.

DEDICATION

To my beloved husband, Ruimin Tan, for his love, understanding, and support.

To my precious daughter, Emily, who means the world to me.

ACKNOWLEDGMENTS

Many people have been important for the completion of my doctoral degree. First and foremost, I thank my mentor, Dr. Patrick Higgins, for giving me the opportunity to study and work in his laboratory and for offering criticism and suggestions for my work. He is one of the most honorable scientists I have known. I really appreciate his time and effort in training me to become a scientist. The time in his laboratory will set the tone for the rest of my research career.

I thank my committee members, Drs. Thomas Broker, Jamila Horabin, Susan Ruppert, and Tim Townes, for their time with me and for their suggestions for my experiments. I always enjoyed my committee meetings and learned a lot from them.

I am also greatly indebted to the members of Dr. Higgins's laboratory for their ideas, technical assistance, and contributions to my research. I enjoyed the friendship and delightful company of every member. I thank them for making the laboratory a fun place to work over the last six years. In particular, I want to thank Dr. Dipankar Manna for the stimulating conversations and for his constant willingness to offer a helping hand. Dr. Manna invested a lot of his time in my scientific career and did so unselfishly. I thank him for his guidance and friendship. I also thank Julie Harrison for her excellent secretarial support.

I cherish the invaluable friendship and help I received from the members of Townes and Detloff laboratories. I appreciate their kindness and generosity in lending reagents and allowing me to use their color printer.

I thank all my friends for their help, kindness, and scientific input through out graduate school. I also thank Jinxiang Ren and her family for making my doctoral journey into Higgins's lab possible and for always encouraging me through these six years.

I thank my parents and my brother, Jun Deng. None of this work would have been possible without their uncompromising guidance and support. Although they did not understand why science is often frustrating, they were always supportive and encouraging in any way possible. They especially helped me take good care of my daughter for years.

The most special acknowledgment goes to Ruimin Tan, my husband, because, without his unlimited love and unconditional support, I would have never been able to make it through the many challenges and difficulties over the years. He is a wonderful and loving husband and friend. I am also very grateful to my daughter, Emily. When I am down and blue, she is the best medicine. She has been and will always be the source of my encouragement and happiness.

TABLE OF CONTENTS

Page

LIST OF TABLES

LIST OF FIGURES

Figure *Page*

LIST OF ABBREVIATIONS

ATP	adenosine triphosphate
bp	base pairs
β-gal	β-galactosidase
X-gal	5-bromo-4-chloro-3-indolyl β-D-galactoside
CHIP	chromatin immunoprecipitation
CLT	chlortetracycline hydrochloride
DNA	deoxyribonucleic acid
DNase	deoxyribonuclease
dsDNA	double strand deoxyribonucleic acid
EM	electron microscopy
ΔG	Gibb's free energy
GFP	green fluorescent protein
IPTG	isopropyl β-D-thiogalactoside
kb	kilobase
LB	Luria Bertani
mRNA	messenger ribonucleic acid
oligo	oligonucleotide
ORF	open reading frame
PCR	polymerase chain reaction

PFGE	pulse field gel electrophoresis
PNAS	*Proceedings of the National Academy of Science of the USA*
REP	repetitive extragenic palindromic
Res	γδ resolvase
RNA	ribonucleic acid
RNase	ribonuclease
SMC	structural maintenance of the chromosome
ssDNA	single strand deoxyribonucleic acid
WT	wild type

INTRODUCTION

The genomes of eubacteria such as *Escherichia coli* and *Salmonella typhimurium* consist of 4-Mb, which is ≈ 1 mm long of B-form, DNA. However, the average length of a bacterium is 1-2 μm. So the chromosome must be compacted about 1,000-fold to fit inside the cell (1). At the same time, the bacterial chromosome must be free enough for transcription and replication to occur continuously. So bacteria face the problem of how to compact DNA in a usable form inside the cell. How the chromosome is condensed to fit in the cell and how it works during replication, transcription, translation, recombination, and other cell functions have remained obscure.

DNA supercoil

Studies of the effect of ethidium bromide intercalation on compaction of isolated "nucleoids" demonstrated that the DNA of the nucleoids is negatively supercoiled, with an estimated specific linking deficit of about $\sigma = -0.05$ (2, 3). This value is similar to that value observed in closed circular DNAs of viruses, phages, and plasmids isolated from both prokaryotes and eukaryotes. The value also differs by about 50% from estimates of the effective superhelical density measured in living bacteria. This is because, *in vivo*, half of the negative supercoil is constrained by being wrapped on the surface of histone-like proteins (4, 5). Only half of the negative supercoil in the bacteria DNA is unrestrained. The unrestrained DNA supercoils in isolated nucleoids appear as plectonemic

supercoils. Plectonemic supercoil is generated by interwinding of DNA duplexes (6).

Negative supercoil is critical for the numerous processes that need unwinding of DNA (7, 8). On the basis of genetic evidence, it has been postulated that the maintenance of a global level of chromosomal negative supercoil within a ±15% range is required for proper growth of *E. coli* cells (9). A modest reduction of negative supercoil is lethal to bacteria (10). So DNA supercoil is essential for viability and is tightly regulated in the cell.

Topoisomerases that control supercoil

DNA topoisomerases solve the topological problems associated with DNA replication, transcription, recombination, and segregation by introducing temporary single- or double-strand breaks in the DNA. In bacteria are four topoisomerases, and each has a role in maintaining DNA supercoil (11-13). Topoisomerases are divided into two classes based on the number of strand breaks per reaction. Type I topoisomerases, which include topoisomerase I and topoisomerase III (14), transiently break one strand and pass another strand through the transient break, changing the linking number by one at a time. Type II topoisomerases, which include gyrase (15) and topoisomerase IV (16), simultaneously break two strands and change the linking number by two at a time. Type I enzymes are not affected by quinolones *in vitro* (17). Type II enzymes are the cellular targets for the quinolone antibiotics (18, 19).

Topoisomerase I, encoded by the *topA* gene, was the first type I enzyme found in *E. coli* (20). Topoisomerase I removes the negative supercoil from a covalently closed DNA molecule without ATP and energy input, and it normally relaxes DNA and prevents

excess supercoil (21). Chromosomes accumulate excess negative supercoils in the absence of topoisomerase I activity. One consequence of the accumulation of the excess supercoils appears to be R-loop formation, which inhibits cell growth (22, 23). The growth defect of *topA* null mutants can be partially corrected by overproduction of RNase H, an enzyme that degrades the RNA moiety of an R-loop (23). It is now thought that a major function of DNA topoisomerase I is to prevent hypernegative supercoil and one of its major consequences, R-loop formation (22, 24).

Topoisomerase III, encoded by the *topB* gene, is also a type I topoisomerase. Topoisomerase III is dispensable for cell viability and has no known role in DNA supercoil; however, topoisomerase III is extremely efficient in the decatenation of multiply interlinked DNA dimers and DNA replication intermediates *in vitro*. On the basis of this observation, it has been proposed that topoisomerase III may play a role in chromosomal segregation during cell division (25).

DNA gyrase is an essential enzyme in bacteria and is encoded by *gyrA* and *gyrB* (26-28). Gyrase is a unique enzyme among topoisomerases in that it can introduce negative superhelical turns into DNA (15). Gyrase needs ATP for this reaction. *topA* deletions in *E. coli* cause an increase in negative supercoil and are tolerated only in the presence of compensatory mutations that reduce the level of supercoil. These mutations have been mapped to the *gyrA* and *gyrB* genes, respectively (29, 30). These mutant alleles compensate for the loss of topoisomerase I by encoding mutant DNA gyrase subunits with reduced supercoil activity (31, 32).

The genes encoding the topoisomerase IV subunits are *parC,* which is homologous to *gyrA* of gyrase, and *parE*, which is homologous to *gyrB* of gyrase (16, 33). To-

poisomerase IV requires ATP to remove either negative or positive supercoils from DNA (13). Topoisomerase IV favors intermolecular strand passage reactions such as decatenation. Positive supercoils generated by replication forks approaching each other in the terminus could be removed by topoisomerase IV acting at *dif* (34). Topoisomerase IV is essential for segregation of chromosomes (35, 36).

Gyrase primarily supports nascent chain elongation during replication of the chromosome, whereas topoisomerase IV separates the topologically linked daughter chromosome during the terminal stage of DNA replication (37). Although there is nearly 40% amino acid sequence identity between gyrase and topoisomerase IV (16), no overlap in specific function has been found.

The in vitro *evidence for chromosomal supercoil domains*

The entire prokaryotic chromosome, or nucleoid, can be isolated from growing bacterial cells as a highly compacted DNA-RNA-protein complex. The original procedure for nucleoid isolation, developed in the early 1970s by Pettijohn, Worcel, and their colleagues, relies on lysis of cells in the presence of sufficient counterions to stabilize DNA charge-charge repulsion (38, 39). Without counterions, the condensed state of the nucleoid DNA is lost as the DNA unfolds during or soon after lysis. In their DNase I nicking experiments, Worcel and Burgi (39) observed that many single-strand DNA breaks per nucleoid were required to relax the entire chromosome. This requirement implied that DNA is organized into independent "domains," thus preventing relaxation from spreading from one chromosomal domain to another. Later, in the mid-1970s, electron micrographs of Kavenoff *et al.* (40, 41) clearly showed that nucleoid preparations appear

as rosettes of many individually plectonemically interwound loops emanating from a central region (Fig. 1*A*). A single loop could be relaxed while the rest of the loops remained supercoiled (42). These supercoiled loops were hypothesized to be topological domains. Recently, members of cozzarelli's laboratory used a gentler method to look at bacterial chromosomes by using electron microscopy (43). They visualized chromosomes as rosettes of tightly supercoiled loops of DNA. Individual loops in a single chromosome could be relaxed by γ-irradiation without affecting supercoil of other loops (Fig. 1*B*) (43).

All of these studies of isolated chromosomes gave *in vitro* evidence supporting the supercoiled domain structure of chromosomes.

The in vivo *evidence of chromosomal supercoil domains*

To examine whether chromosomal domains also exist *in vivo*, methods are required to investigate the domain structure of chromosomes inside living cells. Trimethylpsoralen was exploited as a probe of the distribution of domains *in vivo*. Trimethypsoralen photobinds to duplex DNA at a rate directly proportional to the torsional tension in the double helix, so tension in the winding of the helix can be detected *in vivo* from measurements of the amount of the photobinding in living cells (5). Tension in the DNA double helix is relaxed *in vivo* when single-strand DNA breaks are introduced by γ-irradiation, and ≈160 nicks per genome are required to relax the whole chromosome (44). So bacterial DNA forms domains of supercoil *in vivo*. These domains might be topologically equivalent to loops such as appear in the electron micrographs of isolated nucleoids (43).

Fig. 1. Image of *E. coli* chromosome. (*A*) Electron micrograph of isolated *E. coli* nucleoid after cells were treated with lysozyme and lysed with mild detergent. The nucleoid preparation appeared as rosettes of many supercoiled loops emanating from a central region (40). (*B*) Recent image of *E. coli* chromosome captured by electron microscopy (EM). Isolated chromosome was deposited directly onto carbon-coated EM grids. Unlike A, there was no ethanol washing, crosslinking, or DNA-binding agents. Chromosomes showed rosettes of highly supercoiled loops of DNA (43). (*C*) Model of the bacterial chromosome showing the segregation of the nucleoid DNA into chromosomal domains. Two domains with cuts are shown; such cuts relax any supercoilings in a single domain without affecting supercoilings of other domains.

A

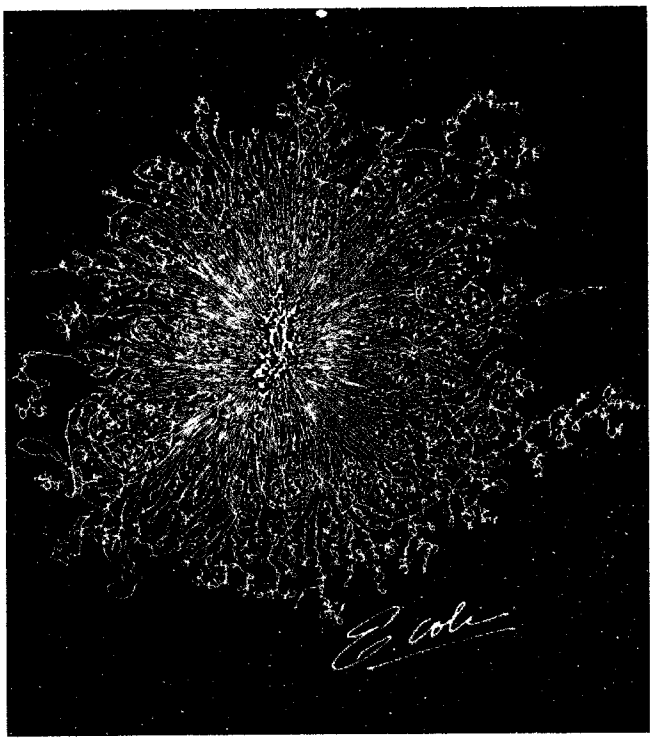

B

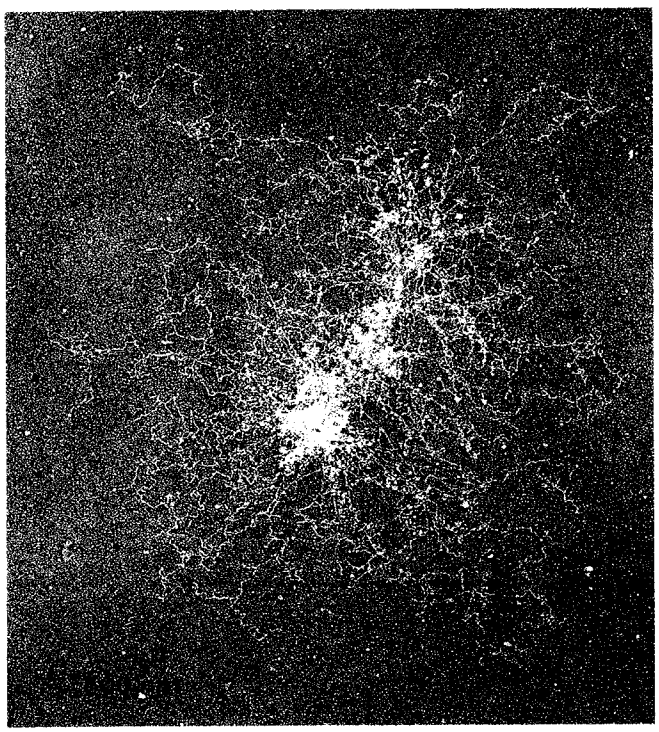

C

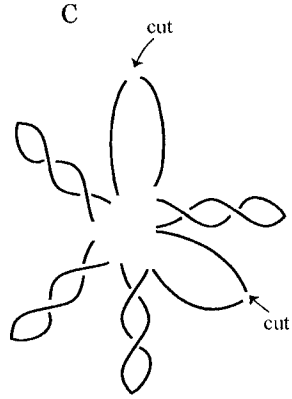

Therefore, both *in vitro* and *in vivo* studies revealed the existence of topologically independent domains. A domain of supercoil is defined as a segment of chromosomal DNA bounded by topological constrains on the rotation of the double helix (45). The operational definition of a domain is the region relaxed by an interruption of DNA (43).

Number and size of DNA domains

In the early experiments, the number of DNase I-induced nicks required to relax the *in vitro* nucleoid led to estimates of 12-80 domains of supercoil per genome (39). Electron micrographs showed 50-100 loops per nucleoid (41). γ-Ray-induced nicks required for complete relaxation of the whole chromosome enabled the number of *in vivo* domains of supercoil to be estimated at 43 ± 10 domains per genome (44). On the basis of these experiments, the size of supercoil domains was estimated to be about 100 kb under an assumption that all domains are equal in size; however, no evidence exists to this assumption. In 1996, Higgins *et al.* (46) developed a less invasive method to study supercoil domains *in vivo*. They used site-specific γδ resolution to sense the domain barriers that inhibit resolution efficiency. They concluded that bacterial DNA is stochastically organized into supercoil domains of variable size, and with a median domain size of 20 kb (6, 46); therefore, there are about 200 domains per genome. However, the WT resolvase used in the assay is a long-lived protein that persists in cells for the entire cell cycle, which led to an underestimation of domains lasting for shorter periods. Recently, Stein *et al.* (manuscript in preparation) modified the resolvase and generated a new resolvase with a half-life of 5 min. The short half-life resolvase suggests that a median domain size is 9 kb and that there are ≈400 supercoil domains per chromosome. Chromosomes are more

dynamic than previously thought. At the same time, members of Cozzarelli's laboratory performed more systemic investigations of the organization of chromosome structure in *E. coli*, both *in vivo* and *in vitro* (43). They found that the whole chromosome *in vivo* is generally accessible to frequent restriction enzymes, which indicated that there are no extensive stably bound structural components. They studied the sizes of supercoiled loops from isolated chromosomes by using EM. The range of loop sizes was 2-66 kb, and the average domain length was 10 kb. By using 300 supercoil-sensitive genes as a probe to sense how far the relaxation from double-strand breaks spreads *in vivo*, these authors demonstrated that domain barriers are randomly distributed and that the domain length is ≈10 kb (43). Thus, both *in vivo* and *in vitro* data are consistent with the idea that domain organization is more dynamic and domain sizes are smaller than previously estimated. The domain model is depicted in Fig. 2.

Nature of domain boundaries

What defines domain boundaries has remained unclear. Initial experiments suggested RNA as a stabilizing molecule: RNase treatment of nucleoids (39) or rifampicin treatment of cells before nucleoid isolation (47) causes unfolding of high-salt isolated nucleoids. However, support for this model has diminished. An intensive study of RNA molecules attached to the isolated nucleoid revealed only nascent RNAs. Treating cells with rifampicin *in vivo* did not diminish domains (44); thus, nascent RNA does not stabilize chromosome domains found in vivo. These results forced a rethinking of the older models of chromosome organization. Now, three models about domain boundaries are commonly accepted .

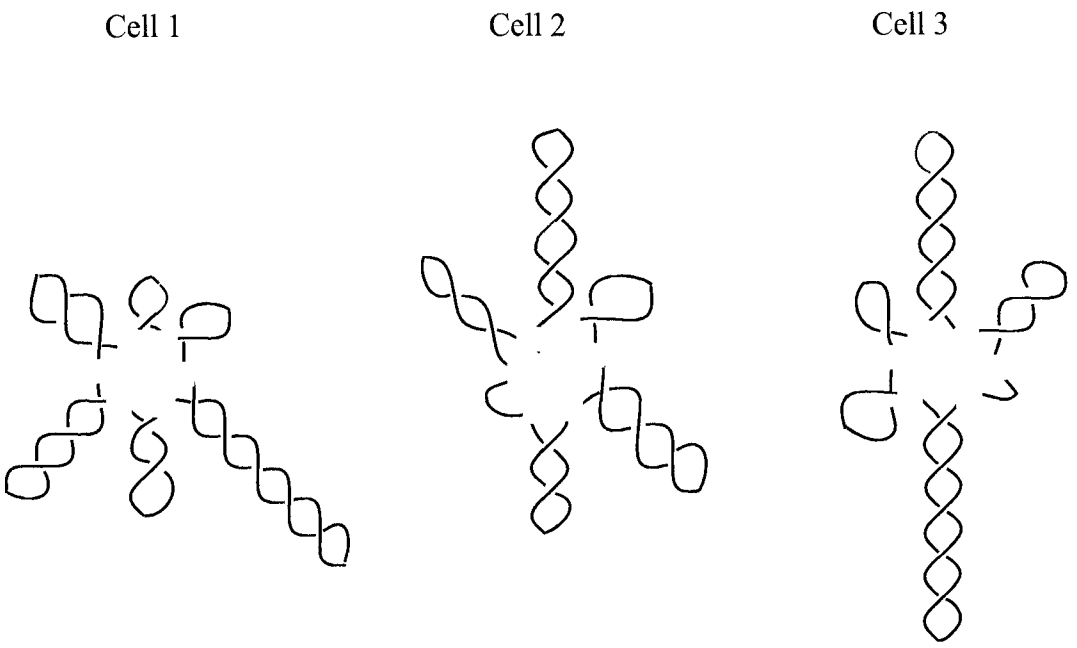

Fig. 2. Model of chromosome domains with variable length and variable placement. Domain barriers are indicated with yellow boxes. A red marker demonstrates the variability in barrier position. For simplicity, each chromosome is divided into only six domains. Three different chromosomes are shown and may depict chromosomes in different cells or in the same cell at different times.

The first model involves DNA gyrase high-affinity binding sites. An early study (48) discovered that in cells treated with oxolinic acid, chromosomes were broken into ≈50 fragments, which is similar to the number observed *in vitro* by EM (39). Snyder and Drlica (48) concluded that gyrase bound to the high-affinity sites on the chromosome and divided it into 50 domains. Yang and Ames (49) demonstrated specific gyrase binding to a single repetitive extragenic palindromic (REP) sequence *in vitro*. The REP sequence is repeated hundreds of times on the *E. coli* chromosome (50). So it has been suggested that REP sequences and their associated proteins could bind DNA gyrase and serve to define the domain boundaries. However, PFGE demonstrated that DNA gyrase cleavage of the chromosome occurs at specific but infrequent sites, which are called toposites (51). REP sequences occur much more frequently than toposites. Moreover, REP cloned onto PBR322 could not produce cleavage. So the interaction between the REP sequence and gyrase has yet to be demonstrated. Recently, topoisomerase IV was found to have high affinity for the *dif* site and to induce DNA cleavage at this site (34). So topoisomerase high-affinity binding sites could serve as domain boundaries in DNA organization.

Second, constraints of chromosomal domains could be caused by anchoring of DNA to the membrane through cotranscriptional membrane association. As transcription proceeds along the helical template, RNA polymerase and its nascent RNA might need to turn around the DNA (52, 53). Recently, relative rotation between *E. coli* RNA polymerase and DNA during transcription was directly visualized by real-time optical microscopy (54). Lynch and Wang (55) showed that membrane-associated nascent proteins with their attached cotranscribed mRNA could act to anchor the associated active RNA polymerase and therefore restrain the rotation of the RNA polymerase around the DNA

template; instead, the DNA might turn around its axis as the transcription complex tracks along. The consequence of DNA rotation is that positive supercoil would be generated in the template ahead of the transcribing polymerase and negative supercoil would be generated behind it. In cells deficient for topoisomerase I, the rotation of the DNA double helix forces plasmids to become hypernegatively supercoiled only when genes coding for the anchoring proteins are actively transcribed. This topology change has been repeatedly observed in plasmids carrying genes specifying membrane proteins (55, 56). Because an anchored RNA polymerase cannot rotate around its DNA template during transcription, the energetics of transcription drives the axial rotation of DNA. This anchored site of transcription therefore has the potential of defining the boundary of a chromosomal domain.

The third hypothetical type of boundaries involves DNA-binding proteins that attach the chromosome to intracellular partitioning machinery. In *Bacillus subtilis*, SpoOJ protein was discovered to bind six to eight specific chromosomal sites *in vivo*. SpOJ is aggregated in living cells and, through its DNA attachments, this complex causes the origin-proximal one-fourth of the chromosome to move to a specific cellular location during cell division (57). In *E. coli*, the SeqA protein binds to nascent hemimethylated DNA and occupies a unique position near the cell's midpoint throughout the cell cycle (57). F plasmid encodes the partition protein SopB. Visualization of SopB fused to the GFP in *E. coli* indicated that SopB is localized to the "quarter-cell" position near the cell poles (58). F plasmid has a centromere-like partitioning site called *sopC*. SopB specifically binds to *sopC* and ensures efficient partitioning of the plasmids during cell division (59). P1 plasmid has a similar mechanism. In the case of P1, ParB binds to the specific site *parS* (60)

and promotes plasmid segregation into daughter cells. DNA-binding proteins anchor the chromosome to intracellular partitioning machinery, and the DNA-binding site has the potential to be a domain boundary

Effect of supercoil and supercoil domains in vivo

Supercoil affects the structure of DNA and hence the interaction between DNA and other molecules. Processes that involve denaturation of the complementary strands are favored with supercoiled DNA. Supercoiled DNA, being under torsional strain, is in a higher energy form; thus, any reaction on the strained DNA substrate that reduces ΔG will be thermodynamically favored. Interactions occurring on DNA that require an input of energy, such as the initiation of DNA replication or transcription, will be favored on supercoiled DNA. Supercoil of DNA influences almost all of the processes involving DNA-DNA and DNA-protein interactions, such as transcription, replication, recombination, and repressor-operator interactions.

Among these influences, the effects of DNA supercoil on transcription is best characterized. The effect of DNA supercoil on gene expression in *E. coli* has been the subject of many studies (8, 61). DNA supercoil affects transcription at several steps: (i) RNA polymerase and regulatory proteins may prefer binding to supercoiled DNA (62-64). (ii) DNA is underwound in open and elongating complexes (65-69), and underwinding is favored by negative supercoil (70, 71). (iii) The step of promoter clearance may also be subject to the influence of DNA supercoil (72, 73). (iv) A pause in transcription elongation was shown to be enhanced by DNA supercoil (74). (v) Supercoil affects transcription

termination (75). So DNA supercoil plays an active rather than a passive role in gene transcription.

The expression of numerous prokaryotic operons is sensitive to DNA supercoil. Negative-supercoil-dependent transcriptional initiation is believed to be at least part of the explanation for altered expression of many genes in mutants defective in DNA topoisomerase I or in cells treated with specific inhibitors of DNA gyrase (73, 76-79). Transcription of the *gyr* and *topA* gene appears to be regulated specifically by the level of DNA supercoils (80, 81). Additionally, DNA supercoil is influenced *in vivo* directly and indirectly by environmental signals such as growth-medium osmolarity (82), oxygen availability (83), pH (84), and nutrient status (85). These environmentally induced changes in DNA supercoil also appear to play a role in regulating gene expression (82, 83).

The *leu-500* mutation in *S. typhimurium* is a good example of negative-supercoil-dependent transcriptional regulation. The *leu-500* mutation is a single-base-pair (AT to GC) transition in the –10 region of the leucine promoter; this transition results in leucine auxotrophy (86). This phenotype can be suppressed by a mutation in the *topA* gene (76, 78, 79, 87). The GC base pair in the *leu-500* is thought to increase the energy barrier to the open complex formation at the mutant promoter. The *topA* mutant causes more negative supercoil on the DNA template, which is important for overcoming the higher energy barrier. Thus, the *topA* mutation restores the ability to synthesize leucine (78).

The existence of separate chromosome domains potentially allows the superhelical density to vary on different parts of same chromosome. When DNA undergoes repair, replication, and recombination in one domain, the topology is changed in that domain.

Because of domain boundaries, the topology of the other domains of the same chromosome may not be affected by this topological change. Thus, gene expression in the neighboring domains could remain unchanged (2).

Effect of transcription on supercoil

Transcription is influenced by supercoil but also affects the supercoil. Inhibition of DNA gyrase in *E. coli* leads to the formation of highly positively supercoiled pBR322 (88). Vector pBR322 isolated from *topA* null mutants exhibits more negative supercoil than the same plasmid isolated from *topA*$^+$ strains shows(89); this increase of negative supercoil is called hypernegative supercoil. Hypernegatively supercoiled plasmid DNA could not be resolved by electrophoresis in agarose gels containing chloroquine (89-91). This *topA*-dependent hypernegative supercoil is plasmid specific because a derivative of pBR322, pUC19, did not show supercoil differences when isolated from *topA* mutant and *topA* WT strains. Further analysis of the pair of plasmids pBR322 and pUC19 led to the conclusion that transcription of *tet*, the gene encoding the tetracycline resistance marker in pBR322, is necessary for the hypernegative supercoil of the plasmid in the absence of DNA topoisomerase I (91). The major mechanism for this hypernegative supercoil is thought to be the consequence of the twin-supercoiled domains described by Liu and Wang (53). According to this model, hindered rotation of an elongating transcription complex leads to the formation of positive supercoil ahead of a translocating RNA polymerase and the formation of negative supercoils behind it (Fig. 3). The anticipated DNA helix rotation during the tracking progress of RNA polymerase has recently been visualized by using real-time optical microscopy (54). DNA topoisomerase I removes the nega-

Fig. 3. A model of formation of twin-supercoiling domain in pBR322. Shown is a single RNA polymerase (RNAP) transcribing the *tetA* gene from the plasmid pBR322. Translational insertion of the nascent TetA protein into the membrane anchors the transcription complex and prevents RNAP from rotating around the DNA template. Instead, DNA is rotated around its helical axis, which leads to the positive supercoiling of DNA ahead of RNAP and the negative supercoiling of DNA behind it. For persistent domains to arise, a constraint to the diffusion of supercoiling must exist elsewhere on the plasmid; and this constraint might be another oppositely oriented transcription unit or DNA-binding proteins, which may anchor DNA to some subcellular structure (shown as yellow circle).

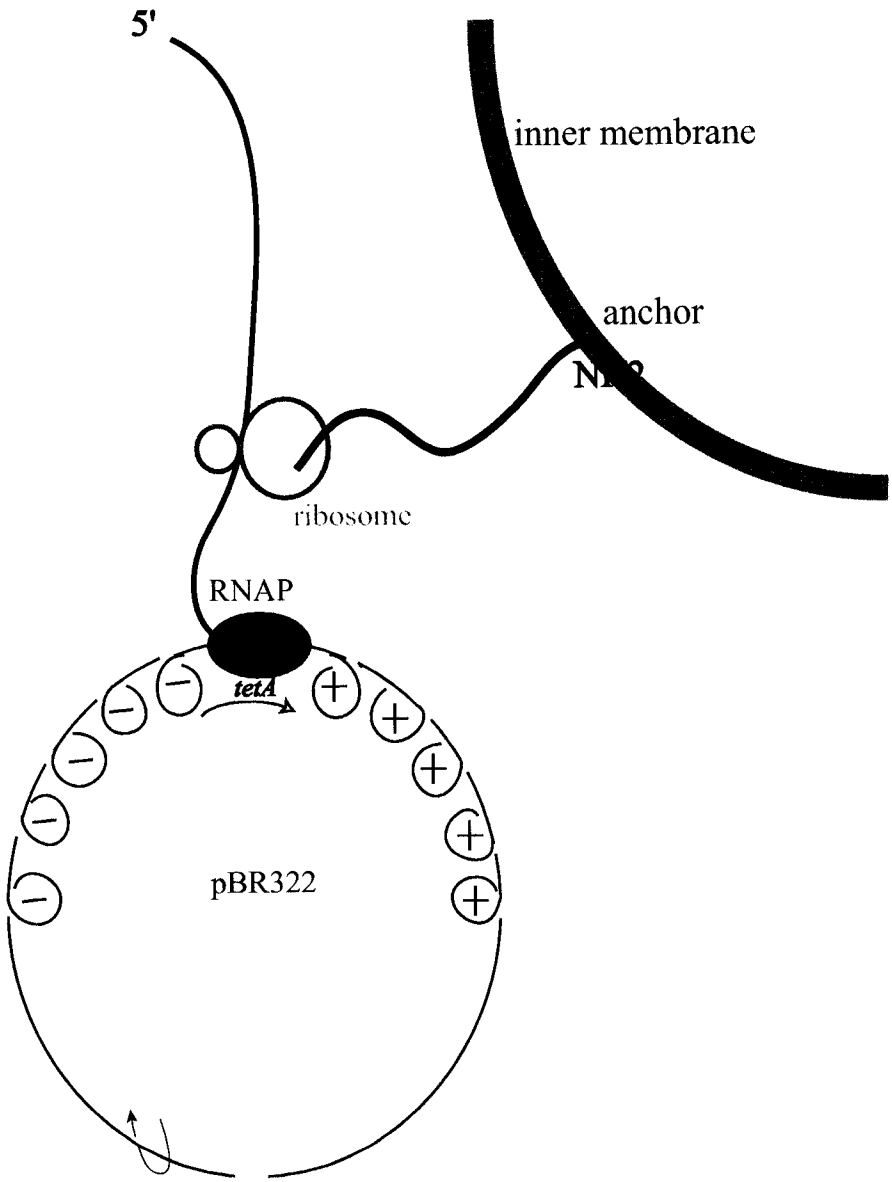

tive supercoils behind the RNA polymerase so that, in the absence of DNA topoisomerase I, plasmids showed hypernegative supercoil. DNA gyrase specifically removes the positive supercoils ahead of the polymerase; therefore in the absence of DNA gyrase, plasmids exhibit highly positive supercoil. Two mechanisms could hinder the rotation of a transcription complex around its DNA template. One mechanism involves cotranscribed translated integral membrane proteins that restrict DNA rotation by tethering the transcription machinery to the membrane, such as transcription of the pBR322 *tetA* gene (55). The other mechanism could be DNA-binding proteins like bacteriophage λ O replication initiator or the *E. coli* lactose or galactose repressors (92). DNA-binding proteins could function as a barrier to the rotational diffusion of nascent supercoils that arise during transcription and stimulate transcription-coupled DNA supercoil.

Inducing transcription from a strong promoter increases negative supercoil in derivatives of pBR322, even when DNA topoisomerase I activities are present (93). Transcription from a strong promoter leads to greater negative supercoil than transcription from a weak one. For a strong promoter, translation is not necessary for generating hypersupercoil of plasmid DNA (93, 94).

The notion that transcription can generate supercoil changes in the DNA template largely stems from work with small circular plasmids. Little is known about the impact of transcription on the topology of the large bacterial chromosome because of the lack of tools to investigate long-range chromosome behavior *in vivo*. Assays used to detect plasmid topology changes are hard to conduct on the bacterial chromosome due to its large size. However, indirect evidence indicates that transcription affects chromosome supercoil. As discussed earlier, the inactive *leu-500* promoter of *S. typhimurium* regains activ-

ity if negative supercoil rises, as is the case in a *topA* mutant (78, 87). Because the activity of the *leu-500* promoter is DNA supercoil-sensitive, whatever factor is responsible for the *leu-500* activation is most likely to generate negative supercol. In a review paper (95), Lilley and Higgins suggested the possible involvement of an adjacent transcription activity in the activation of the DNA supercoil-sensitive *leu-500* promoter. *leu-500* has been used as a supercoil-sensitive promoter to sense superhelicity changes (96). Results showed that induced transcription in the region upstream of the *leu-500* promoter activated the promoter. This finding suggested that transcription could cause local supercoil changes in chromosomal DNA. So far, the evidence for transcription-driven DNA supercoil has been based on the presence of an active promoter. Because of the transient nature of transcription-driven DNA supercoil, a better methodology is needed to directly monitor its presence.

Barriers to supercoil diffusion

DNA is dynamic, and distant sites on the chromosome are able to communicate with each other. Many genetic events require communication between proteins bound to distant sites on DNA. Examples include DNA replication, gene expression and its control, site-specific recombination, and genome rearrangements (97-99). The communication requires a negatively supercoiled substrate. Of these many genetic processes, one of the best characterized is the site-specific recombination system carried out by the γδ transposon (100). Transposition of the γδ transposon involves two sequential steps. The first step is a replicative transposition reaction that creates a cointegrate intermediate of the donor and target sequences, which are joined by two copies of the γδ element ordered as direct

repeats. The second step is a site-specific recombination at the *res* sites of the directly repeated transposons. This second reaction is carried out by γδ resolvase (Res), the product of the transposon *tnpR* gene. Res separates the cointegrate at sites designated *res*; as a result, the original arrangement of donor and recipient is restored, except that the recipient now carries a γδ element, as well (101, 102). The second step, γδ site-specific recombination, has been characterized extensively on plasmids *in vitro* and *in vivo*. Two *res* sites with a direct repeat order were engineered into one plasmid, just like they are positioned in a natural cointegrate. In the presence of resolvase, the plasmid was resolved into two circles interlinked once to form a catenane (103, 104). The reaction process can be divided into three sequential steps (105). The first step is binding of Res dimers to each of the *res* sites (106-108). A *res* site consists of three resolvase-binding sites, called I, II, III, each of which, in turn, is made of an inverted repeat of a 12-bp "half-sites." Although all three sites are required, exchange occurs only between the halves of site I (109). This step only takes about a millisecond *in vitro*. The second step is formation of a specific synapse complex in which the DNA-protein complexes at the two sites interact with each other. The synapse structure captures precisely three supercoil nodes between the two *res* sites. This step also occurs relatively quickly. More than 60% of plasmids form a synapse within 1 sec. The third step involves DNA breakage, strand exchange, and DNA ligation. This step is slow and takes about a min. to complete.

The simplest way of forming a synapse between two sites on a DNA chain is for the sites to meet each other by unconstrained random collisions stemming from the dynamic flexibility of the DNA chain (110). However, Res produces only singly interlinked catenanes, and this particular topology demands that just three negative supercoils be lo-

cated between the synapse *res* sites (104, 111). Rapid formation of a specific topological structure requires that DNA molecules proceed directly to the requisite complex by an ordered motion of the DNA rather than by random collisions. Two ordered motions of the DNA molecule bring distant sites on a single molecule close together and facilitate synapses of directly repeated *res* sites. These motions are called slithering (105, 112) and branch migration (Fig. 4) (113, 114). Slithering is a DNA movement similar to the movement of a conveyor belt, in which all points along the chain move relative to all other points. Branch migration involves axial rotation of supercoil branches and extrusion of a new branch coupled with absorption of old branches. These two motions are able to bring about supercoil diffusion. Supercoil diffusion may cause two distant *res* sites to become juxtaposed in an interwound synapse. Both *in vitro* and *in vivo* experiments demonstrated that γδ recombination requires only supercoiled DNA and that its substrate is a plectonemically tangled pair of *res* sites with three superhelical nodes (115-117). These rigorous topological requirements for site-specific recombination provide a way to study chromosome behavior *in vivo*. Experiments on plasmids implied that γδ recombination could be used as a reporter system to sense long-range interactions between distant sites on DNA (118, 119).

On the basis of γδ recombination, our laboratory constructed a γδ resolution assay to investigate the dynamic chromosomal structure *in vivo* (46). In this system, a pulse of resolvase (Res protein) is given to bacterial cultures by the plasmid pJBRES*c*I. The pJBRES*c*I is a pACYC184-derived vector carrying the tnpR (Res protein) gene of transponson γδ, which is cloned under control of the pL promoter of phage lambda with a nearby copy of λ *cIts* repressor gene (119). Two *res* site-containing genetic elements,

Fig. 4. Two kinds of ordered motions of DNA molecules. (*A*) Slithering movement. During slithering, DNA moves like a conveyor belt, in which all points along the chain move relative to all other points. (*B*) Supercoil branch migration. Branch migration involves axial rotation of supercoil branches and extrusion of a new branch coupled with absorption of old branches, which causes sites to become plectonemically interwound. The recombination products included a deleted interval (shown as the pink circle), which is initially catenated with the recombinant chromosome (shown as the black circle). Decatenation of the two circles is achieved by the activity of topoisomerase IV.

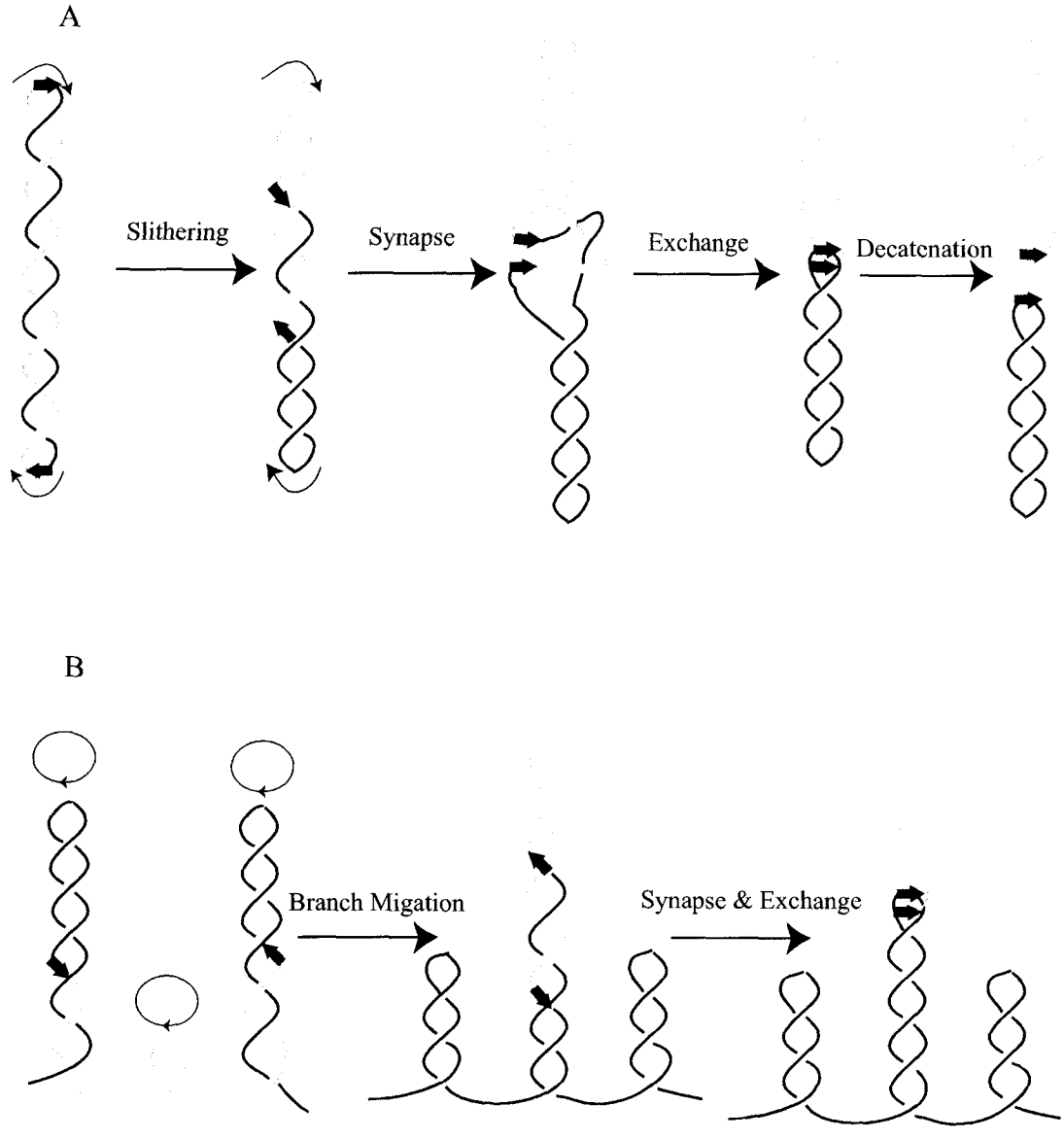

Mu*d*Jr2 and Tn*10d*Gn, were created specifically for use in the γδ resolution assay (46). Mu*d*Jr2 is a Mini-Mu defective for transposition and is based on Mu*d*I (120). Structurally, it is composed of the left and right ends of phage Mu, the promoterless *lacZYA* genes, the kanamycin genes from Tn*903*, and the Mu c repressor. The Mu*d* has been engineered such that the γδ *res* site is positioned between the Mu left end and the promoterless Mu repressor gene and points toward the Mu left end. Tn*10d*Gn is a transposition-defective element based on Tn*10* (121). The γδ *res* site in the Tn*10d*Gn element is positioned downstream of and in the same transcriptional orientation as the gentamicin resistance gene. A pair of *res*-containing elements such as Mu*d*Jr2 and a Tn*10d*Gn were positioned in the bacterial chromosome to provide directly repeated *res* sites (Fig. 5). Inducing a pulse of resolvase synthesis by heat shock resulted in γδ site-specific recombination, which was assayed by deletion frequency of the interval between the pair of *res* sites. Deletion frequency was scored by one of two methods: loss of blue color on 5-bromo-4-chloro-3-indolyl β-D-galactosidase (X-gal) plates or loss of drug resistance. For example, when a Tn*10d*Gn insertion is upstream of a Mu*d*Jr2 insertion and orientation of both *res* sites is clockwise, the deletion product retains *gen* but loses *lacZYA* and *kan*. Cells carrying the deletions form white colonies on plates containing X-gal, whereas cells without the deletions form blue colonies. The deletion frequency was calculated as the percentage of white colonies among white and blue colonies. When a Tn*10d*Gn insertion is downstream of a Mu*d*Jr2 insertion and the orientation of both res sites is clockwise, the deletion product retains *lacZYA* and *kan* but loses *gen*. The deletion frequency was calculated as the percentage of gentamicin sensitive colonies among all colonies, and the rate of deletion was plotted as a function of distance.

Fig. 5. Schematic representation of the γδ resolution assay. (*A*) Two directly repeated *res* elements, Mu*d*Jr2 and Tn*10*dGn, are constructed in the same chromosome. This strain is gentamicin resistant, kanamycin resistant and shows blue color on the X-gal plate. (*B*) In the presence of γδ resolvase, γδ resolution leads to deletion of the DNA sequence between the two *res* sites. The deleted sequence is lost during growth because of the lack of replication origin. Only gentamicin-resistant gene and one *res* site retain in the chromosome. (*C*) Recombinant colonies appear as white, whereas nonrecombinants appear as blue on X-gal-containing indicator plate. The deletion frequency is calculated as the percentage of white colonies among white and blue colonies.

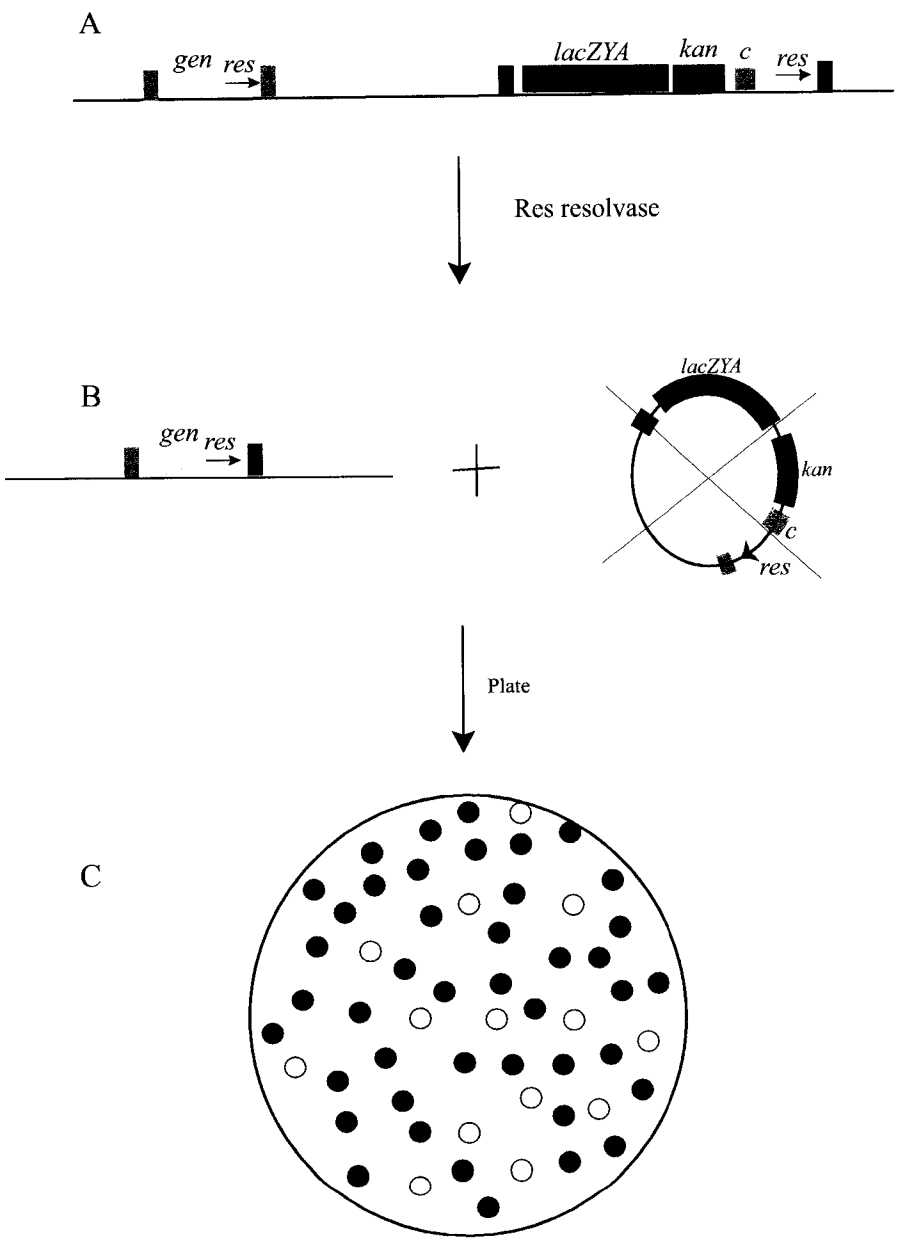

% deletion = W / W+B

In the γδ resolution assay, recombination and deletion formation in the presence of resolvase are determined by the feasibility and rate of synapse formation between the two *res* sites. Domain boundaries that deter supercoil diffusion will presumably inhibit resolution by blocking synapse formation. Therefore, the γδ resolution assay can be used to measure the rate of supercoil diffusion and to detect constraints on DNA structures (Fig. 6).

Studies using this assay in the 43- to 45-centisome (cs) region of the *S. typhimurium* chromosome showed that supercoil diffusion could spread over distances as large as 100 kb. Resolution efficiency decreased as the *res-res* distance increased, indicating the presence of random barriers to supercoil diffusion (46). The nature of these barriers is not clear. The efficiency of γδ recombination was decreased by mutations in type II topoisomerase, gyrase, and topoisomerase IV, suggesting that knots (intramolecular nodes) and catenanes (intermolecular links) were candidates for these barriers (113). In this region, no evidence of fixed barriers has been found.

Supercoil diffusion may also play an important role in Mu transposition. During Mu transposition, two proteins are required: MuA and MuB (122). Mu A binds specifically to the Mu ends (123). Mu B binds to DNA without sequence specificity (124). Mu A bound to Mu ends preferentially captures target DNA molecules that are associated with Mu B protein and transfers Mu strands into the target DNA. However, in the presence of Mu A protein and ATP, Mu B protein preferentially dissociates from DNA molecules that carry Mu A proteins bound to Mu ends. So one Mu sequence insertion can inhibit a second Mu from inserting into neighboring DNA sequences. This phenomenon is called transposition immunity (125). Interaction of Mu A and Mu B proteins bound at a

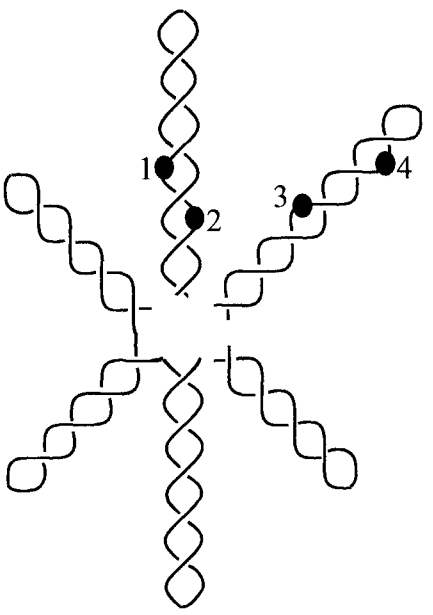

Fig. 6. Effect of domain structure on resolution frequency. In the model of the supercoiled bacterial chromosome, yellow squares represent barriers that divide the chromosome into different domains. Numbered circles represent *res* sites. The sites that are in the same supercoil domain, such as sites 1 and 2 (or sites 3 and 4), are yielding a high-resolution frequency. The sites residing in two different supercoil domains, such as sites 1 and 3, are not expected to interact. The resolution efficiency for such a pair is expected to decrease dramatically.

distance along the same immune DNA underlies transposition immunity in the Mu DNA strand-transfer reaction. How does the Mu A protein interact with the Mu B protein, bound some distance along the DNA to facilitate Mu B dissociation? Adzuma and Mizuuchi (126) proposed a DNA-looping model in which two proteins simply collide with each other by looping out of the DNA segment between them. By using a PCR-based technique called Muprinting, Manna and Higgins (127) measured the Mu transposition pattern over a 35-kb segment of the *S. typhimurium* chromosome around the *cob* region. They found that a Mini-Mu element in the *cobT* gene conferred transposition immunity in both directions in the range of 20 kb from its insertion point. Immunity strength decreased with increasing distance between the transposition target and Mu sequence. *gyrB* mutants produced a smaller transposition immunity zone. These results are very similar to the findings obtained from the γδ resolution assay; resolution efficiency decreased as *res-res* distance increased. Also, type II topoisomerase mutants had a decreased efficiency of γδ recombination. So these similarities suggested that both systems use the same mechanism of supercoil diffusion to juxtapose protein-bound sites along DNA.

Observations from γδ recombination and Mu transposition immunity are indicative of the presence of stochastic barriers to supercoil diffusion. These barriers might be knots and catenanes. The γδ resolution assay is best suited to *in vivo* studies of such barriers to supercoil diffusio.

Construction of res-res *interval by using a novel recombination method*

The key step in constructing the γδ resolution assay system is to engineer γδ res element pairs so that each carries a *res* site such as Mu*d*Jr2 and Tn*10d*Gn into various lo-

cations of the bacterial chromosome. Previously, *res* elements were inserted into the chromosome by random insertional mutagenesis (46). The insertion locus was estimated by genetic linkage analysis and PCR assays. This process is time consuming and limited by the target preference of transposons used.

A recently developed technology called Red recombineering (128) significantly reduces the strain construction time. "Recombineering" is genetic engineering that is homology-dependent and recombination-mediated. (129, 130). Red recombineering is a phage λ-based recombination system. The phage system has a unique advantage in that it can catalyze efficient recombination with very short regions of sequence homology (<50 bp) (131-135). The λ Red-mediated recombination requires the phage Gam, Exo, and Beta proteins but does not need *E. coli* RecA function. The three proteins provide homologous recombination activity with linear dsDNA or ssDNA. λ Gam inhibits the host RecBCD activity, thereby protecting the electroporated linear dsDNA from degradation (136, 137); λ Exo is a dsDNA-dependent exonuclease that digests in the 5' to 3' direction, leaving 3' overhangs intact that act as substrates for recombination (32). λ Beta is a ssDNA-binding protein. Beta binds 3' overhangs to protect the DNA from ssDNA nuclease attack and anneal these overhangs to complementary sequences (138-140). A model for Red-mediated recombination is shown in Fig. 7.

With Red recombineering, antibiotic cassettes with appropriate flanking homology can be conveniently used to target specific genes or regions of the chromosome for replacement if the sequence of the target DNA is known. Such replacements are directly selected as drug resistant. Drug-resistant recombinants were confirmed by PCR to ascertain that targeting took place at the site and not at an unintended site. This technology

Fig. 7. Recombineering a liner PCR product. The PCR template is the cassette to be inserted into chromosome (shown as red). Primers contain two parts: (i) 5' end of 35~45 bp (black) that is homologous to flanks of the target DNA. (ii) 3' end of 20 bp (red) that primes the cassette DNA for amplification. PCR reaction generates the PCR product with cassette flanked by homologous DNA. The PCR product is transformed into cells with Red recombination proteins. The lambda Gam product inhibits the nuclease activity of RecBCD. Exo, which is 5' to 3' exonuclease, degrades the 5' end of the PCR product, leaving behind the intact 3' overhang. Beta binds to ssDNA and protects DNA from single-strand nuclease attack. Beta searches for homology and promotes annealing between complementary ssDNAs. In the presence of the lambda Red recombination system, the linear DNA is integrated into the chromosome at the target sequence after recombination.

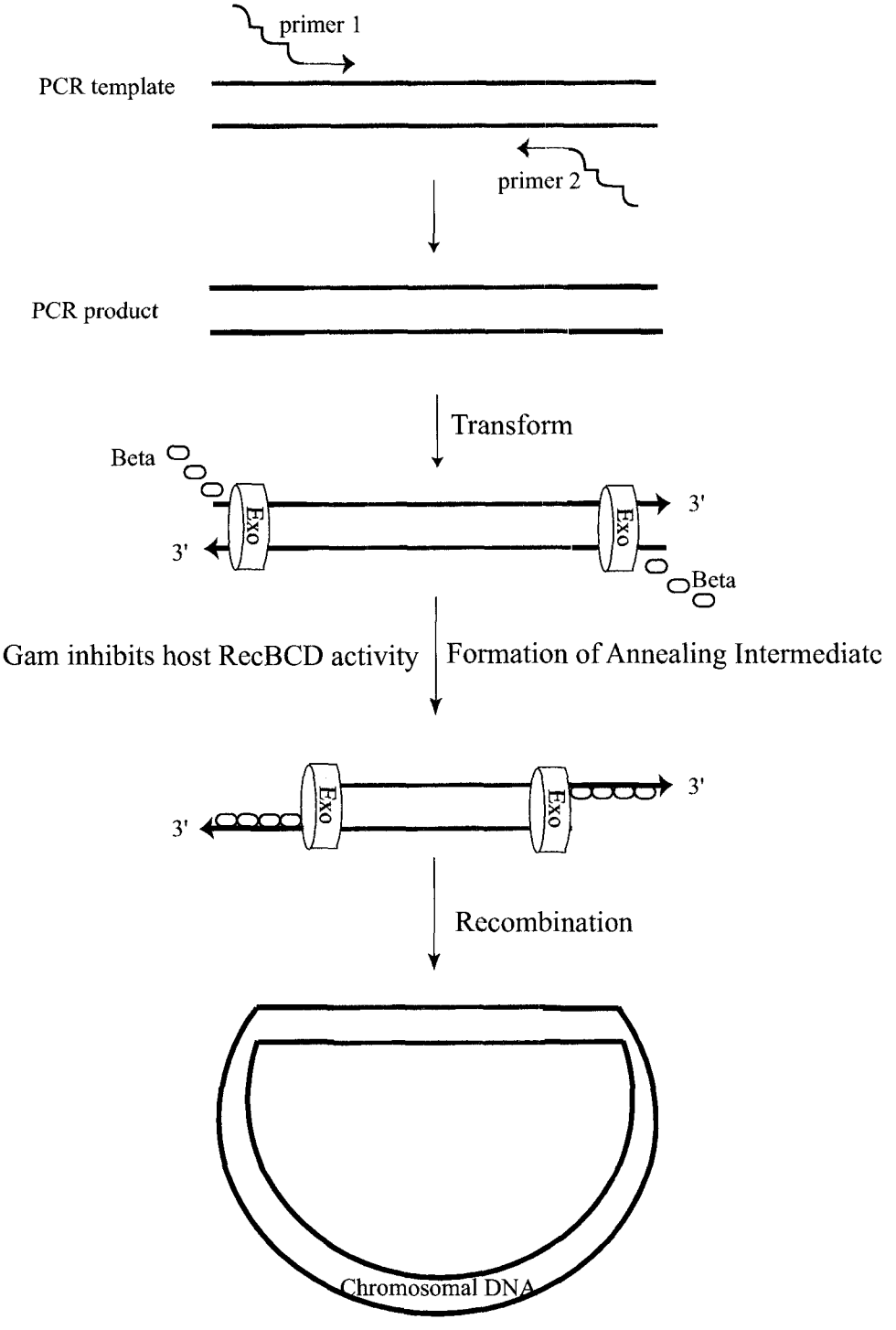

was used to insert DNA cassettes between two adjacent base pairs without deleting any bases (130, 132), as well as to replace as much as 70kb with the insertion cassette (141). Under optimal conditions, the efficiency of recombination can be as high as 1 in 1,000 surviving cells from a standard electroporation. At this efficiency, even without a selection marker, recombinants could be screened with PCR. Thus, Red recombineering makes the bacterial chromosome amenable to almost any type of desired change. Recently, genomic sequencing has provided the complete genome information for *S. typhimurium* (142). Therefore, *res* elements carrying an antibiotic gene can now be inserted at nearly any site except in single copy essential genes in the *S. typhimurium* chromosome.

Two Red-recombineering systems are available. In the first system, the recombination genes are carried as a single copy on the bacterial genome and expressed from the powerful λP_L promoter. Expression from this promoter is tightly regulated by the temperature-sensitive λ CI857 repressor. At 30°C the repressor blocks the P_L promoter; inactivating the repressor by a temperature shift to 42°C turns on the promoter, allowing coordinated expression of the *gam, bet,* and *exo* genes (130, 131, 143). In the second recombineering system, recombination genes are expressed from an arabinose-controlled promoter, P_{araBAD}. The three recombination genes are constructed under the control of an arabinose-inducible promoter in the Red helper plasmid pKD20 (135). In the presence of arabinose, the araC activator, present on the vector, induces expression of Exo, Beta and Gam proteins. pKD20 can be simply cured by growth at 37°C because it is a temperature-sensitive replicon. Both systems were used in this study to engineer multiple insertions and deletions on the chromosome.

TRANSCRIPTION-INDUCED BARRIERS TO SUPERCOIL DIFFUSION IN THE *SALMONELLA TYPHIMURIUM* CHROMOSOME

by

SHUANG DENG, RICHARD A. STEIN, AND N. PATRICK HIGGINS

Proceedings of the National Academy of Science of the USA **101,** 3398-3403

ABSTRACT

Transcription and replication both influence and are influenced by superhelical changes in DNA. Explaining how supercoil movement is channeled in living chromosomes has been a major problem for 30 years. Transcription of membrane-associated proteins leads to localized hypersupercoiling of plasmid DNA, and this behavior indicates the presence of aberrant supercoil diffusion. Using the lambda Red recombination system, we constructed model domains in the *Salmonella typhimurium* chromosome to analyze supercoiling dynamics of regions encoding membrane proteins. Regulation of Tn*10*-derived tetracycline resistance involves a repressor, TetR, and a membrane-bound export pump, TetA. Strains deficient in TetR repressor activity had 60-fold higher transcription levels (from P_A) than TetR-positive strains. High *tetA* transcription caused a 10- to 80-fold decrease in the γδ resolution efficiency for the domain that includes the Tet module. Replacing *tetA* with genes encoding cytosolic proteins LacZ and Kan also caused the appearance of supercoil diffusion barriers in a defined region of the chromosome. In strains containing a functional TetR repressor located next to a regulated *lacZ* reporter (P_R*tetR*-P_A*lacZ*), induction of transcription with chlortetracycline caused a 5-fold drop in resolution efficiency in the test domain interval. A short half-life resolvase showed that barriers appeared and disappeared over a 10- to 20 min span. These studies demonstrate the importance of transcription in chromosome structure and the plasticity of supercoil domains in bacterial chromosomes.

INTRODUCTION

Numerous studies demonstrate that bacterial chromosomes are partitioned into independent domains that limit supercoil diffusion (1, 2). Early analyses of bacterial chromosomes liberated from cells by treatment with lysozyme and detergent showed that "nucleoids" were negatively supercoiled objects and that multiple single-strand breaks were needed to relax all supercoils (3, 4). Sinden and Pettijohn subsequently confirmed that chromosomes were segregated into multiple independent domains *in vivo* by using tri-methylpsoralen crosslinking (5). In 1996, an assay was developed to measure supercoil diffusion inside living cells using the site-specific recombination reaction of Tn*3* or the closely related element γδ (6). In this assay, the ability to delete specific chromosome segments separated by two γδ *res* sites spaced along the chromosome measures supercoil diffusion (7, 8). What elements are responsible for domain structure is a long-standing question.

One advantage of the site-specific resolution assay is that it shows how supercoil structure at specified locations is modified when growth rate or biological activity changes. Most resolution barriers are random with respect to DNA sequence, but the appearance of a new barrier has been documented. For example, induction of the early promoter of the bacteriophage Mu caused a new barrier to supercoil diffusion that was restricted to the region near the virus center (9).

The impact of transcription on DNA structure is well documented in plasmids (10). For example, transcription of the pBR322 *tetA* gene causes dramatic hyper-supercoiling when the cell also harbors a mutation in the *topA* gene, which encodes a type I topoisomerase (ω protein) (11-14). Studies by Lynch and Wang showed that hyper-

supercoiling from a moderate-strength promoter required both the presence of a *topA* mutation plus transcription of a protein that was cotranscriptionally inserted into the membrane or exported to the periplasm or outer membrane (15). Similar studies have been difficult to conduct in the bacterial chromosome for two reasons. First, it has been difficult to construct test intervals in the 4-Mb bacterial genome. Second, bacterial chromosomes have supercoiling domains larger than most multicopy plasmids.

A new supercoil diffusion barrier appears after induction of *tetA* transcription. Moreover, transcription of two cytosolic proteins, LacZ and Kan, showed similar effects. A short half-life resolvase revealed that barriers appear and disappear over a 10- to 20-min span. These studies demonstrate an extremely dynamic domain structure for bacterial chromosomes.

MATERIALS AND METHODS

Media

LB media and minimal media were prepared as described (6). Antibiotics were added to medium at concentrations of 50 μg/ml for kanamycin and ampicillin, 20 μg/ml for chloramphenicol, 12 μg/ml for tetracycline, and 10 μg/ml for gentamicin. Bochner plates were made as described (16).

Plasmids

Plasmid pJBRESc*I* is a pACYC184-derived vector carrying the *tnpR* (WT Res resolvase protein) gene of transposon γδ cloned under control of the λP_L promoter with a nearby copy of λ *c*Its repressor gene (17). Plasmid pJBRESc*I*-SSRA carries a short half-

life Res resolvase in which the sequence tag encoded by *ssrA* RNA was added to the carboxyl terminus of Res. λ Red helper plasmid pKD20 is a derivative of pint-ts that encodes Red recombinase under the control of the P_{araB} promoter (18).

Chromosomal modification with Red recombination

Insertion mutagenesis of the *Salmonella typhimurium* chromosome was done with the lambda Red recombination system of plasmid pKD20 (18). Synthetic oligos used for each construct is described in Table 2, which is published as supporting information on the PNAS web site. Oligonucleotides were purchased from IDT (Coralville, IA). *Taq* polymerase (Sigma) and *Taq* extender (Stratagene) were mixed 1:1 to generate DNA for sequence analysis and to make gene replacement substrates. Recombinants with the correct insertions were selected for tetracycline resistance or kanamycin resistance or screened for blue-color phenotype and tested as described (6, 19). Details of strain constructions are given in *Supporting Text,* which is published as supporting information on the PNAS web site.

Assays

To measure resolution, log phase cultures grown at 30°C to 50 Klett units (filter no. 54) were induced for Res expression by a 10-min incubation at 42°C followed by 10-fold dilution in LB containing chloramphenicol. Cells were incubated overnight at 30°C and then diluted $1:10^6$ and plated on minimal medium with chloramphenicol and 5-bromo-4-chloro-3-indolyl β–D-galactosidase (X-gal). Deletion frequencies were scored by loss of color or loss of antibiotic resistance (6). To measure *lacZ* expression, overnight

bacterial cultures diluted 1:100 in 5 ml of LB were grown to 50 Klett units. β-galactosidase (β-gal) assays were done in triplicate as described (20).

RESULTS

Supercoil diffusion in the 17-min region of S. typhimurium

Transcription can lead to anomalous DNA structure and a hypernegative supercoiling phenotype in plasmid DNA (14, 15, 21, 22). For efficient promoters like the hybrid *tac* promoter under control of the Lac repressor, transcriptional effects on plasmid DNA topology can be documented in WT cells (23). With weaker promoters like the one regulating the tetracycline resistance gene on pBR322, cotranscriptional translation of membrane proteins stimulate hypernegative supercoiling only in *topA* mutants (15, 24). Although several examples of translation-driven supercoiling are restricted to *topA* mutants, the behavior has led to theories of cotranscription membrane association helping to organize chromosomal DNA after replication (25, 26). A serendipitous result suggested that the *tetA* gene of Tn*10* might also cause topological anomalies in the chromosome. A genetic interval in *S. typhimurium* was flanked with a pair of *res* sites by using two combinations of drug markers. Strain NH3470 had a Tn*5* kanamycin resistance gene (*kan*) upstream and a Tn*10*-derived *tetR/tetA* module downstream. Strain NH3471 had a Tn*1696*-derived gentamicin resistance gene upstream (*gen*) and the Tn5 *kan* gene downstream (Table1 and Fig. 1*A*). Recombination between *res* sites in strain NH3470 (Fig. 1*A Upper*) results in sensitivity to tetracycline, and in NH3471 (Fig. 1*A lower*) resolution leads to kanamycin sensitivity.

Table 1. Strains used

Strain	Genotype	Plasmid
NH3470	*zbj8904*::Tn*10d*(Gn)<>(*kan*) (*yliI*)<>(P_R*tetR435-*P_A*tetA-res*)	pJBRESc*I*
NH3471	*zbj8904*::Tn*10d*Gn (*yliI*)<>(*kan-res*)	pJBRESc*I*
NH3472	*zbj8904*::Tn*10d*(Gn)<>(*kan*) (*yliI*)<>(P_R*tetR-*P_A*tetA-res*)	pJBRESc*I*
NH3475	*zbj8904*::Tn*10d*(Gn)<>(*kan*) (*yliI*)<>(P_A*tetA-res*)	pJBRESc*I*
NH3477	(*yliI*)<>(P_R*tetR435-*P_A*lacZ-res*)	
NH3478	(*yliI*)<>(P_R*tetR-*P_A*lacZ-res*)	
NH3479	(*yliI*)<>(P_A*lacZ-res*)	
NH3480	*zbj8904*::Tn*10d*k*an* (*yliI*)<>(P_A*tetA-rrnB-res*)	pJBRESc*I*
NH3481	*cobP712*::Tn*10d*Gn *cobT714*::Mud*J*r2	pJBRESc*I*
NH3482	*cob-708*::Tn*10d*Gn *cobT714*::Mud*J*r2	pJBRESc*I*
NH3483	*cobT712*::Tn*10d*Gn *cobT714*::Mud*J*r2(*kan*)<>(P_A*tetA*)	pJBRESc*I*
NH3484	*cobP712*::Tn*10d*Gn *cobT714*::Mud*J*r2(*kan*)<>(P_A*tetA*$_{inv}$)	pJBRESc*I*
NH3485	*cob-708*::Tn*10d*Gn *cobT714*::Mud*J*r2(*kan*)<>(P_A*tetA*)	pJBRESc*I*
NH3486	*cob-708*::Tn*10d*Gn *cobT714*::Mud*J*r2(*kan*)<>(P_A*tetA*$_{inv}$)	pJBRESc*I*
NH3487	*zbj8904*::Tn*10d*(Gn)<>(*kan*) (*yliI*)<>(P_R*tetR-*P_A*lacZ-rrnB-res*)	pJBRESc*I*
NH3488	*zbj8904*::Tn*10d*(Gn)<>(*kan*) (*yliI*)<>(P_A*lacZ-rrnB-res*)	pJBRESc*I*
NH3489	*zbj8904*::Tn*10d*Gn (*yliI*)<>(P_R*tetR-*P_A*kan-rrnB-res*)	pJBRESc*I*
NH3490	*zbj8904*::Tn*10d*Gn (*yliI*)<>(P_A*kan-rrnB-res*)	pJBRESc*I*
NH3491	(*recN*)<>(P_R*tetR-*P_A*tetA*) *zbj8904*::Tn*10d*(Gn)<>(*kan*) (*yliI*)<>(P_A*lacZ-rrnB-res*)	pJBRESc*I*
NH3492	*zbj8904*::Tn*10d*(Gn)<>(*kan*) (*yliI*)<>(P_R*tetR-*P_A*lacZ-rrnB-res*)	pJBRESc*I*-SSRA

All strains were derived from *S. typhimurium* LT2 and were constructed during this work. The Tn*10d*Gn and Mud*J*r2 elements were described in (6). <> indicates a replacement generated by lambda Red recombineering (47).

Fig. 1. Effect of WT *tetR*, a mutant *tetR*, and a *tetR* deletion on γδ resolution efficiency. (*A*) Physical and genetic map of a 12-kb interval between *zbj8904* and *yliI* in the 17- to 20-min region of *S. typhimurium* includes ORFs flanked by drug markers and *res* sites. Two arrangements of selectable drug markers involve kanamycin and tetracycline resistance (*Upper*) and gentamicin and kanamycin resistance (*Lower*). (*B*) Resolution efficiency comparison among different module insertions in the gene *yliI* in the 12-kb interval in the log phase. Resolution efficiency for a 12-kb interval in the 43- to 45-min region (6) is designated as the expected resolution efficiency.

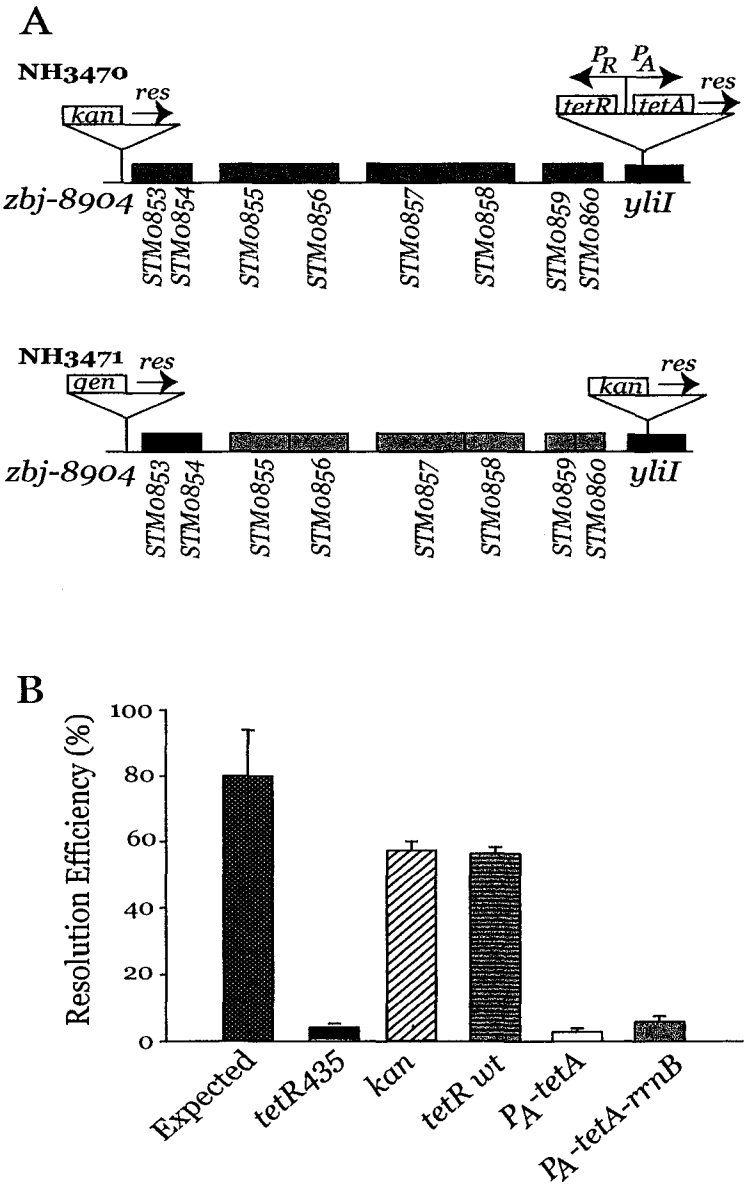

Based on studies of the genetic segment between the cob and his operons, we expected resolution efficiency for a 12-kb interval to be 80% (Fig. 1*B* first column). However, NH3470 had a resolution efficiency of only 3%, which is 26-fold lower than expected (see Fig. 1*B* second column). Strain NH3471, analyzed by using the same protocol except that kanamycin sensitivity was scored, had a resolution frequency of 57%, which is close to the expected level (Fig. 1*B* third column). This unexpected low efficiency suggested that the *tet* cassette in strain NH3470 caused a low-resolution phenotype.

We have used Tn*10*-derived *tet-res* elements for resolution analyses in many different intervals where they did not show a low-resolution phenotype. One explanation is that a mutation (like an altered *res* site) generated during PCR amplification reduced resolution efficiency. To test this hypothesis, a new strain was made by using different PCR reactions to generate the *tet-res* module. A resulting strain (NH3472) had a resolution efficiency of 56%, which was similar to the efficiency of the strain NH3471 (57%). This experiment supports the notion that the *tet* module in strain NH3470 was unusual.

Sequence analysis of *tet* modules from NH3470 and NH3472 showed that NH3470 *res* site was unaltered, but it had a deletion of base pair 435 in the *tetR* gene (ΔA-435). Hereafter, we refer to this allele as *tetR435*. The deletion causes a frameshift and premature translation stop that eliminates 66 amino acids of the WT TetR protein (Fig. 6, which is published as supporting information on the PNAS web site). Although the DNA-binding domain of TetR435 repressor is unaltered (27), destabilization of the TetR dimer interface might lead to constitutive *tetA* gene expression (28).

Tet expression in strains with WT *tetR* and *tetR435* alleles was measured in two ways. First, Bochner plates were used to test sensitivity to fusaric acid. These plates are

commonly used to counterselect against strains carrying Tn*10*-derived tetracycline resistance (16). TetA expression is toxic at 42°C in the presence of fusaric acid. Standard Bochner plates contain chlortetracycline hydrochloride (CLT), which induces the Tet operon by binding the TetR, causing its dissociation from DNA and transcription of both *tetA* and *tetR* (28). Fusaric acid sensitivity was measured in normal Bochner plates and modified plates lacking CLT. Strain NH3472 with a WT *tetR* gene grew well on Bochner plates without CLT but was killed on a standard Bochner plate (Fig. 7, which is published as supporting information on the PNAS web site). Strain NH3470 died on Bochner plates with or without CLT, which indicates constitutive TetA expression.

Second, to quantify transcription from the *tetA* promoter, chromosomal *lacZ* was fused to a *tetA* promoter (P_A) using lambda Red substitution. NH3478 (WT *tetR*) made 15 units of β-Gal in the absence of CLT and 688 units of β-gal after addition of 5 μg/ml CLT. NH3477 (*tetR435*) made 959 units of β-gal with or without CLT addition (Table 3, which is published as supporting information on the PNAS web site). Thus, *tetR435* had a higher level of *tetA* expression than a WT *tetR* construct induced with the optimal amount of CLT. The effect of *tetA* expression was local and not generally inhibitory to resolution because a Tet element, 1800 kb away from the test interval had no impact when the region had no *tetA* promoter (data not shown).

Transcription hinders supercoil diffusion

Although the expression data shown above reveal a correlation between *tetA* expression and reduced γδ resolution, transcription and translation levels of TetA are not the only differences between these strains. The TetR435 protein might cause DNA dam-

age or alter DNA structure by unexpected mechanisms. To check this possibility, strains NH3475 and NH3479 were made, which lack TetR and constitutively express *tetA* or *lacZ*, respectively, from the P_A promoter. NH3475 (P_A*tetA* allele) was similar to NH3470, being inviable on Bochner plates with or without CLT (Fig. 7). Strain NH3479 was similar to NH3477 because it expressed 915 units of β-gal (Table 3). The resolution efficiency of a strain lacking TetR (NH3475) (*yliI*)<>(P_A*tetA-res*) was identical (3%) with the strain carrying the *tetR435* allele (Fig. 1*B*, fifth column). Thus, *tetR435* and a *tetR* deletion have the same phenotype.

The hypothesis at this point was that TetA protein expression induces a position-specific barrier to chromosome supercoil diffusion, perhaps by handcuffing the DNA to the cell membrane during translation. However, a trivial explanation is that RNA polymerase transcribes through the *res* site, causing Res protein to dissociate. This mechanism would block site-specific resolution by occluding Res binding to one *res* site. To address this possibility, a pair of efficient transcription terminators (*rrnB* T/T2) was placed at the 3'-end of *tetA*. After the TetA termination codon is a 105-bp sequence followed by the *rrnB* T1/T2 terminators (158 bp in length), and the γδ *res* site is 129 bp beyond the terminators. In this configuration the *res* site is shielded from occlusion by efficient (>95%) transcription terminators. Strain NH3480, which contains this construct (*yliI*)<>(P_A*tetA-rrnB-res*), retained a low-resolution phenotype (6% recombinants, see Fig. 1*B*, sixth column). A 2-fold occlusion effect is possible, because the resolution efficiency rose from 3% without the terminator to 6% when the terminator was present. Nonetheless, most of the inhibitory effect of *tetA* expression on resolution remained to be explained.

tetA *barriers are mobile*

To see whether *tetA* expression alters supercoiling behavior in a different chromosomal setting, several *tetA* configurations were moved to the *his-cob* region. This genetic interval has been thoroughly characterized, and it has no sequence- or region-specific barriers (6, 19, 29). Two intervals that normally resolve at high frequency include a 14-kb segment defined by *cobP712*::Tn*10d*Gn and *cobT714*::Mu*d*Jr2 (Fig. 2*A*, NH3481) and a 28-kb interval defined by *cob-708*::Tn*10d*Gn and *cobT714*::Mu*d*Jr2 (Fig. 2*A*, NH3482). In these experiments, a Δ*tetR* P_A*tetA* module was substituted for the *kan* gene in *cobT714*::Mu*d*Jr2 (Fig. 2*B*). Replacements were made in two orientations to control for transcription occlusion. In NH3483 and NH3485, *tetA* transcription points toward the nearby *res* site (Fig. 2*B*, Mu*d*Jr2 (*kan*)<>(P_A*tetA*)). In NH3484 and NH3486 *tetA* transcription is directed away from the *res* site [Fig. 2*B*, Mu*d*Jr2 (*kan*)<>(P_A*tetA-inv*)]. In this orientation RNA polymerase cannot occlude a *res* site.

Resolution efficiency over the 14-kb interval between *cobP712*::Tn*10d*Gn and *cobT714*::Mu*d*Jr2 (NH3481) was 98% (Fig. 2*Ca*, Mu*d*Jr2). When the *kan* gene in Mu*d*Jr2 was replaced by P_A*tetA* (NH3483), resolution efficiency dropped to 2% (Fig. 2*Ca*, P_A*tetA*). When the *kan* gene was replaced by inverted P_A*tetA* (NH3484), resolution efficiency was 5% (Fig. 2*Ca*, P_A*tetA-inv*). Thus, constitutive t*etA* expression caused a 20- to 50-fold decrease in resolution efficiency for this 14-kb interval. Resolution efficiency for the 28-kb interval between *cob-708*::Tn*10d*Gn and *cobT714*::Mu*d*Jr2 (NH3482) was 78%. (Fig. 2*Cb*, Mu*d*Jr2). Replacement of the *kan* gene in Mu*d*Jr2 with P_A*tetA* (NH3485) caused resolution efficiency to decrease to 1% (Fig. 2*Cb*, P_A*tetA*). When *kan* gene was replaced by an inverted P_A*tetA* (NH3486), resolution efficiency was

Fig. 2. γδ resolution in the 43- to 45-min. of *S. typhimurium* chromosome. (*A*) Physical map of two intervals. The 14-kb interval from *cobP712* to *cobT714* is labeled a, and the 28-kb interval from *cob-708* and *cobT714* is labeled interval b. (*B*) Genetic map of *res* elements placed at the *cobT714* location: Mu*d*Jr2, Mu*d*Jr2(*kan*)<>(P_A*tetA*), and Mu*d*Jr2(*kan*)<>(P_A*tetA-inv*). (*C*) Resolution efficiencies for different 14-kb (*a*) and 28-kb (*b*) intervals.

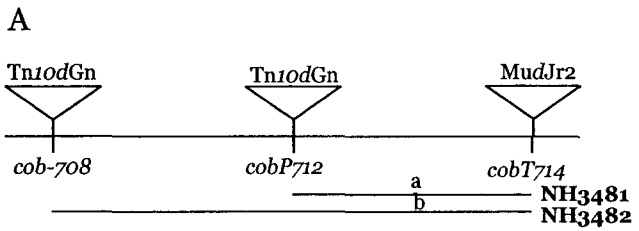

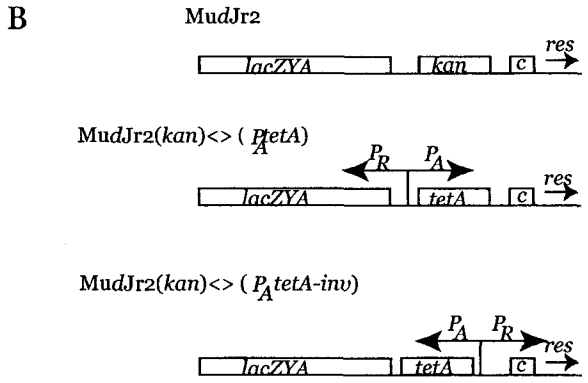

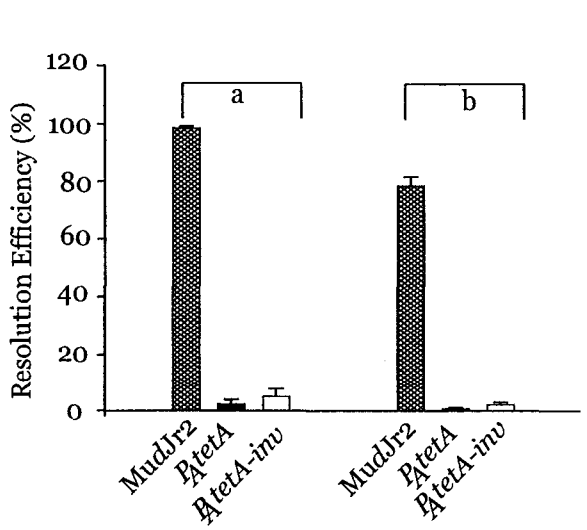

2% (Fig. 2*Cb*, P_A*tetA-inv*). Constitutive *tetA* expression reduced resolution efficiency in the 28-kb interval by 40- to 80-fold. These results prove that the *tetA* gene is a mobile element that can disrupt supercoil diffusion. Occlusion here is unlikely in either case, so the major impact is due to transcription and/or translation of *tetA*.

Genes encoding cytoplasmic proteins also create supercoil barriers

Is membrane association necessary to disrupt supercoil diffusion? To address this question, we measured γδ resolution in intervals with *lacZ* and *kan* genes fused to the *tetA* promoter. When *lacZ* expression was repressed by TetR (NH3487), γδ resolution was efficient (65% in Fig. 3 *A* and *B* column 2), but when *lacZ* expression was unregulated (NH3488), γδ resolution was very inefficient (4% in Fig. 3 *A* and *B* column 3). The magnitude of disruption to supercoil diffusion in NH3488 was similar to a strain constitutive for TetA expression (6% in Fig. 3 *A* and *B* column 1). Similarly, when *kan* was placed at P_A under the control of TetR (NH3489), γδ resolution was efficient (70% in Fig. 3 *A* and *B* column 5). But unregulated *kan* expression (NH3490) caused γδ resolution to fall to the level of cells expressing TetA (7% in Fig. 3 *A* and *B* column 6). Clearly, a membrane anchor is not prerequisite for generating barriers to supercoil diffusion; transcription of two genes encoding cytoplasmic proteins reduced γδ resolution as much as transcription of *tetA*.

To see whether resolution could be modulated by using a distant source of *tetR* repressor, *tetR* was cloned into *recN* (NH3491), which is 1,800 kb away from gene *ylil*. With no source of TetR, strain NH3488 made dark-blue colonies, and resolution was in

Fig. 3. Effect of genes encoding cytoplasmic proteins on the γδ resolution efficiency in the 12-kb interval between *zbj8904* and *yliI*. (*A*) Genetic map of different protein coding sequences (*tetA*, *lacZ,* and *kan*) fused to *tetA* promoter $P_{A.}$ (*B*) Resolution efficiency comparison among different insertions in the gene *yliI* in the 12-kb interval in the log phase.

A

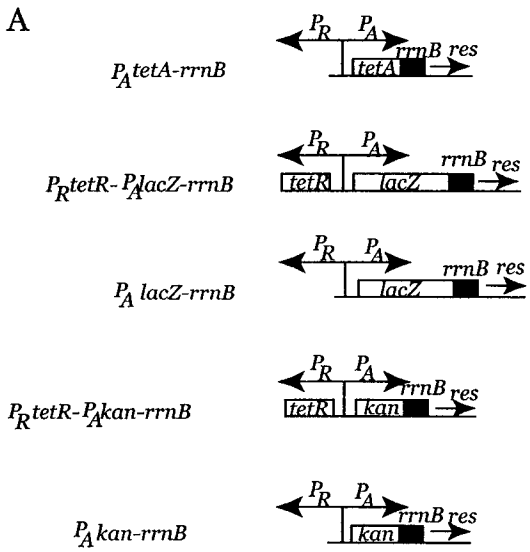

B

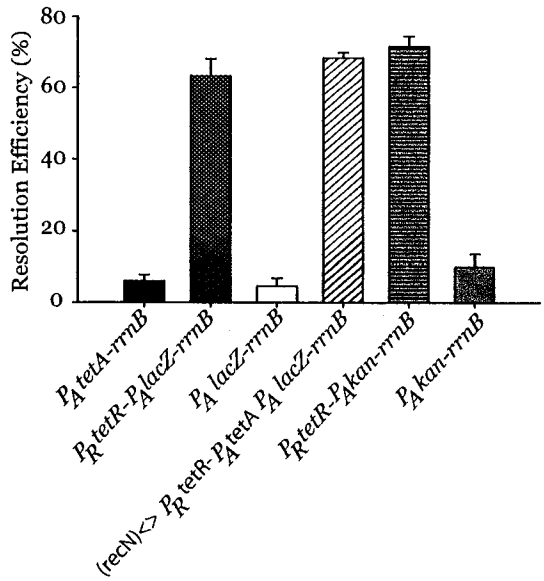

efficient 4% (Fig. 3 *A* and *B* column 3). When TetR protein was provided in trans, NH3491 made light-blue colonies and γδ resolution was efficient (67%, Fig. 3 *A* and *B* column 4). Thus, TetR regulation of the *tetA* promoter clearly determines the efficiency of resolution reactions.

Barrier Kinetics

Supercoil barriers in two regions of the genome appear when genes encoding *tetA*, *lacZ*, or *kan* are expressed from a *tetA* promoter P_A (Figs, 1-3). To explore the correlation between transcription level and γδ resolution efficiency, a dose-response experiment was carried out in strain NH3492, which has the *lacZ* fused to the *tetA* promoter next to a WT *tetR* repressor. Cultures grown overnight in LB were diluted 100- fold in medium containing 0, 0.1, 0.5, 1, 5, 10, or 20 μg/ml CLT. Cell growth at 30°C was monitored in Nephlo flasks by using a Klett meter, and when cultures reached the value of 50 Klett units, half of the cells were harvested by centrifugation and assayed for β-gal activity. The remaining half of each culture was incubated at 42°C for 10 min to induce expression of a tagged form of γδ Res protein (see below). Cells were put back in culture at 30°C to allow chromosome segregation and then diluted and spread on plates containing the chromogenic indicator X-gal. Resolution efficiency was calculated as the percentage of white colonies among all colonies. WT Res protein is stable, and once induced, it can catalyze recombination for a time lasting longer than two cell divisions, which obscures the kinetic analysis of barrier disappearance. The Res-SsrA protein has a C-terminal extension of 11 amino acid residues that are identical with the Clp-XP proteolysis tag of the SsrA system (30). Work to be reported elsewhere (Stein, R., unpublished work) shows

that this protein has a half-life of 5 min in exponential cultures of *S. typhimurium*. The Res-SsrA protein is fully functional and has the same *in vivo* resolution efficiency as WT Res if either the expressing cells lack functional ClpXP protease or the 11-aa tag is modified so that it is no longer recognized as a ClpXP/P substrate (data not shown). For a 10-min induction followed by outgrowth at 30°C, 90% of all resolution in strains with the Res-SsrA protein occurs in a 5- to 12-min window after the shift to 42°C.

A reciprocal relationship between β-gal activity and γδ resolution efficiency was observed (Fig. 4). At 0.1 μg/ml CLT, a small induction of β-Gal expression produced a small inhibitory effect on resolution (Fig. 4 *Inset*). With the increase of CLT concentration, β-gal expression increased and resolution decreased. At 5 μg/ml of CLT, β-gal activity peaked and γδ resolution efficiency approached a minimum. At very high concentrations of CLT, cells grow poorly, which complicates both resolution and β-gal assays.

To study the kinetics of barrier appearance, fresh overnight cultures of NH3492 were diluted 100-fold into LB at 30°C and cell growth was followed in a Klett meter. At a density of 50 Klett units, 5 μg/ml of CLT was added. One aliquot was immediately induced for the resolution assay, then at various later time points aliquots were removed and shifted to 42°C for resolution assays (Fig. 5). Each time point in Fig. 5 marks the elapsed time from addition of CLT to the end of the 42°C induction period. Resolution frequencies changed 5-fold from 50% to 10% over a 20-min window of growth and induction with CLT.

The kinetics of barrier disappearance was also examined. An overnight culture of NH3492 was diluted 100-fold into LB plus 5 μg/ml CLT. At a density of 50 Klett units, cells were harvested and resuspended in CLT-free medium, and 10-min shifts to 42°C

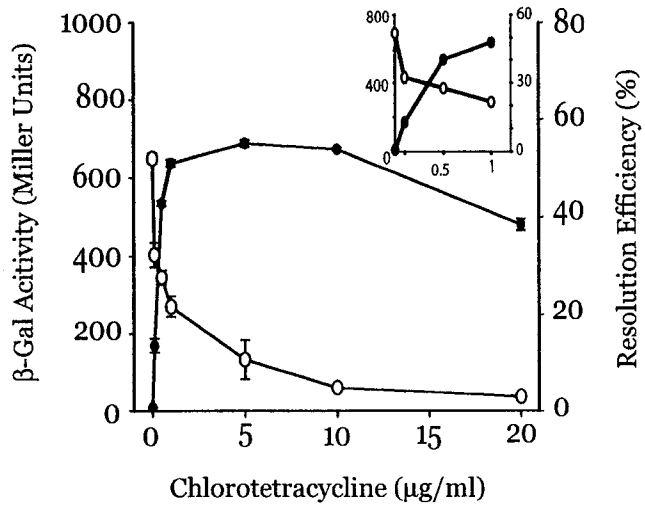

Fig. 4. Effect of chlortetracycline concentration on β-gal activity and γδ resolution efficiency. NH3492 was subcultured in 0, 0.1, 0.5, 1, 5, 10, 20 μg/ml chlortetracycline and was grown to a cell density of 50 Klett units. Both β-gal assays(●)and γδ assays (O)were done on each sample.

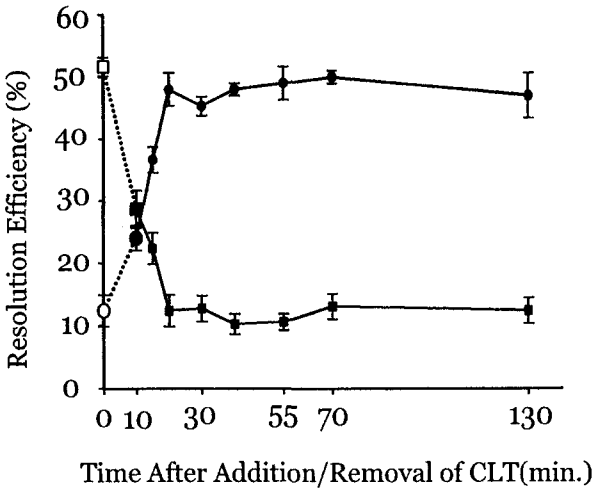

Fig. 5. Barrier appearance and disappearance in response to chlortetracycline. □, overnight cultures of NH3492 subcultured in LB without chlortetracycline. γδ resolution assays were done when cell density reached 50 Klett units. ■, 5 μg/ml chlortetracycline added at a cell density of 50 Klett units. Samples were taken at various points after addition of chlortetracycline and subjected to γδ resolution assays. ○, NH3492 grown in LB with 5 μg/ml chlortetracycline. γδ resolution were initiated when cell density reached 50 Klett units. ●, chlortetracycline removed by quickly washing and then resuspending cells in LB. Samples taken at various times were tested for γδ resolution.

were done in the same manner described above. Resolution efficiency increased from 10% to 50% after CLT removal. Barriers appeared and disappeared with similar kinetics (Fig. 5).

DISCUSSION

Transcription changes the dynamic behavior of plasmid DNA in several ways. First, RNA polymerase unwinds the double helix as it transcribes RNA. Induction of a moderate-strength promoter can add six new RNA polymerase molecules to a small plasmid, which changes the average linking number by 10 negative supercoils (31). Second, transcription causes a temporary segregation of positive supercoils in front of a transcribed gene and negative supercoils in the transcription wake (32-34). In strains carrying a *topA* mutation, expression of a membrane-inserted protein can result in a dramatic increase in negative supercoil of plasmids (14, 15, 21). Both of these effects are visible because rapid plasmid extraction freezes the population in its current topological state, and agarose gel electrophoresis can detect subtle changes in plasmid topology (35). Two effects of transcription have been noted in the large bacterial chromosome. First, if a highly transcribed operon like *rrnB*, which encodes ribosomal RNAs, is positioned head to head with a replication fork, transcription markedly delays the time required for forks to cross the transcription unit (36). Second, induction of the strong phage Mu early promoter causes a new supercoil barrier to appear in the vicinity of the transcription unit (9).

In this work we found three effects of transcription on supercoil dynamics in the *S. typhimurium* genome. First, constitutive *tetA* transcription caused a persistent 20-fold reduction in γδ site-specific recombination over a 14-kb interval by (Fig. 2). The effect

was larger for longer intervals, with an impact of a 40-fold reduction for a 28-kb domain. Second, transcription effects were not restricted membrane proteins. Similar effects on γδ resolution efficiency were found with aminoglycoside-3'-*O*-phosphotransferase, which is the product of the Tn*5* *kan* gene and β-gal, the product of *Escherichia coli lacZ*. Barriers were detected by using a WT resolvase in combination with modules that either lacked a functional copy of the TetR repressor, or modules with WT TetR protein but in presence of the inducer CLT. The critical determinant was transcription strength. Even though the eight genes separating the *res* sites in strain NH3470 include five membrane-associated proteins, the level of transcription of these genes, estimated by microarray analysis of total-cell RNA (data not shown), was too low to disrupt supercoil diffusion. At the *atp* operon, consisting of nine genes encoding membrane-associated proteins, and the *nmpC* operon, which regulates a single gene, the mRNA abundance measured from microarray analysis accurately predicted the impact on γδ resolution (Fig. 8, which is published as supporting information on the PNAS web site). Third, by using a modified form of γδ resolvase with a cellular half-life of 5 min, barriers to supercoil diffusion appeared and disappeared within 10-20 min of the point when CLT was either added or washed out of cell cultures. The impact of transcription over a 14-kb interval was correlated with the level of transcription over a 40-fold range of expression measured with β-gal assays.

Because transcription alters chromosome dynamics of both plasmid and the bacterial chromosomal DNA, the question arises as to how many transcription-related barriers exist in a bacterial cell. Microarray analyses provide important information on genome-wide transcription profiles (37, 38). Cells growing under the same conditions employed

in our experiments (exponential cultures in LB) give detectable RNA signals for >4,000 *E. coli* genes (38). However, steady-state mRNA abundance exhibits a strikingly skewed distribution. For 70% of the genes (3,034 ORFs) mRNA abundance is less than one molecule per cell. Genes in this category include the uninduced RNA for *lacZ* (which yields ≈15 Miller units of β-gal activity) and 69 of the 321 known essential genes. Genes in this low-transcription category probably have little impact on DNA dynamics. The second class is genes with a steady state abundance of one to four copies of RNA/DNA, which results in 40-160 Miller units of β-gal activity. Genes in this class (≈1,000) include 86 essential genes, and they are also predicted to have a modest topological impact. Fig. 4 suggests that over a 14-kb interval these genes would decrease resolution by 30% or less. The third gene class includes genes with RNA/DNA ratios >4. Included in this category would be a *lacZ* gene induced with 1 mM isopropyl β-D-thigalactoside (IPTG), which causes a 40- to 60-fold derepression of transcription to ≈600 Miller units. Protein-coding genes in *E. coli* with RNA/DNA ratios of 10 or greater represent 85 genes. The predicted impact on chromosome domains of these top 85 genes is given in Table 4, which is published as supporting information on the PNAS web site. The abundance of *lacZ* mRNA in uninduced cultures yields an RNA/DNA ratio of 0.45 (38), so a culture with 600 Miller units would have an RNA/DNA ratio of ≈20. This expression change is nearly identical with the change in levels of β-gal expression we observe in *S. typhimurium* going from a repressed P_R*tetR*-P_A*lacZ* culture to steady-state expression in the presence of 5 μg/ml CLT (Fig. 4). Extrapolating from the plot in Fig. 4, the number of chromosomal sites with diffusion barriers that would inhibit resolution by 5-fold or more would be <8. If we add the seven ribosomal operons, we predict that only ≈15 sites

would show persistent 5-fold effects on resolution. This number of barriers is small compared to our estimate of 300 barriers that are stochastic and associated with DNA replication.

Several implications of these results are noteworthy. First, because transcription of many genes, including a significant fraction of the essential genes, is intermittent in many parts of the chromosome, domain structure is likely to be both dynamic and variable. Recent studies show that cell-to-cell expression variation is high for the *lac* operon at low inducer levels (39, 40). In specific instances, a burst of transcription can lead to a large amount of protein production in some cells and none at all in most cells. Considering the fact that operons like *araBAD* respond in similar fashion (41), no two organisms in a bacterial culture may ever have the same genome organization. This makes chromosome structure behave like a quasispecies, which is a collection of organisms that vary in structure around a common mean (42). Second, the genome behavior of the highly expressed operons may have special mechanisms to insulate their transcriptional effects from surrounding chromosome regions. The highly transcribed genes may be under selection for interspersion. Examples are known where chromosomal inversions involving specific inverting sites are disfavored, whereas other inversions using the same end points are permitted (43, 44). Finding the rules governing such behavior has been difficult. It is possible that apposition of two chromosomal segments with high-transcription activity may be unstable, just as placing a replication origin in front of a strong transcription unit leads to an impediment to replication (36). Third, recent reports in both bacteria and yeast show that high levels of transcription can cause formation of persistent RNA:DNA hybrids (R-loops) that interfere with both transcription and replication (22, 45, 46).

Whether R-loop formation is responsible for some examples of chromosomal domain behavior is a difficult question, but it is one well worth pursuing.

ACKNOWLEDGMENTS

We thank Dipankar Manna, Keith Champion, and Zhenhua Pang for critical comments on the manuscript. This work was supported by National Institutes of Health Grant GM33143-15.

REFERENCES

1. Pettijohn, D. E. (1996) in *Escherichia coli and Salmonella*, ed. Neidhardt, F. C. (Am. Soc. Microbiol., Washington, D.C.), Vol. 1, pp. 158-166.

2. Higgins, N. P. (1999) in *Organization of the Prokaryotic Genome*, ed. Charlebois, R. L. (Am. Soc. Microbiol., Washington, D.C.), Vol. 1, pp. 189-202.

3. Stonington, G. O. & Pettijohn, D. (1971) *Proc. Natl. Acad. Sci. USA* **68,** 6-9.

4. Worcel, A. & Burgi, E. (1972) *J. Mol. Biol.* **71,** 127-147.

5. Sinden, R. R. & Pettijohn, D. E. (1981) *Proc. Natl. Acad. Sci. USA* **78,** 224-228.

6. Higgins, N. P., Yang, X., Fu, Q. & Roth, J. R. (1996) *J. Bacteriol.* **178,** 2825-2835.

7. Krasnow, M. A. & Cozzarelli, N. R. (1983) *Cell* **32,** 1313-1324.

8. Boocock, M. R., Brown, J. S. & Sherratt, D. J. (1986) *Biochem. Soc. Trans.* **14,** 214-216.

9. Scheirer, K. & Higgins, N. P. (2001) *Biochimie* **83,** 155-159.

10. Lilley, D. M. J. (1992) *Methods Enzymology* **212**, 133-139.

11. Pruss, G. (1985) *J. Mol. Biol.* **185,** 51-63.

12. Pruss, G. & Drlica, K. (1985) *J. Bacteriol.* **164,** 947-949.

13. Margolin, P., Zumstein, L., Sternglanz, R. & Wang, J. C. (1985) *Proc. Natl. Acad. Sci. USA* **82,** 5437-5441.

14. Lodge, J. K., Kazic, T. & Berg, D. E. (1989) *J. Bacteriol.* **171,** 2181-2187.

15. Lynch, A. S. & Wang, J. C. (1993) *J. Bacteriol.* **175,** 1645-1655.

16. Bochner, B. R., Huang, G.-C., Schieven, G. L. & Ames, B. N. (1980) *J. Bacteriol.* **143,** 926-933.

17. Bliska, J. B., Benjamin, H. W. & Cozzarelli, N. R. (1991) *J. Biol. Chem.* **266,** 2041-2047.

18. Datsenko, K. A. & Wanner, B. L. (2000) *Proc. Natl. Acad. Sci. USA* **97**, 6640-6645.

19. Staczek, P. & Higgins, N. P. (1998) *Mol. Microbiol.* **29,** 1435-1448.

20. Miller, J. H. (1972) *Experiments in Molecular Genetics* (Cold Spring Harbor Lab. Press, Plainview, NY).

21. Pruss, G. & Drlica, K. (1986) *Proc. Natl. Acad. Sci. USA* **83,** 8952-8956.

22. Drolet, M., Broccoli, S., Rallu, F., Hraiky, C., Fortin, C., Masse, E. & Baaklini, I. (2003) *Front. Biosci.* **8,** D210-D221.

23. Figueroa, N. & Bossi, L. (1988) *Proc. Natl. Acad. Sci. USA* **85,** 9416-9420.

24. Pruss, G. J. & Drlica, K. (1989) *Cell* **56,** 521-523.

25. Norris, V. (1995) *Mol. Microbiol.* **16,** 1051-1057.

26. Woldringh, C. L., Jensen, P. R. & Westerhoff, H. V. (1995) *FEMS Microbiol. Lett.* **131,** 235-242.

27. Berens, C., Pfleiderer, K., Helbl, V. & Hillen, W. (1995) *Mol. Microbiol.* **18,** 437-448.

28. Hinrichs, W., Kisker, C., Duvel, M., Muller, A., Tovar, K., Hillen, W. & Saenger, W. (1994) *Science* **264,** 418-420.

29. Manna, D. & Higgins, N. P. (1999) *Mol. Microbiol.* **32,** 595-606.

30. Keiler, K. C., Waller, P. R. H. & Sauer, R. T. (1996) *Science* **271,** 990-993.

31. Cook, D. N., Ma, D., Pon, N. G. & Hearst, J. E. (1992) *Proc. Natl. Acad. Sci. USA* **89,** 10603-10607.

32. Gamper, H. B. & Hearst, J. E. (1982) *Cell* **29,** 81-90.

33. Liu, L. F. & Wang, J. C. (1987) *Proc. Natl. Acad. Sci. USA* **84,** 7024-7027.

34. Wu, H.-Y., Shyy, S., Wang, J. C. & Liu, L. F. (1988) *Cell* **53,** 433-440.

35. Higgins, N. P. & Vologodskii, A., in *Plasmid Biology*, ed. Funnell, B. (Am. Soc. Microbiol., Washington, D.C.), in press.

36. French, S. (1992) *Science* **258,** 1362-1365.

37. Wei, Y., Lee, J.-M., Richmond, C., Blattner, F. R., Rafalski, J. A. & LaRossa, R. A. (2001) *J. Bacteriol.* **183,** 545-556.

38. Bernstein, J. A., Khodursky, A. B., Lin, P.-H., Lin-Chao, S. L. & Cohen, S. N. (2002) *Proc. Natl. Acad. Sci. USA* **99,** 9697-9702.

39. Elowitz, M. B., Levine, A. J., Siggia, E. D. & Swain, P. S. (2002) *Science* **297,** 1183-1186.

40. Ozbudak, E. M., Thattai, M., Kurtser, I., Grossman, A. D. & van Oudenaarden, A. (2002) *Nature Genetics* **31,** 69-73.

41. Siegele, D. A. & Hu, J. C. (1997) *Proc. Natl. Acad. Sci. USA* **94,** 8168-8172.

42. Domingo, E., Martinez-Salas, E., Sobrino, F., de la Torre, J. C., Portela, A., Ortin, J., Lopez-Galindez, C., Perez-Brefia, P., Villanueva, N., Najera, R., *et al.* J. (1985) *Gene* **40,** 1-8.

43. Segall, A. M. & Roth, J. R. (1994) *Genetics* **136,** 27-39.

44. Miesel, L., Segall, A. & Roth, J. R. (1994) *Genetics* **137,** 919-932.

45. Takeuchi, Y., Horiuchi, T. & Kobayashi, T. (2003) *Genes Dev.* **17,** 1497-1506.

46. Huertas, P. & Aguilera, A. (2003) *Mol. Cell* **12,** 711-721.

47. Yu, D., Sawitzke, J. A., Ellis, H. & Court, D. L. (2003) *Proc. Natl. Acad. Sci. USA* **100,** 7099–7104.

SUPPORTING MATERIAL AND METHODS

Plasmids

Plasmids pTrcHis-Topo-*tet*, pTrcHis-Topo-*lacZ*, and pTrcHis-Topo-*kan* were derived from pTrcHis-Topo (Invitrogen). PTrcHis-Topo has two strong *rrnB* transcription terminators T*1* and T2. The *tet*, *lacZ*, and *kan* genes were cloned into this vector, respectively, according to the manual (catalog nos. K4400-01). Positive clones were checked by sequence analysis.

Construction of Strains

P_R*tetR*-P_A*tetA* cassette was amplified from Tn*10* with primers Tn*10*FtetF1 and Tn*10*R*tetR* (Table 2). The P_R*tetR*-P_A*tetA* PCR product was used to transform strain NH3467, which harbors Tn*10d*Gn and pKD20 plasmid. After recombination, the Gn element in Tn*10d*Gn was replaced by P_R*tetR*-P_A*tetA* gene to yield the strain NH3468 and a new Tn*10d*(*Gn*)<>(*tet*) module. NH3468 chromosomal DNA was used as a template to amplify a new module. P_R*tetR*-P_A*tetA-res* substituted for 17 bp of *yliI* and created a *yliI* mutation, (*yliI* Δ 17bp)<>(P_R*tetR*-P_A*tetA-res*) (hereafter referred to as (*yliI*)<>(P_R*tetR*-P_A*tetA-res*). The PCR primers were *yliI* FtetF1 and *yliI* RTn*10*R-2. Two different insertions, (*yliI*)<>(P_R*tetR435*-P_A*tetA-res*) and (*yliI*)<>(P_R*tetR*-P_A*tetA-res*), were obtained from two independent experiments. The kanamycin-resistant cassette *kan* was amplified from Mu*d*Jr2 with primers *yliI* FknF-2 and Tn10RknR-2. The *kan* replaced *tet* gene in strain NH3472 [(*yliI*)<>(P_R*tetR435*-P_A*tetA-res*)]. P_A*tetA* was amplified from NH3468 with primers *yliI* FP_R and Tn10RtetR.

Table 2. Oligonucleotide primers used for strain constructions

Name of primers	Primer sequence*
Tn10FTetF1	GAGGTCTTCCGATCTCCTGAAGCCAGGGCAGATCCGTGC/TATGATTCCCTTTGTCAACAGC
Tn10RtetR	ACGGCCACAGTAACCAACAAATCAATATCGCTGTATGGC/GCTATGCATCAAGCTTGGTAC
ylil FKnF-2	CCCGGAAAAAGGCAAAAATTATGGCTGGCCGCTGGCCAC/TGTAGGCTGGAGCTGCTTCG
Tn10RKnR-2	ACGGCCACAGTAACCAACAAATCAATATCGCTGTATGGC/GTCGCTTGGTCGGTCATTTCG
ylil FTetF1	CCCGGAAAAAGGCAAAAATTATGGCTGGCCGCTGGCCAC/TATGATTCCCTTTGTCAACAGCA
ylil RTn10R-2	CGACAATTTCACCTTTGGCTTCCGGCACTTTCAGACCAC/TTAAGGTGGTCACACATCTTGTC
ylil Fp_R	CCCGGAAAAAGGCAAAAATTATGGCTGGCCGCTGGCCAC/CATTAATTCCTAATTTTTGTTGACACTC
p_ALacF	TTTTACCACTCCCTATCAGTGATAGAGAAAAGTGAAATG/ACCATGATTACGGATTCACTG
Tn10RLacR	ACGGCCACAGTAACCAACAAATCAATATCGCTGTATGGC/TTATTTTTGACACCAGACCAACTG
Tn10RterminatorR	ACGGCCACAGTAACCAACAAATCAATATCGCTGTATGGC/CTCAGGAGAGCGTTCACCGA
p_AKnL-2	TTTTACCACTCCCTATCAGTGATAGAGAAAAGTGAAATG/ATTGAACAAGATGGATTGCACGC
$KnRP_R$	CAGAAGAACTCGTCAAGAAGGCGATAGAAGGCGATGCGC/CATTAATTCCTAATTTTTGTTGACACTC
RepressorRTetR	AGCTTATGCCGTTTAGGTATGTTACATGTGTGATTATGTG/GCTATGCATCAAGCTTGGTA
KnRTetR	CAGAAGAACTCGTCAAGAAGGCGATAGAAGGCGATGCGC/GCTATGCATCAAGCTTGGTAC
$RepressorRP_R$	AGCTTATGCCGTTTAGGTATGTTACATGTGTGATTATGTG/CATTAATTCCTAATTTTTGTTGACACT C

The primers contain two parts, a 5′ end that is homologous (35-45 bases long) to flanks of the target DNA, and a 3′ end of 20 bases that primes the cassette DNA for replication. The "/" in the primers indicates the junction between the target homology on the 5′ end and inserted cassette primers on the 3′ end of each oligo. Bases complementary to the template are underlined.

The *tetA* sequence in the constructs above was replaced with the *lacZ* gene amplified from *E. coli* chromosomal DNA with primers $P_A$lacF and Tn*10*RlacR. P_A*lacZ-rrnB* was amplified from plasmid pTrcHis-Topo-*lacZ* with primers $P_A$lacF and Tn*10*RterminatorR. P_A*kan-rrnB* was amplified from pTrcHis-Topo-*kan* with primers $P_A$knL-2 and Tn*10*FterminatorR. The *tetA* gene in the P_R*tetR-*P_A*tetA-res* element was replaced by *lacZ-rrnB* or *kan-rrnB* to form (*yliI*)<>(P_R*tetR-*P_A*lacZ-rrnB-res*) and (*yliI*)<>(P_R*tetR-*P_A*kan-rrnB-res*), respectively. The *tetA* gene in the P_A*tetA-res* was also replaced by *lacZ-rrnB* or *kan-rrnB* to make (*yliI*)<>(P_A*lacZ-rrnB-res*) and (*yliI*)<>(P_A*kan-rrnB-res*), respectively. Both *lacZ* and *kan* were driven by *tetA* promoter P_A. The *kan* gene in the *cobT714*::Mu*d*Jr2 was replaced with the *tetA* module amplified from NH3468. One replacement was made by exchanging *kan* with *tetA* by using primers KnRP$_R$ and RepressorRTetR [*cobT714*::Mu*d*Jr2(*kan-c*)<>(*tetA*)]. Another replacement was made by using primer RepressorRP$_R$ and KnRTetR [*cobT714*::Mu*d*Jr2(*kn-c*)<>($tetA_{inv}$)]. Strains that carry *res-res* sites combination and pJBRES*cI* were made by transduction crosses as described (1).

1. Higgins, N. P., Yang, X., Fu, Q. & Roth, J. R. (1996) *J. Bacteriol.* **178**, 2825-2835.

Fig. 6. The gene sequence and protein sequence of *tetR* gene in both mutant *tetR* and WT *tetR*. The first line is the number of amino acids. The second line is the WT tetR protein sequence. The third line is the mutant protein sequence. The fourth line is the WT gene sequence. The highlighted nucleotide "A" was missing in the mutant *tetR*. It happened at position 435 from the transcription start site. It leads to amino acid H-139 changed into L. At the position L-142, mutant *tetR* encounters a premature stop codon leaving the TetR-435 repressor 66 amino acids short of the WT TetR.

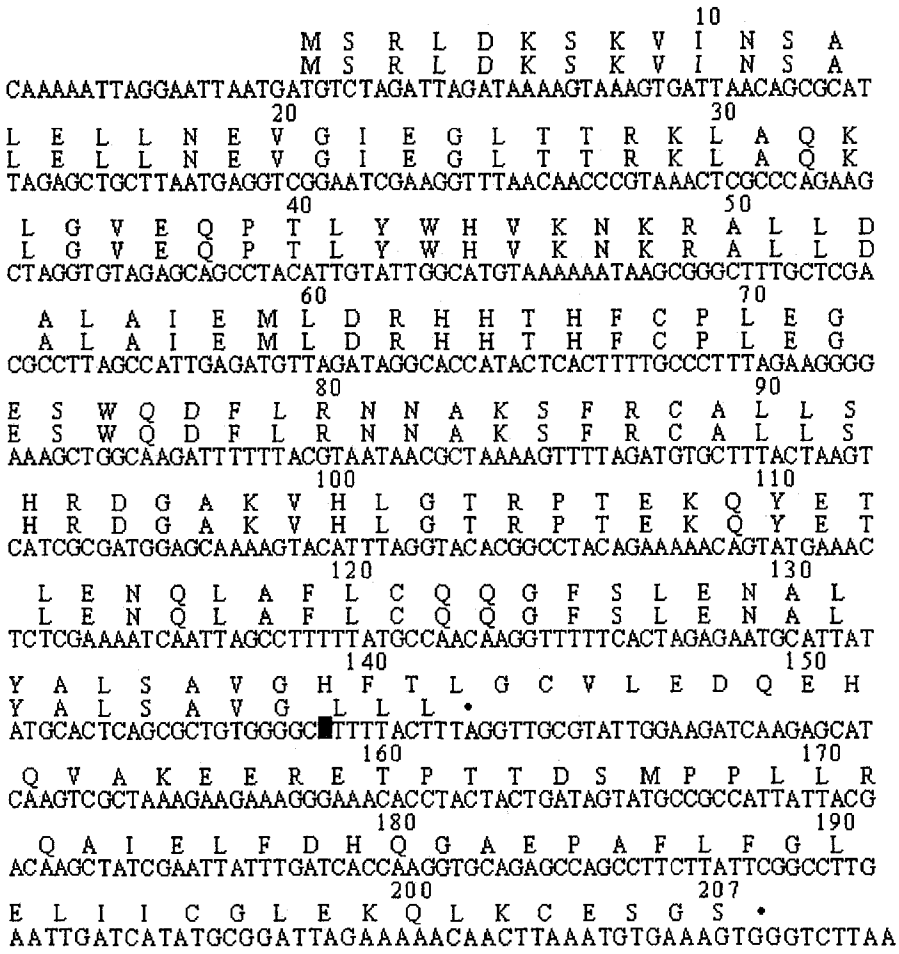

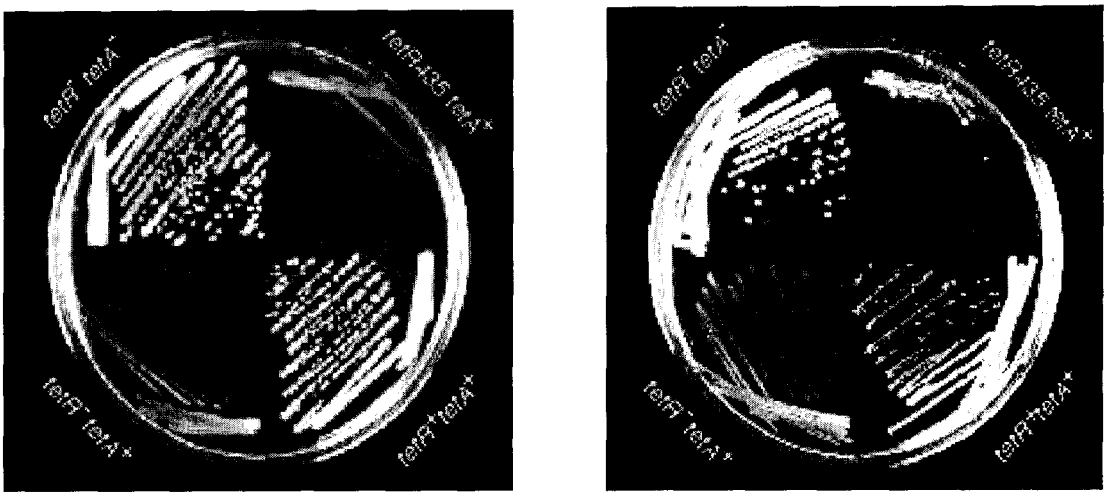

Bochner plate without CLT Bochner plate

Fig. 7. Cell growth at 42°C on the modified Bochner plates without CLT and standard Bochner plates. On the Bochner plate without CLT, the WT *tetR* and *tetA* (NH3471: $tetR^{+}tetA^{+}$) grew as well as WT LT2 (NH3358: $tetR^{-}tetA^{-}$). Neither *tetR435* (NH3470) nor *tetR* deletion (NH3475) grew on the Bochner plate without CLT. On standard Bochner plates, all strains having a functional *tetA* gene grew very poorly.

Table 3. β-galactosidase activity (Miller units) of *tetA* promoter fusions of different *S. typhimurium* strains

Strains	Gene arrangement	Activity (grown in LB), mean ± SD	Activity (in LB + 5 μg/ml CLT)*, mean ± SD
NH2002	———	<1	<1
NH3477	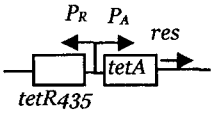	959 ± 24	928 ± 15
NH3478	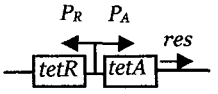	15 ± 1	688 ± 9
NH3479	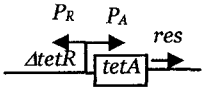	915 ± 2	896 ± 12

Means and standard deviations are derived from at least three independent assays.
*Strains were grown in the LB containing 5 μg/ml chlortetracycline (CLT) and grew to a cell density of 50 Klett units.

Fig. 8. Resolution analysis for two *S. typhimurium* intervals predicted to have different domain behavior based on RNA abundance measured by microarray analysis. (*Upper*) the genetic and physical map of the *atp* operons. This 6-kb cluster is highly conserved between *E. coli* and *Salmonella,* and it includes nine-membrane-associated proteins from *atpI* to *atpC*. (*Lower*) the genetic and physical map of an interval containing the highly transcribed gene *nmpC*. The *nmpC* gene is transcribed as a single ORF operon and has one of the highest transcription rates of all protein-encoding *S. typhimurium* genes. The microarray analysis RNA/DNA ratio is shown above each gene, and arrows are shown below each gene that indicate the direction and start of transcripts. Lines with asterisks indicate the positions at which *res*-containing modules were inserted into the *S. typhimurium* chromosome. The impact factor is the resolution efficiency of an 8- or 15-kb interval in the *his-cob* region divided by the observed resolution efficiency.

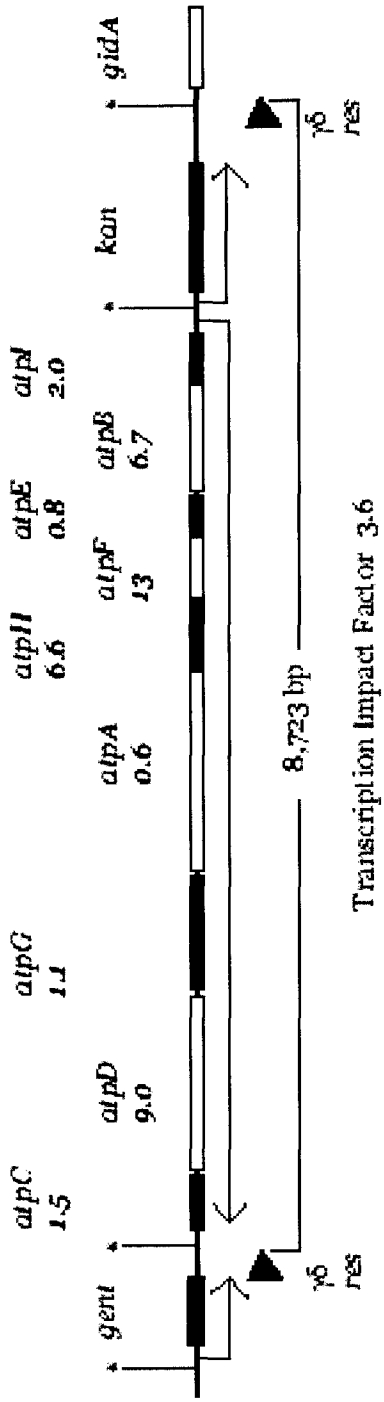

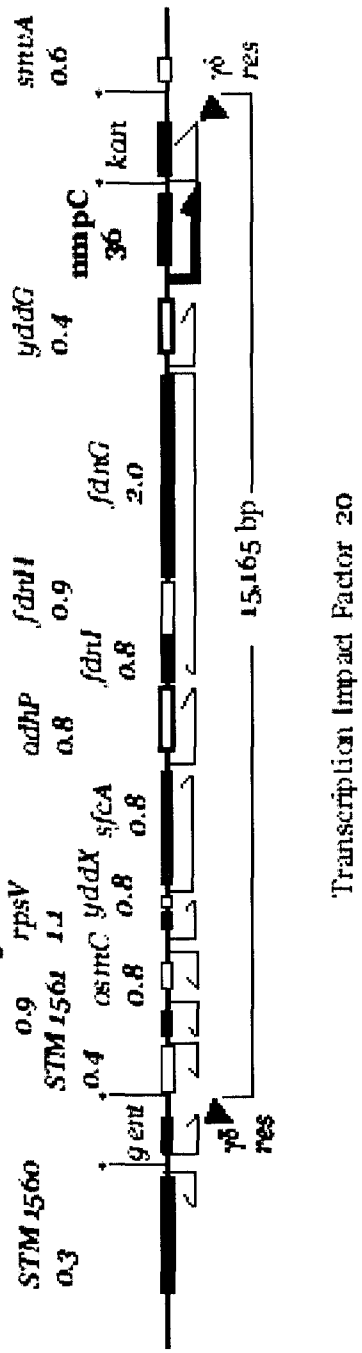

Table 4. Predicted impact of highly transcribed *Escherichia coli* genes on chromosome domains based on microarray-measured abundance of encoded cellular RNAs in cells grown in LB

Cluster name	Predicted impact on resolution	Region size, bp	Location, kb
rrsH, rrlH, rrfH	>20	5104	224
rrfG, rrlG, rrsG	>20	5089	2724
rrfD, rrlD, rrsD	>20	5094	3421
rrsC, rrlC, rrfC	>20	5012	3939
rrsA, rrlA, rrfA	>20	5096	4033
rrsB, rrlB, rrfB	>20	5097	4164
rrsE, rrlE, rrfE	>20	5013	4206
TnaA: tnaA, tnaL	8	1711	3886
fliC: fliC, fliD, fliA, fliZ	6	4806	2000
rpsH: rpsD, rplC,rpoA, rplE, rpsS,rplW, rpsN, rpsE,rpsK, rplB, rplD, rpmD, rplF, rplX, rpsJ, rpsM, rplN, rplV, rpmC, rplO, prlA, rpsC, rplQ, rplR, rplP	5	13655	3444
RpsA	5	1674	961
tufA: fusA	4	3370	3468
tufB	4	1185	4174
acpP: fabG	3	2182	1151
ompC	3	1104	2310
TrmD: rimD, rplS	3	1745	2743
rplU	2	312	3331
flgD: flgB, flgE, flgL, flgC, flgM	2	11152	1131
ompT	2	954	584
hns	2	414	1292
rplJ: rplK, rplA, rplL	2	2479	4178
ompF	2	1089	985
rplY	2	285	2281
mdh	2	939	3381
rpsB: tsf	2	1835	190
ompA	2	1041	1018
rplM: rpsl	2	837	3376
icdA	2	1251	1194
slyB	2	468	1718
priB: rpsR	2	548	4423
glpK: glpF	2	2377	4113
infC: rpml, rplT	2	1246	1798
rpsO	2	270	3309
wbbK: wbbJ	2	1694	2101
ymfK: b1146	2	966	1201
glpQ	2	1077	2348
rpmB: rpmG	2	425	3809
gatY: gatA, gatB	2	2929	2174
tig	2	1299	454
atpH: atpF	2	1019	3917

Table 4. Predicted impact of highly transcribed *Escherichia coli* genes on chromosome domains based on microarray-measured abundance of encoded cellular RNAs in cells grown in LB (Continued)

rpsU	2	216	3208
tatA	2	312	4019
nmpC	2	1128	575
ahpC	2	564	638
groS	2	294	4368
cyoA	2	948	450
b0725	2	261	758
infA	2	219	925
gapA	2	996	1861
hlpA	2	486	200
rpmE	2	213	4125
rpsT	2	264	21
ycgY	2	441	1244
yjjY	2	141	4638
lit	2	894	1198

Genes with predicted impact factors >2 for resolution of a 12-kb interval. Note that one gene cluster (*rpsH*) is >12 kb. Microarray RNA data are from Bernstein, J. A., Khodursky, A. B., Lin, P.-H., Lin-Chao, S. L. & Cohen, S. N. (2002) *Proc. Natl. Acad. Sci. USA* **99**, 9697-9702 .

THE MODEL OF TRANSCRIPTION-INDUCED BARRIERS TO SUPERCOIL DIFFUSION IN THE *SALMONELLA TYPHIMURIUM* CHROMOSOME

by

SHUANG DENG AND N. PATRICK HIGGINS

In preparation for *Molecular Microbiology*

Format adapted for dissertation

ABSTRACT

Previous work has shown that transcription from the *tetA* promoter leads to a new barrier to supercoil diffusion as measured by γδ resolution. The magnitude of inhibition on γδ *res*olution was dependent on transcription level. In this paper, we further characterize the *tetA* transcription-induced barrier. Placing the *tetA* gene between two *res* sites (namely, within the *res-res* interval) resulted in low-resolution efficiency no matter how far the *tetA* gene was from either of the *res* sites. However, when *tetA* was located outside the *res-res* interval, the inhibition was felt as long as the *tetA* gene was 1 kb from the interval. We also tested three chromosomal intervals that contain genes of different transcription levels and confirmed that, irrespective of the nature of the gene or its location on the chromosome, high transcription causes a chromosomal barrier to supercoil diffusion. Last, we proposed a model in which highly transcribed genes are organized into domains that acts as barriers to supercoil diffusion.

INTRODUCTION

Bacterial chromosomes are segregated into separate supercoiled domains (1, 2). A domain structure is apparent in electron micrographs of the *Escherichia coli* nucleoid (3, 4). However, the nature of specific domain boundaries has been elusive.

Many major cellular DNA transactions, including transcription, replication, and recombination, require negative supercoil of DNA for optimal function (5-8). It is well known that the transcription of many genes is influenced when the DNA supercoil is perturbed (9-11). Transcription is influenced by supercoil, but also affects the supercoil. Studies on small circular plasmids demonstrated that transcription could generate super-

coils in the DNA template (12-14). The major mechanism is thought to be the twin-supercoiled-domains described by Liu and Wang (15). According to this model, hindered rotation of an elongating transcription complex leads to the formation of positive supercoils ahead of a translocating RNA polymerase and to the formation of negative supercoils behind it. In the absence of DNA topoisomerase I, plasmids showed hypernegative supercoil. Two processes could hinder the rotation of a transcription complex around its DNA template. One process involves cotranscriptionally translated integral membrane proteins that restrict DNA rotation by tethering the transcription machinery to the membrane, such as transcription of the pBR322 *tetA* gene (16). The other process can be DNA-binding proteins like bacteriophage λ O replication initiator or the *E. coli* lactose or galactose repressor that loops DNA between successive binding sites (17). DNA-binding proteins could function as barriers to the rotational diffusion of nascent supercoils that arise during transcription and stimulate transcription-coupled DNA supercoil. Inducing transcription from a strong promoter increases negative supercoil in derivatives of pBR322 even when DNA topoisomerase I activities are present (18). Transcription from a strong promoter leads to greater negative supercoil than transcription from a weak one. For a strong promoter, translation is not necessary for generating hypersupercoil of plasmid DNA (18, 19).

The notion that transcription can generate supercoils in the DNA template largely stems from work with small circular plasmids. Little is known about the impact of transcription on the topology of the large bacterial chromosome because of the lack of tools to investigate long-range chromosome behavior *in vivo*. Transcription studies (20) and studies of nucleoid structure showed that nucleoid DNA has a dynamic organization. In

1996, a site-specific recombination assay based on the resolvase of transposon γδ was developed to investigate dynamic chromosomal structure *in vivo* (21). This assay can probe domain barriers that deter supercoil diffusion by measuring resolution efficiency. By using this assay, Scheirer and coworkers found that the strong Mu early promoter induces the appearance of a domain barrier to γδ resolution in the *his-cob* region of the *Salmonella typhimurium* chromosome (22). Later Deng *et al.* discovered that transcription from the *tetA* promoter in the absence of TetR repressor caused a new barrier to resolution in the chromosome (23). Membrane attachment was not involved in the generation of a transcription-induced barrier in the chromosome. Only the transcription level from the *tetA* promoter was important. Also, the magnitude of inhibition of resolution depended on the level of transcription. A kinetic study showed that this barrier persists for 20 min. However, the mechanism of the transcription-induced barrier in the chromosome remains unknown.

In this report, we show that *tetA* inserted within a *res-res* interval always causes a new barrier to supercoil diffusion but that *tetA* positioned outside the *res-res* interval affected resolution only when the interval was within 1 kb. We also demonstrate that genes of different transcription strength have different impacts on resolution efficiency in the *S. typhimurium* chromosome. Impact factor was proportional to transcription level. Last, we propose a domain model of transcription-induced barrier to supercoil diffusion.

MATERIALS AND METHODS

Bacterial Strains and Plasmids

Genotypes of the bacterial strains used in this work (all derivatives of *S. typhimurium* LT2) are listed in Table 1. Details of construction of those strains are described in *Construction of Strains*. Plasmid pJBRESc*I* is a pACYC184-derived construct carrying the *tnpR* (Res resolvase) gene of transposon γδ cloned under the control of a λP_L promoter, which is regulated by a nearby copy of λ *c*Its repressor gene (24). pKD20 is a derivative of pINT-ts that encodes Red recombinase under the control of the P_{araB} promoter (25).

Table 1. Strains used

Strain	Genotype	Plasmid
NH3466	LT2	pKD20
NH3500	(*ylil*)<>(P_R*tetR*-P_A*tetA-res*) (*madA*)<>(*kan-res*)	pJBRESc*I*
NH3501	(*atpC*)<>(*gen-res*) (*atpI*)<>(*kan-res*)	pJBRESc*I*
NH3502	(*STM1560*)<>(*gen-res*) (*STM1573*)<>(*kan-res*)	pJBRESc*I*
NH3503	(*STM0925*)<>(*gen-res*) *zbj8905*::MudJr2	pJBRESc*I*
NH3504	(*STM0925*)<>(*gen-res*) *zbj8905*::MudJr2(*kan*)<>(P_A*tetA-rrnB*)	pJBRESc*I*
NH3505	(*STM0925*)<>(*gen-res*) *STM0929*(P_A*tetA-rrnB*)*STM0930* *zbj8905*::MudJr2	pJBRESc*I*
NH3506	(*STM0925*)<>(*gen-res*) STM0927(P_A*tetA-rrnB*)*STM0928* *zbj8905*::MudJr2	pJBRESc*I*
NH3507	(*STM0925*)<>(P_A*tetA-rrnB-res*) *zbj8905*::MudJr2	pJBRESc*I*
NH3508	(*STM0925*)<>(PAtetA-rrnB-200bp-res) zbj8905::MudJr2	pJBRESc*I*
NH3509	(*STM0925*)<>(PAtetA-rrnB-500bp-res) zbj8905::MudJr2	pJBRESc*I*
NH3510	(*STM0925*)<>(P_A*tetA-rrnB-1kb-res*) *zbj8905*::MudJr2	pJBRESc*I*
NH3511	*STM0923*(P_A*tetA-rrnB-res*)*STM0924 zbj8905*::MudJr2	pJBRESc*I*
NH3512	(*STM0925*)<>(*gen-res*) *zbj8905*::MudJr2 *seqA-*	pJBRESc*I*
NH3513	(*STM0925*)<>(*gen-res*) *zbj8905*::MudJr2(*kan*)<>P_A*tetA-rrnB seqA-*	pJBRESc*I*

All strains were derived from *S. typhimurium* LT2 and were constructed during this work. <> indicates a replacement generated by lambda Red recombineering (25, 26).

PCRs

PCRs were done with the recombinant Klen*Tag* from Sigma and the thremo-cycling conditions, time, and buffers recommended by Sigma. Oligonucleotides were purchased from IDT (Coralville, IA) and are described in Table 2. Primer sequences are designed as described earlier (25, 26).

Construction of Strains

All of the insertion mutagenesis of the *S. typhimurium* chromosome was made by using the lambda Red recombination system that is carried on plasmid pKD20 (25). The PCR products were used for homologous recombination. Recombinants that had inserted cassette were selected as antibiotic-resistant colonies and verified as such by PCR (25, 26).

Mutation (*yliI*)<>(P_R*tetR*-P_A*tetA*-*res*) was from a previous study (23). The *gen-res* cassette was amplified from Tn*10d*Gn. The *gen-res* element amplified with primers atpCFGnF/atpCRGnR-2 substituted 26 bp of *atpC* and created an *atpC* mutation, (*atpC*Δ26bp)<>(*gen-res*) [hereafter referred to as (*atpC*)<>(*gen-res*)]. The *gen-res* amplified with primers STM1560FGnG/STM1560RGnR-2 inserted in ORF STM1560 and made a mutation, (*STM1560*)<>(*gen-res*). The *gen-res* element amplified with primers STM0925FGnF/STM0925RGnR-2 substituted 339 bp of *atpC* and created a *STM0925* mutation, (*STM0925*Δ339bp)<>(*gen-res*) [hereafter referred to as (*STM0925*)<>(gen-*res*)]. The *kan-res* was amplified from NH3471 chromosome DNA. *kan-res* element amplified with primers madAFKnF-2/madARTn10R-2 substituted 12 bp of *atpC* and created a *madA* mutation, (*madA*Δ12bp)<>(*kan-res*) [hereafter referred to as (*madA*)<>(*kan-res*)].

Table 2. oligonucleotide primers used for strain constructions

STM0925GnF	CACCTGCAATGCGTATCTGACGGACCAGCGTAAAGCGTGGACCCAGTTGACATAAGCCTG
STM0925GnR-2	CCACCGTCTGCGTTTCCAGTAATTCGGTGGTGATGGCCCCGGAATTAGCTTGCATGCCTG
STM0927FTetAP1	GATACCTCAAATCCTGATTGGCCGGAACAACCAGTCTGACATTAATTCCTAATTTTTGTTGACACTC
STM0928TermR	GCTGCTATATAACATATAGCAGCAGTCTCTACTACATAGCCTCAGGAGAGCGTTCACCGAC
$KnRP_R$	CAGAAGAACTCGTCAAGAAGGCGATAGAAGGCGATGCGC/CATTAATTCCTAATTTTTGTTGACACTC
RepressorRtermR	AGCTTATGCCGTTTAGGTATGTTACATGTGTGATTATGTG/ CTCAGGAGAGCG TTCACCGAC
STM0929FtetAP1	GCAATACTATTGATTGTTGTAAGGTGATTGACCGATATCATTCGGTGA/CATTAATTCCTAATTTTTGTTGACACTC
STM0930RTermR	CCAGTGCGGATAACCCTATATTTGACAACATTCACATACAATAGCTC CTCAGGAGAGCG TTCACCGAC
STM0925FTetAP1	CACCTGCAATGCGTATCTGACGGACCAGCGTAAAGCGTG/ CATTAATTC CTAATTTTTGTTGACACTC
Tn10RTermR	ACGGCCACAGTAACCAACAAATCAATATCGCTGTATGGC/CTCAGGAGAGCGTTCACCGAC
GnR_{200}TermR	CACCGCTACCCTCATGATGTCTAACGGCCAAGGTAA GCG/CTCAGGAGAGCG TTCACCGAC
GnR_{500}TermR	AAGCCGGAGCGCTTTGCGGCCGCGGCGTTGTGACAATTT/ CTC AGG AGA GCG TTC ACC GAC
GnR_{1kb}TermR	GCCTACATGTGCGAATGATGCCCATACTTGAGCCACCTA/CTCAGGAGAGCG TTCACCGAC
STM0923FTetAP1	GGTGATCATCGGTCGATAAAACGAGCCGCCGGTCATGGA/ CATTAATTCCTA ATTTTTGTTGACACTC
STM0924RtermR	CGCCTGTGGCGTTATAAAATAAAATTCACTCTGTGAGGCACTGTT/CTCAGGAGAGCGTTCACCGAC
MadAFknF-2	GCCTGCCGAGCTTGTGGTTCATGAGAACCAGTATCAACCTGTAGGCTGGAGCTGCTTCG
MadARTn10R-2	CAGATAATACTCAGCCAACTGCTCGTCATAGCGCGCCAGCAGTTAAGGTGGTCACACATCTTGTC
AtpCFGnF	CGCCTTCAGCCGCTTGTTTTTGTCGTTGCTAGTTTATCGACCCAGTTGACATAAGCCTG
AtpCRGnR-2	CCGGCTTGAAAGCATAAAACCAGTCTGATTGCGGACTGGCGGAATTAGCTTGCATGCCTG
AtpIKnF-2	TCATGCTTACGCAATTCATTTACGTGTCAATTCATGCCTAGCAGGTAGCTTGCAGTGGGC
GlmURGnR-2	CTGGTATATTTTGCGGATTTTTATGTCGCGTAATTAAGTCGGAATTAGCTTGCATGCCTG
STM1560FGnF	CACTTAACAGGCATTCTTTTTCGTATCTGCGTGTAAAAC/ ACCCAGTTG ACATAAGCCTG
STM1560RGnR-2	CTTCGGTACATCTGAGCAATCCCGACAATAATTCCACG/CGGAATTAGC TTGCATGCCTG
STM1573FKnF-2	TTTGTTGTGTCTGAATACAAAGCCAGTCCTTTCAGGGC/AGCAGGTAGCTT GCAGTGGGC
STM1573RGnR-2	ACTCCTTATGACCGAGTCTACATCAAGAGAAAAAGCCA/CGGAATTAGCTTGCATGCCTG

The primers contain two parts, a 5' end that is homologous (35~45 bases long) to flanks of the target DNA and a 3' end of 20 bases that primes the cassette DNA for replication. The "/" in the primer sequence indicates the junction between the target homology on the 5' end and inserted cassette primers on the 3' end of each oligo. Bases complementary to the template are underlined.

The *kan-res* element amplified with primers atpIKnF-2/glmUGnR-2 created an insertion in *atpI* and duplication from *glmU* to *atpI*. This mutation is described as d(*atpI-glimU*) <> (*kan-res*). *kan-res* amplified with primers STM1573FKnF-2/STM1573RGnR-2 inserted in ORF STM1573 made a mutation, (*STM1573*)<>(*kan-res*). The module P_A*tetA-rrnB* was amplified from NH3480 [(*yliI*)<>(P_A*tetA-rrnB-res*)] chromosome DNA and primers KnRP_R/ RepressorRtermR. The *kan* gene in the Mu*d*Jr2 elements was replaced by module P_A*tetA-rrnB* to form *zbj8905*::Mu*d*Jr2 (*kan*)<>P_A*tetA-rrnB*. P_A*tetA-rrnB* module amplified with STM0929F*tetA*P1/STM0930RtermR was inserted in the intergenic region between *STM0929* and *STM0930*. The P_A*tetA-rrnB* module amplified with STM0927F*tetA*P1/STM0928termR was inserted in the intergenic region between STM0927 and STM0928. The *gen* gene in the *gen-res* was replaced by P_A*tetA-rrnB* amplified with primers STM0925F*TetA*P1/ Tn10RtermR to form (*STM0925*)<>(P_A*tetA*-rrnB-*res*). Part of the *gen* gene in the *gen-res* was replaced by P_A*tetA-rrnB* amplified with primers STM0925F*TetA*P1/ GnR_{200}TermR, with 200 bp from the *gen* gene left between the end of *rrnB* and the beginning of *res*. Part of the *gen* gene in the *gen-res* was replaced by P_A*tetA-rrnB* amplified with primers STM0925F*TetA*P1/ GnR_{500}TermR, with a 500 bp sequence from the *gen* gene left between the end of *rrnB* and the beginning of *res*. Part of the *gen* gene in the *gen-res* was replaced by P_A*tetA-rrnB* amplified with primers STM0925F*TetA*P1/ GnR_{1kb}TermR, with 1 kb from the *gen* gene left between the end of *rrnB* and the beginning of *res*. P_A*tetA-rrnB-res* amplified from NH3507 chromosome DNA with primers STM0923F*TetA*P1/STM0924RtermR was inserted between *STM0923* and *STM0924*.

Strains that carry *res-res* sites combination and pJBRES*c*I were made by transduction crosses as described (21) with P22 HT105/1 int-201, a high-efficiency transducing mutant of bacteriophage P22.

γδ Resolution Assay

Stationary-phase culture (overnight) and log-phase culture (50 Klett units) were induced 10 min at 42°C and then immediately diluted 1:10 in LB medium. Culture was incubated overnight at 30°C. On the next day, 100 μl of 10^{-6} dilution was plated on minimal medium containing chloramphenicol and 5-bromo-4-chloro-3-indolyl β-D-galactoside (X-gal). Deletion frequency was scored by one of two methods: loss of color or loss of drug sensitivity. LB and minimal media were prepared as described (21). Antibiotics were added as described (23).

RESULTS

tetA *inserted at various locations within the interval does not affect the resolution efficiency*

In our previous experiments (23), *tetA* was always placed next to the downstream *res* sites. Does the highly transcribed gene have to be next to the *res* site to block supercoil diffusion? To address this question, we constructed several strains (Fig. 1*A*). In NH3503, the *res-res* interval between (*STM0925*<>(*gen-res*) and *zbj8905*::Mu*d*Jr2 is 20 kb. Resolution efficiency for this interval was 37% (Fig. 1*B*, first column). When the *kan* in the Mu*d*Jr2 element was changed to P_A*tetA-rrnB* (NH3504), the resolution efficiency decreased to 3% (Fig. 1*B*, second column). When the P_A*tetA-rrnB* module was inserted at the middle of the interval (NH3505), the resolution efficiency was still as low as 8% (Fig.

Fig. 1. Effect of *tetA* inserted within *res-res* interval on resolution efficiency of the interval. (*A*) Physical map of *tetA* insertion in the 20-kb interval. 1. No *tetA* insertion. 2. *tetA* is next to the downstream *res* site, and the distance between terminator *rrnB* and *res* site is 129bp. 3. *tetA* is located at the one-quarter postion within the interval near the downstream *res* site. 4. *tetA* is at the middle of the *res-res* interval. 5. *tetA* is located at the one-quarter position within the interval near the upstream *res* site. (*B*) Resolution efficiency comparison among constructs with *tetA* inserted at the different locations within the interval.

A

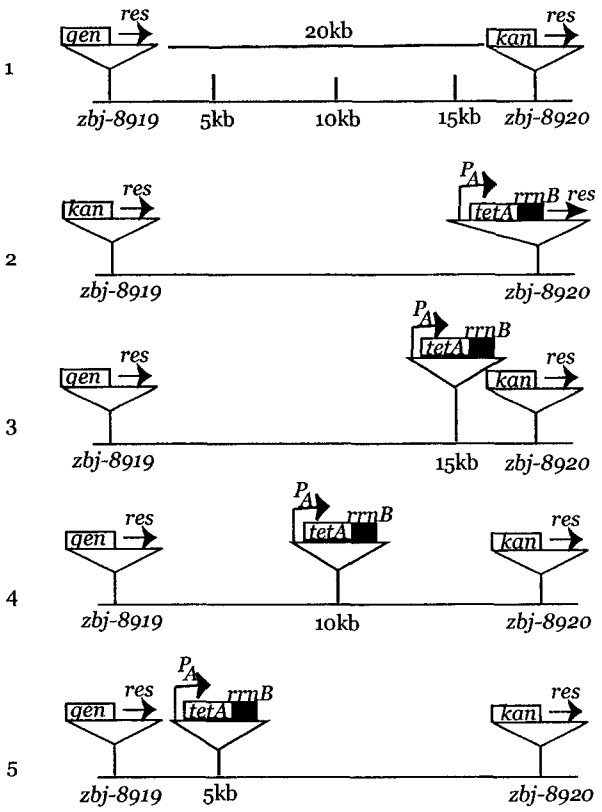

B

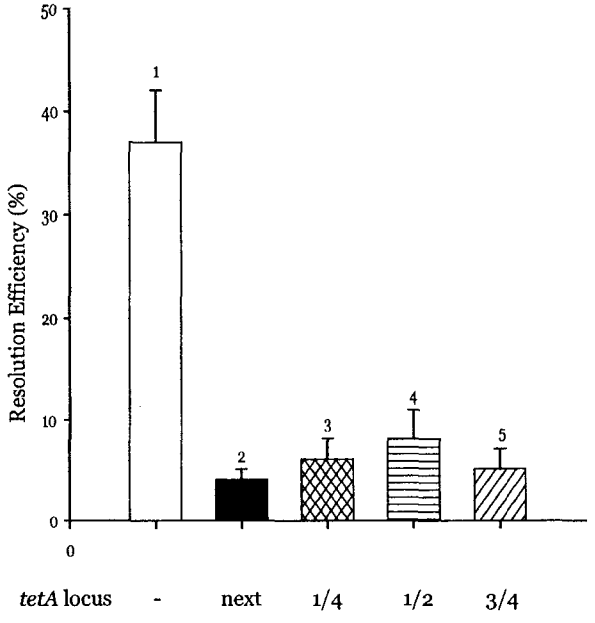

1*B*, third column). When the P_A*tetA-rrnB* module was inserted at the upstream quarter position of the interval (NH3506), the resolution efficiency was 4% (Fig. 1*B*, fourth column). So when the *tetA* gene was moved around within the res-res interval, the resolution did not change much. As long as *tetA* was within the interval, transcription from *tetA* gave a similar effect on the dynamics of the bacterial chromosome.

When tetA *was outside of the interval, the effect on resolution efficiency decreased with the distance between the* tetA *gene and the* res *site*

We already knew that, when *tetA* is located within the *res-res* interval, it always blocks the supercoil diffusion irrespective of its position within the interval. Next we asked how the *tetA* gene affects the supercoil diffusion when it is put outside of the *res-res* interval. The *gen* gene at the locus *STM0925* was replaced by P_A*tetA-rrnB* (NH3507, Fig. 2*A*), in which the end of *tetA-rrnB* was 129 bp away from the *res* site. Resolution efficiency was as low as 3% (Fig. 2*B*, third column). This construct is like the one we always used before (like NH3504), in which *tetA-rrnB* is next to the *res* site (129 bp). The difference between NH3507 and NH3504 is that *tetA* is outside the *res-res* interval in NH3507, whereras *tetA* is inside of the interval in NH3504. However, *tetA* influenced the resolution efficiency to the same extent in both constructs. Next a series of *tetA-rrnB* insertions were made in which the distance between the end of *tetA-rrnB* and the *res* site varies. In NH3508, the end of *tetA-rrnB* is 200 bp away from the *res* site. In NH3509, NH3510, and NH3511, the distance between the end of *tetA-rrnB* and beginning of the *res* site is 500 bp, 1 kb and 2 kb respectively (Fig. 2*A*). The resolution efficiency was 7% in NH3508 (Fig. 2*B*, fourth column). Resolution efficiency went up to 25% when the *tetA*

Fig 2. Effect of *tetA* inserted ouside *res-res* interval on resolution efficiency. (*A*) Physical and genetic map of *tetA* inserted outside of *res-res* interval. The distance between the end of *tetA-rrnB* and the *res* site is, respectively, 0.1 kb (1), 0.2 kb (2), 0.5 kb (3), 1 kb (4), and 2 kb (5). (*B*) Resolution efficiency comparison among the constructs that have *tetA* inserted at different locations outside the *res-res* interval (columns 3-7). Column 1 and 2 are controls. Column 1 is for the construct without *tetA* insertion (column 1 in Fig. 1). Column 2 is for the construct with *tetA* inside the interval (column 2 in Fig. 1).

A

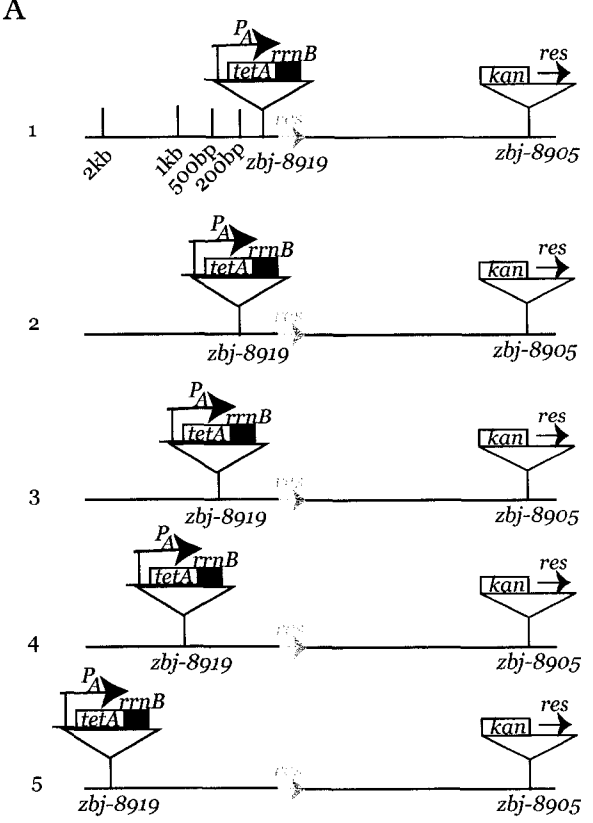

B

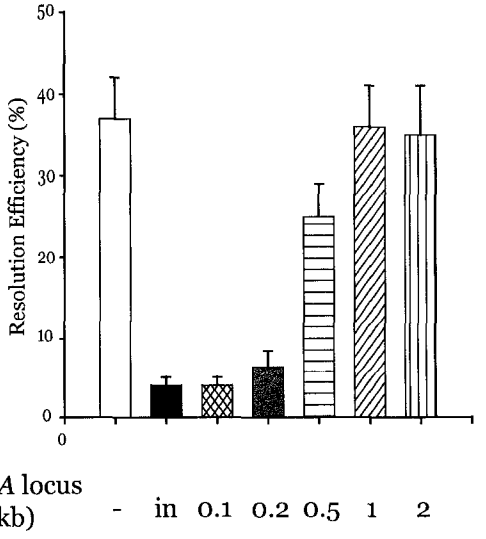

was 500 bp away from the *res* site (NH3509, Fig. 2*B*, fifth column). When *tetA* was 1kb away from the *res* site (NH3510), the resolution efficiency was 36%, which is just as high as the strain without the *tetA* insertion (NH3503, Fig. 2*B*, first column). In strain NH3511, in which *tetA* is 2 kb away from the *res* site, the resolution frequency was 35%, which is almost like the results found for NH3510. So when *tetA* was outside the *res-res* interval, the effect on the resolution efficiency decreased as the distance between *tetA* and *res* site increased. The shorter the distance is, the more pronounced the effect. When the distance reaches 1 kb, there is no more effect on the resolution efficiency. The effect of *tetA* transcription on resolution efficiency can only extend to 1 kb when *tetA* is outside the *res-res* interval. Inhibition was detected within a range of approximately 1 kb from the end of the transcribed gene.

Effect of transcription from promoters of different strength on γδ resolution efficiency

A previous study by members of our laboratory has shown that transcription from a constitutive *tetA* promoter causes a dramatic decrease in γδ site-specific recombination (23). Any coding sequence expressed from the *tetA* promoter, either membrane or non-membrane protein-coding sequence, gave a similar effect. We drew the conclusions that transcription alters chromosome dynamics and that transcription strength determines the effect extent on supercoil diffusion. On the basis of these experiments (23) it was not clear whether this relationship between transcription and resolution is also true for the genes in the bacterial genome.

We further tested this conclusion by using *S. typhimurium* promoters of different transcription strength. Genome-wide transcription analyses using microarray technology

provide us with a basic idea about the transcription level of each gene. We made three intervals. One interval spanned from *ylil* (*STM0861*) to *madA* (*STM0874*). We flanked the interval with P_R*tetA*-P_A*tetA*-*res* and *kan-res*. The length of the interval was 14 kb, and there are 11 genes in this interval. The transcription level of these 11 genes is very low; all of the genes have RNA/DNA ratios of <1. Previous data on the induced *tetA* promoter (23) indicate that this low transcription level has little impact on DNA dynamics and resolution efficiency. The resolution efficiency expected from previous data for a 14 kb interval is 63% (21). We observed 65% ± 7%, (Fig. 3, group 1). So resolution efficiency did not show any difference from the expected one.

The second interval is from *atpC* to *atpI*. We flanked this interval with *gen-res* and *kan-res*. The *atp* operon is essential for cell survival. γδ resolution that deletes the *atpC-atpI* interval produces a nonviable recombinant. Such recombination events cannot be scored by kanamycin sensitivity. We made an *atp* operon duplication so that recombinant cells could survive. We designed the specific primers atpIFKnF-2 and glmURGnR-2. The homology part of atpIFknF-2 matched the end of *atpI*. The homology part of glmURGnR-2 matched the beginning of *glmU*, which is upstream of the atp operon. The PCR product amplified by using primers atpIFKnF-2 and glmURGnR-2 could only integrate into the strain that has *atp* operon duplication. In this way, the *kan*-resistant strain NH3501 has *kan* inserted in *atpI* and the *atp* operon duplication *dup*(*glum-atpI*). The length of the interval consisting of the *atp* operon was 9 kb and there were seven genes in the interval. Among these genes, three showed a high transcription level. Microarray analyses yielded RNA/DNA ratios for *atpD*, *atpF*, and *atpB* of 9, 13, and 6, respectively. We expected a resolution efficiency of 80% for the 9-kb interval. However, resolution in

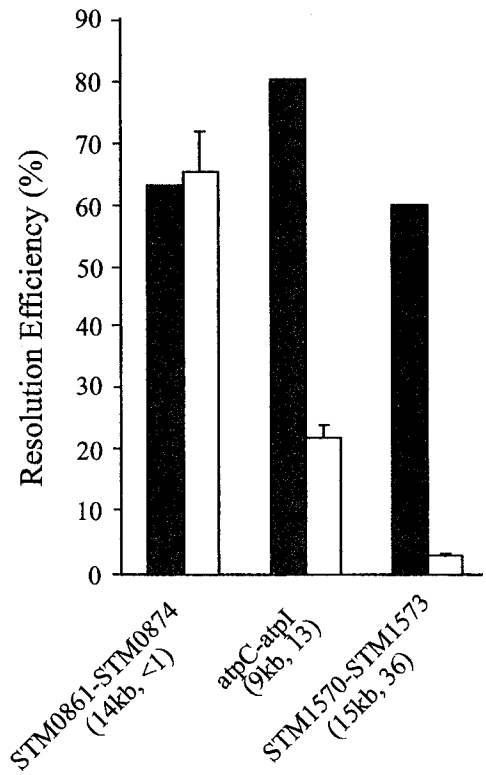

Fig. 3. Effect of transcription from bacterial chromosomal promoters of different strength on resolution efficiency. The three intervals tested were *STM0861-STM0874*, *atpC-atpI* and *STM1570-STM1573*. The gray column indicates the expected resolution efficiency for a nontranscribing region of the same size. The white column shows the observed resolution data for the same interval. The length of each interval is shown in paratheses followed, by the strength of transcription as the RNA/DNA ratio for that interval.

strain NH3501 was 22%, which was 3.6-fold lower than what we expected for the 9-kb interval (Fig. 3, group 2).

The third interval is from *STM1570* to *STM1573*. This interval was also flanked by *gen-res* and *kan-res*. There are 12 genes in this interval, and length of the interval is 15kb. The *nmpC* gene in this interval gave the highest RNA/DNA ratio, which was 36. The expected resolution efficiency for 15 kb is 60% (21). However, this interval only gave a 3% deletion frequency. *nmpC* had a 20-fold lower resolution efficiency compared to the control interval (Fig. 3, group 3).

These data clearly demonstrated the reciprocal relationship between transcription strength and effect on γδ resolution efficiency on the *Salmonella* chromosome. Transcription affects the dynamics of the bacterial chromosome. The higher the transcription is, the lower the resolution efficiency.

Effect of seqA *mutant on resolution efficiency*

seqA is known to affect transcription profile of many genes (27). We made a *seqA* knockout mutant that carried pJBRESc*I* (NH3512). The *res-res* interval without *tetA* insertion [(*STM0925*)<>(*gen-res*) *zbj8905*::Mu*d*Jr2] or with *tetA* insertion [(*STM0925*)<>(*gen-res*) *zbj8905*::Mu*d*Jr2 (*kan*)<>(P_A*tetA-rrnB*)] was moved into the *seqA* deletion background by a transduction cross. γδ resolution assay was performed in both log phase and stationary phase. Interestingly, in log phase, *seqA* deletion did not affect resolution efficiency at all in either the strain without *tetA* or the strain with *tetA* inserted next to the *res* site (Fig. 4*A*). In the stationary phase, the strain without *tetA* insertion also behaved similarly in both the *seqA*$^+$ and *seqA*$^-$ backgrounds and gave 83% reso-

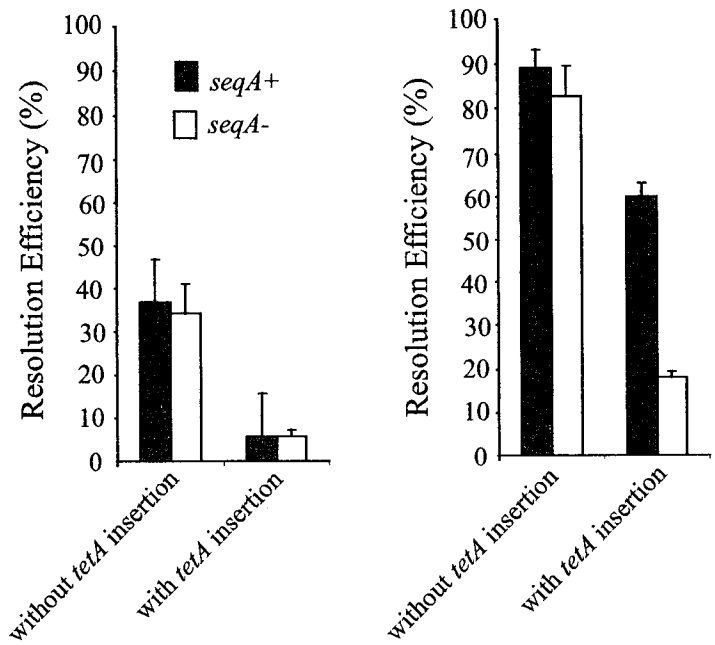

Fig. 4. Effect of *seqA* on resolution efficiency at different growth phases. Column 1 (gray) in both panels A and B represent the construct that has no *tetA* insertion. Column 2 (White) in both panels A and B represents the construct that has *tetA* inserted within the *res-res* interval. (*A*) Log phase. (*B*) Stationary phase.

lution efficiency (Fig. 4*B*). However, the strain with *tetA* inserted next to the *res* site gave 60% resolution efficiency in *seqA* WT strain and 18% in *seqA* deletion strain (Fig. 4*B*). So *seqA* only affected the stationary-phase resolution of the strain that carried a *tetA* module. The *seqA* mutant did not affect the resolution of the strain without a transcription-induced barrier in either the stationary phase or log phase.

A Model of transcription-induced barrier in S. typhimurium

On the basis of the data above, we proposed a model for how transcription generates barriers to supercoil diffusion in the bacterial chromosome (Fig. 5). When the transcription is off (like in the P_R*tetR*-P_A*lacZ* module) or when transcription of genes in the interval is very low, there is no barrier in the region. However, when the transcription is on (for example, when induced by chlortetracycline in the P_R*tetR*-P_A*lacZ* module) or when transcription of one or more genes in a region is very strong, the region is organized into a domain. We also propose that the domain includes sequences nearby and that prevents interaction between sites inside the domain with sites outside the domain. The domain organizes highly transcribed genes and sequences that are within a 1 kb range surrounding the highly transcribed gene. If inside the *res-res* interval, the domain structure blocks the supercoil diffusion between two *res* sites no matter where the domain structure is. When the domain structure is outside the *res-res* interval, the frequency with which the *res* site is organized into the domain is dependent on the distance between the highly transcribed gene and the *res* site. When the gene and *res* site are closer to each other, the *res* site is looped in more frequently and has a greater effect on the resolution efficiency. If the distance is beyond 1 kb, the *res* site cannot be organized into the domain.

Fig. 5. Model of transcription-driven domain. Shown is the schematic of a *res-res* interval that contains 10 ORFs (shaded square). One *res* site is attached to the kanamycin-resistant gene. The other one is next to the *lacZ* gene, which is fused to the *tetA* promoter under the control of the WT *tetR* repressor. (*A*) Transcription is off; there are no domains. (*B*) Transcription is turned on; high transcription causes topological change, which organizes the highly transcribed *lacZ* gene and its neighbor sequence into a domain structure. The domain constitutes a roadblock to the supercoiling diffusion or organizes the *res* site near the *lacZ* gene into the domain, preventing the *res* site inside the domain from interacting with the other *res* site outside the domain. In both cases, the resolution is inhibited.

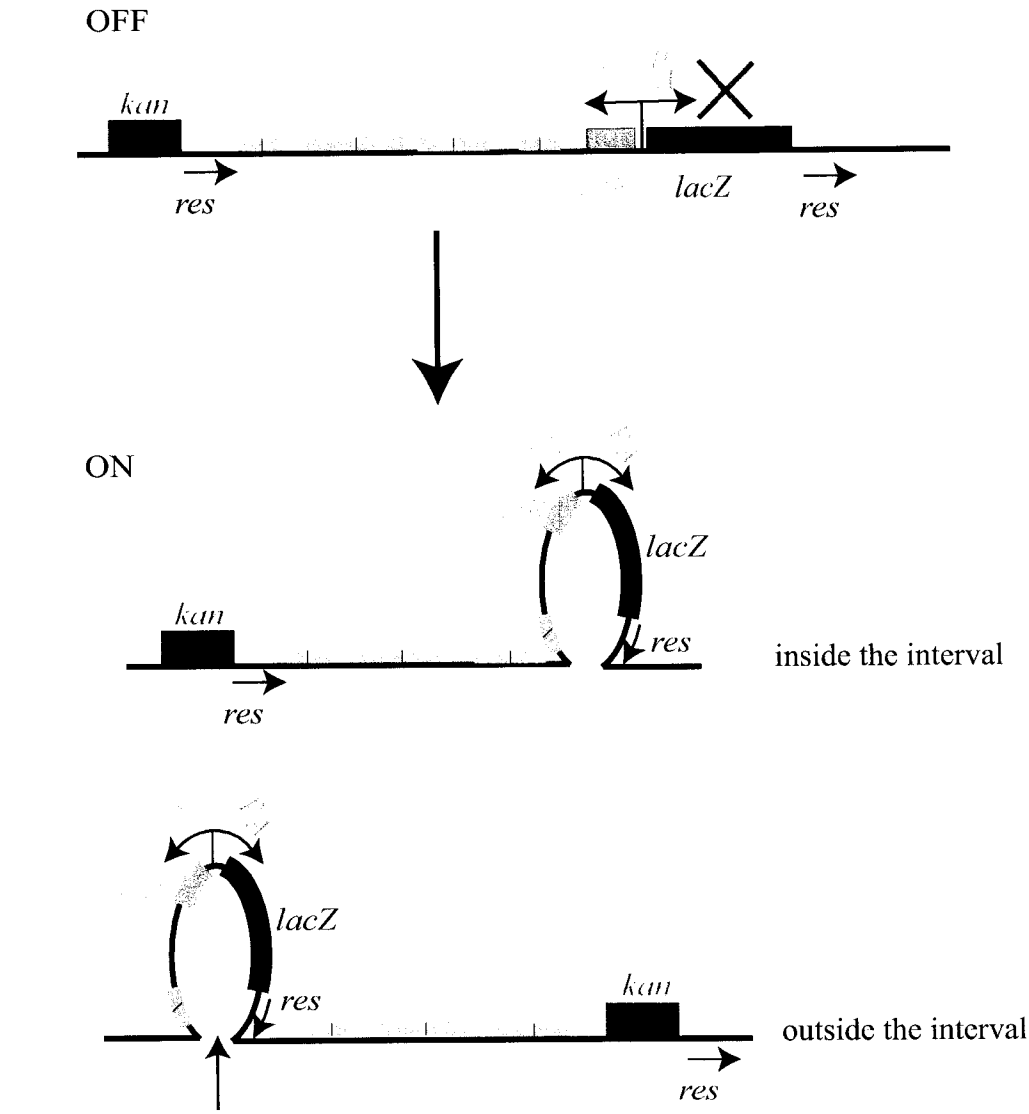

DISCUSSION

In this study, we used the γδ resolution system to study supercoil diffusion of chromosomal DNA. γδ resolution requires only supercoiled DNA, and its substrate is a plectonemically tangled pair of *res* sites with three superhelical nodes (24, 28, 29). These rigorous topological requirements for resolution reactions provide an opportunity to study supercoil movement *in vivo*. Barriers, which block supercoil diffusion, will make recombination difficult and decrease the γδ resolution efficiency between two *res* sites (21, 30). So the γδ resolution assay system can reveal impediments to supercoil diffusion of chromosomal DNA (22, 23). Those impediments are defined as barriers or domain boundaries (21). Previous work in our laboratory demonstrated that transcription from strong *tetA* promoter causes a new barrier to resolution on the *S. typhimurium* chromosome (23). We concluded that the magnitude of inhibition on the resolution depends on the level of transcription. In this work, we further confirm this conclusion that is applicable to genes of *S. typhimurium*. We chose three promoters of different transcription strengths that were determined by microarray transcription profile (personal communication). They gave the expected resolution efficiency that had been predicted from transcription data. Higher transcription gave lower resolution. So the transcription-induced barrier not only is restricted to the *tetA* promoter but is a feature of the strong promoter on the bacterial chromosome.

What defines the domain barrier? Studies in both bacteria and yeast show that high levels of transcription can form stretches of DNA::RNA hybrids (R-loops) that may be an obstacle for transcription elongation (31, 32). Could R-loop formation also lead to chromosomal domain barriers? The presence of an R-loop could explain the observations

made when the *tetA* gene was placed in the interval. High transcription from *tetA* could form R-loops that block the supercoil diffusion. This possibility explains the low resolution in the case of *tetA* located inside the *res-res* interval. However, when *tetA* is located outside the interval, the effect on resolution still can be seen to a distance of 1 kb. This effect is difficult to explain by using the R-loop model.

So we proposed that high transcription causes a domain that can organize the *res* site located within a 1 kb range of the transcribed gene. This domain inhibits resolution either by blocking supercoil diffusion or by looping in one nearby *res* site and precluding *res* site interaction.

What factors organize the loop is unknown. Some attractive candidates could be MukB and SeqA. MukB and SeqA are involved in maintaining chromosome topology and have opposing influences on the organization of the bacterial nucleoid. The *mukB* mutation causes unfolding of the nucleoid, whereas the *seqA* mutation leads to a more compact packaging of the chromosome (33-36). The *mukB seqA* double mutant regained the WT nucleoid organization.

SeqA is a DNA-binding protein that binds to multiple hemimethylated GATC sequences (37). Bound SeqA proteins are likely to maintain contact with each other by looping out the intervening DNA (34). Genes that are highly expressed in WT show decreased expression in *seqA* mutant cells, whereas genes with low expression in WT show increased expression in *seqA* cells (27). Interestingly, *seqA* deletion did not affect resolution in the log phase in strains with or without *tetA* insertion. In the stationary phase, *seqA* deletion did not change resolution in the strain without the *tetA* insertion but decreased resolution 3-fold in the strain with the *tetA* insertion. This result suggests that the effect of

the *seqA* mutation is only felt in stationary-phase cells for the interval that carries a highly transcribed *tetA* gene.

The structural maintenance of the chromosome (SMC) family of eukaryotic proteins that includes condensin has bacterial analogues (38). The *E. coli* MukB does not share sequence homology with the SMC family of proteins but shows remarkable similarity in domain organization at the protein level (39-41). Condensin promotes condensation by forming and stabilizing positively large supercoiled DNA loops (42). MukB may form a similar loop domain in regions that carry highly transcribed genes.

REFERENCES

1. Sinden, R. R. & Pettijohn, D. E. (1981) *Proc. Natl. Acad. Sci. USA* **78,** 224-228.
2. Pettijohn, D. E. (1996) in *Escherichia coli and Salmonella*, ed. Neidhardt, F. C. (Am. Soc. Microbiol., Washington, D.C.), Vol. 1, pp. 158-166.
3. Kavenoff, R. & Bowen, B. C. (1976) *Chromosoma* **59,** 89-101.
4. Kavenoff, R. & Ryder, O. A. (1976) *Chromosoma* **55,** 13-25.
5. Mizuuchi, K. & Nash, H. A. (1976) *Proc. Natl. Acad. Sci. USA* **73,** 3524-3528.
6. Mertens, G., Hoffmann, A., Blocker, H., Frank, R. & Kahmann, R. (1984) *EMBO J.* **3,** 2415-2421.
7. Marians, K. J. (1987) *J. Biol. Chem.* **262,** 10362-10368.
8. Benjamin, K. R., Abola, A. P., Kanaar, R. & Cozzarelli, N. R. (1996) *J. Mol. Biol.* **256,** 50-65.
9. Menzel, R. & Gellert, M. (1983) *Cell* **34,** 105-113.
10. Tse-Dinh, Y.-C. (1985) *Nucleic Acids Res.* **13**. 4751-4763.
11. Drlica, K. (1992) *Mol. Microbiol.* **6,** 425-433.
12. Pruss, G. J. & Drlica, K. (1989) *Cell* **56,** 521-523.
13. Pruss, G. J. & Drlica, K. (1986) *Proc. Natl. Acad. Sci. USA* **83,** 8952-8956.

14. Lockshon, D. & Morris, D. R. (1983) *Nucleic Acids Res.* **11,** 2999-3017.

15. Liu, L. F. & Wang, J. C. (1987) *Proc. Natl. Acad. Sci. USA* **84,** 7024-7027.

16. Lynch, A. S. & Wang, J. C. (1993) *J. Bacteriol.* **175,** 1645-1655.

17. Leng, F. & McMacken, R. (2002) *Proc. Natl. Acad. Sci. USA* **99,** 9139-44.

18. Figueroa, N. & Bossi, L. (1988) *Proc. Natl. Acad. Sci. USA* **85,** 9416-9420.

19. Chen, D. & Lilley, D. M. (1999) *J. Mol. Biol.* **285,** 443-448.

20. Durrenberger, M., Bjornsti, M.-A., Uetz, U., Hobot, J. A. & Kellenberger, E. (1988) *J. Bacteriol.* **170,** 4757-4768.

21. Higgins, N. P., Yang, X., Fu, Q. & Roth, J. R. (1996) *J. Bacteriol.* **178,** 2825-2835.

22. Scheirer, K. E. & Higgins, N. P. (2001) *Biochimie* **83,** 155-159.

23. Deng, S., Stein, R. A. & Higgins, N. P. (2004) *Proc. Natl. Acad. Sci. USA* **101,** 3398-3403.

24. Bliska, J. B., Benjamin, H. W. & Cozzarelli, N. R. (1991) *J. Biol. Chem.* **266,** 2041-2047.

25. Datsenko, K. A. & Wanner, B. L. (2000) *Proc. Natl. Acad. Sci. USA* **97,** 6640-6645.

26. Yu, D., Ellis, H. M., Lee, E. C., Jenkins, N. A., Copeland, N. G. & Court, D. L. (2000) *Proc. Natl. Acad. Sci. USA* **97,** 5978-5983.

27. Lobner-Olesen, A., Marinus, M. G. & Hansen, F. G. (2003) *Proc. Natl. Acad. Sci. USA* **100,** 4672-4677.

28. Benjamin, H. W. & Cozzarelli, N. R. (1988) *EMBO J.* **7,** 1897-1905.

29. Stark, W. M., Sherratt, D. J. & Boocock, M. R. (1989) *Cell* **58,** 779-790.

30. Manna, D. & Higgins, N. P. (1999) *Mol. Microbiol.* **32,** 595-606.

31. Drolet, M., Broccoli, S., Rallu, F., Hraiky, C., Fortin, C., Masse, E. & Baaklini, I. (2003) *Front Biosci.* **8,** D210-221.

32. Huertas, P. & Aguilera, A. (2003) *Mol. Cell* **12,** 711-721.

33. von Freiesleben, U., Krekling, M. A., Hansen, F. G. & Lobner-Olesen, A. (2000) *EMBO J.* **19,** 6240-6248.

34. Brendler, T., Sawitzke, J., Sergueev, K. & Austin, S. (2000) *EMBO J.* **19,** 6249-6258.

35. Weitao, T., Nordstrom, K. & Dasgupta, S. (1999) *Mol. Microbiol.* **34,** 157-168.

36. Weitao, T., Dasgupta, S. & Nordstrom, K. (2000) *Mol. Microbiol.* **38,** 392-400.

37. Brendler, T. & Austin, S. (1999) *EMBO J.* **18,** 2304-2310.

38. Hirano, T. (1999) *Genes Dev.* **13,** 11-19.

39. Hirano, M. & Hirano, T. (1998) *EMBO J.* **17,** 7139-7148.

40. Niki, H., Imamura, R., Kitaoka, M., Yamanaka, K., Ogura, T. & Hiraga, S. (1992) *EMBO J.* **11,** 5101-5109.

41. Melby, T. E., Ciampaglio, C. N., Briscoe, G. & Erickson, H. P. (1998) *J. Cell Biol.* **142,** 1595-1604.

42. Hagstrom, K. A. & Meyer, B. J. (2003) *Nat. Rev. Genet.* **4,** 520-534.

SUMMARY

Transcription and other processes involving the tracking of a macromolecular ensemble along dsDNA can have profound effects on the topological state of the template. If the transcription machinery cannot rotate freely about the DNA during elongation, the DNA will rotate. This rotation would lead to two distinct regions of localized DNA supercoils (53). Positive supercoils are generated as a consequence of the topological overwinding ahead of the advancing RNA polymerase, whereas negative supercoils result from an underwinding in the DNA behind it. Substantial evidence from *in vitro* and *in vivo* studies on plasmids supports this "twin-domain model" of transcription-induced supercoil (144-146). However, little is known about the impact of transcription on the topology of the large bacterial chromosome because of the lack of tools to investigate long-range chromosome behavior *in vivo*. The goal of this dissertation research was to gain further insight into the effect of transcription on chromosomal DNA topology. We employed an *in vivo* system (namely, site-specific recombination by Res) to study dynamic chromosomal structure (46). Res catalyzes recombination between two directly repeated *res* sites that are plectonemically interwound. A barrier to supercoil diffusion between two *res* sites blocks *res* recombination. γδ resolution assay is the only assay that can detect transient domain barriers in living cells. A regulated and highly transcribed gene cassette was derived from the transponson Tn*10*. Regulation of Tn*10*-derived tetracycline resistance involves a repressor, TetR, and a membrane-bound export pump, TetA. Because the *tetA* gene was previously demonstrated to cause topological change for the plasmid,

we tested the effect of the *tetA* gene upon chromosomal topology by using a γδ resolution assay.

In the first part of our work, transcription of the *tetA* gene was shown to modulate supercoil dynamics in the *S. typhimurium* genome. First, constitutive transcription of a *tetA* gene caused a persistent barrier to supercoil diffusion that reduced γδ site-specific recombination over a 14-kb interval by 20-fold. Second, transcription effects were not restricted to the expression of membrane proteins. Similar effects of transcription on γδ resolution efficiency were found by using two cytosolic proteins, aminoglycoside-3'-*O*-phosphotransferase, which is the product of the Tn*5* *kan* gene and β-galactosidase (β-gal), the product of *E. coli lacZ*. Diffusion barriers were detected by using a WT resolvase in combination with modules that either lacked a functional copy of the TetR repressor or contained WT TetR protein but in presence of the inducer chlortetracycline hydrochroride (CLT). Third, the effect on resolution efficiency was proportional to the transcription level. In the strain that has the *lacZ* fused to the *tetA* promoter next to a WT *tetR* repressor, the addition of CLT induces expression from the *tetA* promoter. With the increase in CLT concentration, the transcription level increased and the resolution efficiency decreased. The transcription level reached 600 Miller units in the presence of 5 μg/ml CLT, whereas resolution was inhibited by 5-fold. Fourth, by using a modified form of Res with a cellular half-life of 5 min., barriers to supercoil diffusion were deteceted to appear and disappear within 10-20 minutes after the point when CLT was either added or washed out of cell cultures, respectively.

Because transcription alters chromosome dynamics of both the plasmid and the bacterial chromosomal DNA, the question arises of how many transcription-related barri-

ers exist in a bacterial cell. Microarray analyses provide important information on genome-wide transcription profiles (147, 148). Cells growing under the same conditions employed in our experiments (exponential cultures in LB) give detectable RNA signals for over 4,000 *E. coli* genes (147). However, steady-state mRNA abundance exhibits a strikingly skewed distribution. On the basis of steady-state transcription copy number, we divided over 4,000 genes into three classes.

In the first class, which contained 70% of the genes (3,034 ORFs), mRNA abundance is less than one molecule per cell. Genes in this category include the uninduced RNA for *lacZ* (which yields about 15 Miller units of β-gal activity) and 69 of the 321 known essential genes. Genes in this low-transcription category probably have little impact on DNA dynamics.

The second class includes genes with a steady-state abundance of one to four copies of RNA, which results in 40-160 Miller units of β-gal activity. Genes in this class (about 1,000) include 86 essential genes and are also predicted to have a modest topological impact.

The third gene class includes the ones with mRNA abundance >4, which would inhibit resolution over a 14 kb interval by more than 2-fold. There are about 110 genes that are transcribed equal to or greater than this level. Those genes are located at 50 different sites around chromosome. Therefore, if we define a decrease of 2-fold in resolution as an indication of a barrier, we predict about 50 sites would show transcription-driven domains in the chromosome. Included in this category would be a *lacZ* gene induced with 1 mM IPTG, which causes a 40- to 60-fold derepression of transcription to about 600 Miller units. The abundance of *lacZ* mRNA in uninduced cultures yields an mRNA copy

number of 0.45 (147), so a culture with 600 Miller units would have a copy number of ≈15. This change in expression is nearly identical to the change in levels of β-gal expression that we observe in *S. typhimurium* going from a repressed P_R*tetR*-P_A*lacZ* to steady state expression in the presence of 5 μg/ml CLT (Fig. 4 in the first paper to this dissertation). Under these conditions, a 5-fold inhibition of resolution results. Very few chromosomal locations have this level of transcriptional activity. The number of chromosomal sites with supercoil diffusion barriers that would inhibit resolution by 5-fold would be <8. If the seven ribosomal operons are added, we predict that only ≈15 sites would show 5-fold effects on resolution. This number of barriers is small compared to our estimate of 400 barriers that are stochastic and associated with DNA replication (43).

Why is the membrane attachment not necessary for generating transcription-driven domains in the chromosome but required for this purpose in plsamids? There are two possible reasons. First, the chromosome is 4,000 kb long and the plasmid is only several kilobases long. Their topology might respond to transcription differently. Second, the *tetA* in the Tn*10* module is different from the *tetA* in pBR322 (149). The former *tetA* is much stronger than latter because the strain carrying Tn*10* can grow at a concentration of 12 μg/ml tetracycline medium, whereas the strain carrying a single copy of *tetA* from pBR322 can grow only in medium with 2 μg/ml tetracycline (unpublished results). Even on a plasmid, membrane attachment is not required to generate transcription-mediated hypernegative supercoil when transcription is driven from a strong promoter like P_{tac} (93).

In the second part of our work, we tested whether bacterial chromosomal genes of different transcription levels have different impacts on the resolution efficiency of the chromosomal interval in which they reside. Results validated our previous conclusion

that the magnitude of inhibition on the resolution depends on the level of transcription. Therefore, transcription affects the dynamics of the bacterial chromosome, and transcription strength is a critical determinant of DNA topology. Further characterization of transcription-induced barriers demonstrated that the position of highly transcribed genes is important for their effect on resolution efficiency. If within the *res-res* interval, the transcribed gene always inhibited the resolution efficiency. However, if the transcribed gene was outside of the *res-res* interval, inhibition was detected only when the end of the transcribing gene was within a range of 1 kb from the *res* site.

Our data clearly suggested that low resolution is caused by high transcription and the membrane attachment is not required. Kinetic analysis with a short-lived Res indicated that the barrier to resolution caused by transcription responds to but is not contemporaneous with transcription. Barriers fully appear 20 min. after turning on transcription and completely disappear 20 min. after turning off transcription. We suspect that the domain barriers might be some transient structures caused by high transcription.

How might high transcription induce a structure change leading to a domain barrier without membrane attachment? So far, there are two possible mechanisms.
First, high level of transcription can form stretches of DNA::RNA hybrids (R-loop) (150). In an R-loop, the RNA is hybridized with the corresponding DNA template, leaving the nontemplate strand unpaired. In this manner, ssDNA regions flanked by dsDNA ones are generated (Fig. 1). R-loop formation was hypothesized to be due to the unpairing of template DNA by RNA polymerase, leaving the template DNA single stranded for pairing with the nascent RNA. Alternatively, a transient decoupling of translation and transcrip

Fig. 1. A model of R-loop formation during transcription. – and + represent negative and positive supercoiling, respectively. (*A*) The tight coupling of translation and transcription inhibits R-loop formation. (*B*) A weak coupling of translation and transcription leads to free nascent RNA not bound by the ribosomes. High transcription also causes a higher negative supercoiling behind the moving RNA polymerase, which promotes DNA opening. Nascent RNA binds to this unpaired DNA strand and forms an R-loop, which might constitute a roadblock to transcription elongation.

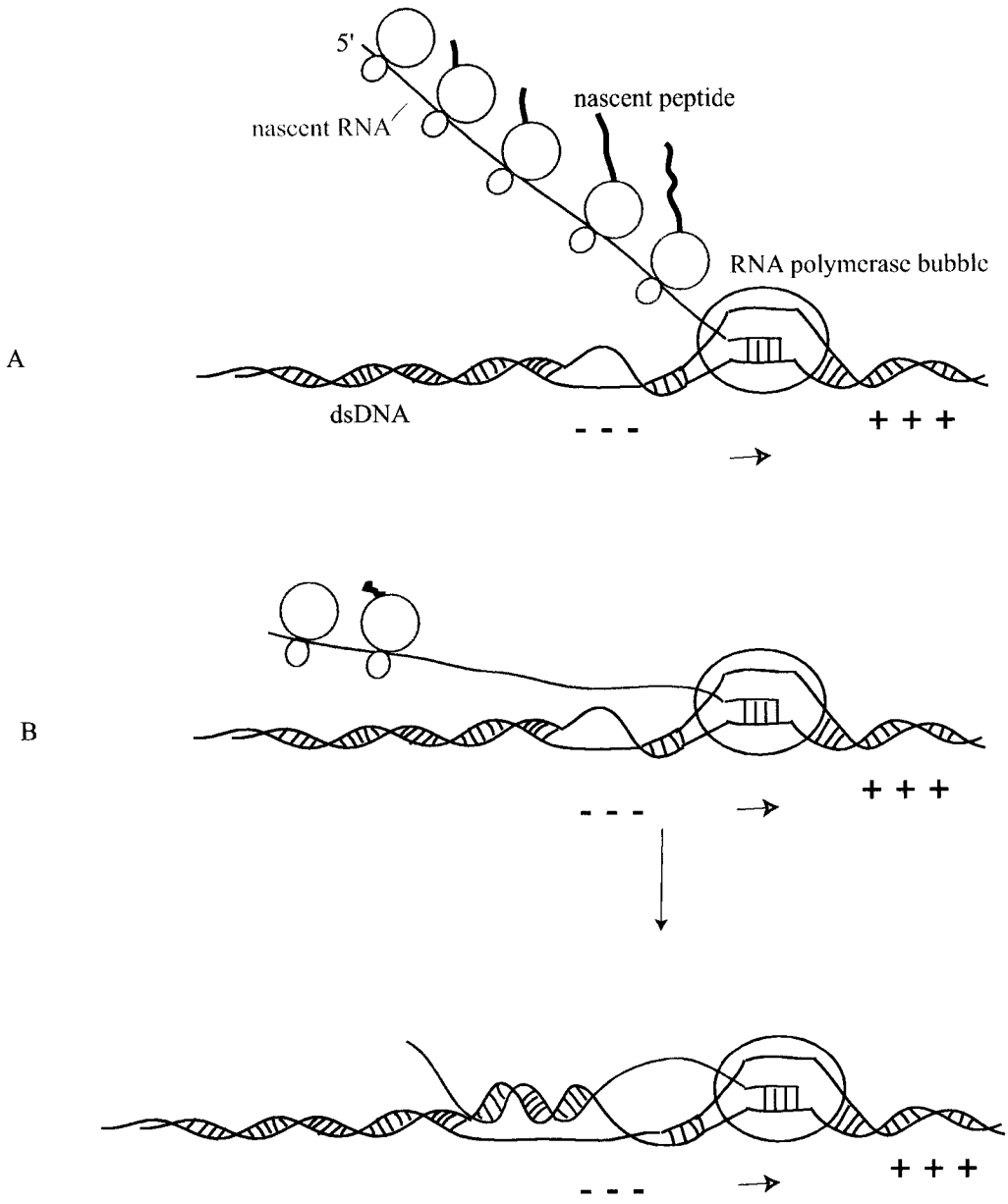

tion may lead to R-loop formation (151). Binding of ribosomes to the nascent RNA renders this RNA unavailable for reannealing with the complementary DNA template region and inhibits R-loop formation. High transcription may result in more transcription than translation and lead to decoupling of translation and transcription, probably causing an R-loop to form. R-loops can inhibit transcription elongation by constituting roadblocks (150). We suspect that R-loops can also block the supercoil diffusion in the same way. We can test this possibility by overproducing RNase H, an enzyme that degrades the RNA moiety of an R-loop (23). RNase H could remove the block produced by the R-loop and restore the high-resolution phenotype of this region. R-loop caused by the *tetA* transcription might block supercoil diffusion, thus explaining the finding obtained when the *tetA* gene was inside the interval. However, when *tetA* is located outside the interval, inhibition is still detected within 1 kb away from the end of the *tetA* gene. We cannot imagine how the R-loop formed before the end of *tetA* will affect the resolution of the interval that is 1 kb away from the *tetA* end because the R-loop cannot form downstream of transcribed genes. On the basis of these data, we suggest that R-loops are unlikely to be involved in the formation of domain barriers to supercoil diffusion.

The other possible model is that, during high transcription, condensing-like protein MukB (152) reorganizes highly transcribed genes into a domain structure, which prevents synapse formation across such a structure. MukB is a functional and structural bacterial analog of structural maintenance of the chromosome (SMC) proteins (153). SMC proteins are involved in chromosome condensation, sister chromatid cohesion, dosage compensation, DNA repair, and recombination (1, 154, 155).

SMC proteins have globular amino- and carboxyl-terminal domains separated by long coiled-coil regions with a central flexible hinge (156). The SMC protein forms a homodimer that hydrolyzes ATP and binds DNA *in vitro* (157, 158). Recently, Melby et al. (159) used higher resolution EM to provide an analysis of MukB. MukB showed two thin rods with globular domains at the ends emerging from the hinge. Both "folded-rod" and "open-V" conformations were seen frequently when EM was used. The open-V molecules demonstrate the potential of the terminal domains to separate and undergo a scissoring motion. The two long coiled coils are in an antiparallel arrangement. The hinge seems flexible; the coiled arms can open up to 180°, separating the terminal domains by 100 nm, or close to near 0°, bringing the terminal domains together. The antiparallel arrangement produces a symmetrical molecule with both an amino- and a carboxyl-terminal domain at each end. Each terminus of the molecule contains a complete and identical functional unit, which means that the two ends of the molecule can operate identically on two strands of DNA that are separated by 100 nm when for the molecule is fully open, or can interact with adjacent DNA sites when the molecule is folded (Fig. 2*A*).

In eukaryotes, condensin, which contains SMC proteins, is required for the substantial reorganization of chromosome structure because chromosomes compact during mitosis. Condesin is hypothesized to act as an intramolecular crosslinker by grabbing sites on an individual DNA strand and bringing them together (160). Condensin promotes condensation by stabilizing supercoiled DNA loops (Fig. 2*B*). On the basis of these properties of SMC proteins, we proposed a model for formation of transcription-driven domains in bacteria. In this model, high transcription leads to localized supercoil change, which facilitates MukB loading onto DNA. MukB then organizes the intervening DNA

Fig. 2. Structural maintenance of the chromosome (SMC) proteins in both eukaryotes and prokaryotes. (*A*) In eukaryotes, condesin, which belongs to SMC protein family, promotes condensation by grabbing sites on a single DNA strand and bringing them together. Condensin stabilizes supercoiled loops and reorganizes chromosomes into their highly compact structure during mitosis. (*B*) In *E. coli,* MukB is an analog of SMC. Shown is the model of the MukB protein structure, which is implied from electron micrographs. MukB homodimers are arranged into an antiparallel fashion. Each monomer has two globular domains connected by two long coiled coils that are separated by a hinge. The hinge is flexible, permitting a scissoring movement, with the coils separated at angles of 0° (folded-rod conformation) to 180° (open-V conformation).

A **Condensin**
Intra-molecular crosslinker

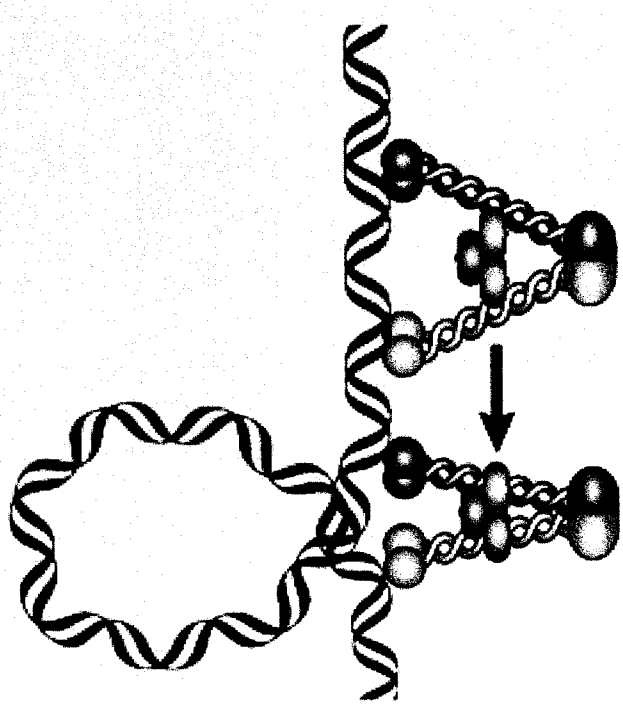

Hagstrom et al *Nature* 2003

B MukB

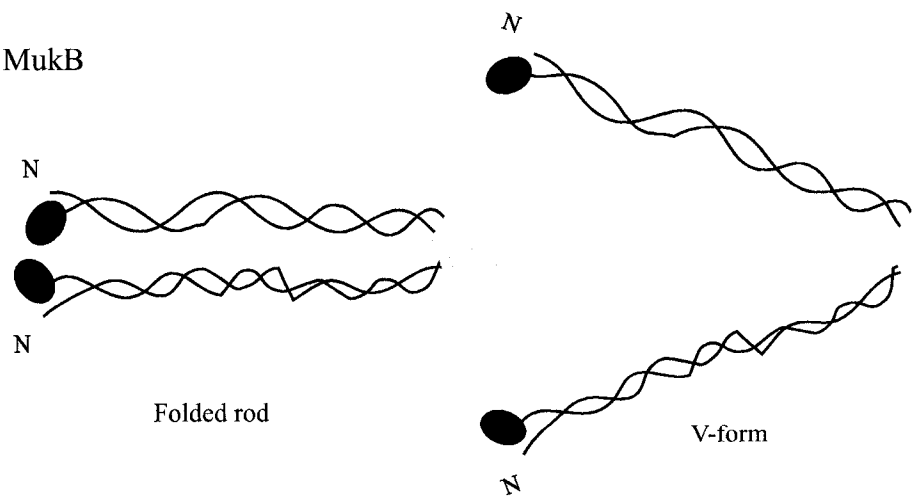

Melby et al JCB 1998

into a domain structure by a scissoring motion. The domain includes the highly transcribed sequence and neighboring DNA up to 1 kb (see Fig. 5 in the second paper of this dissertation). Such a domain structure could block supercoil diffusion across it or prevent a site from inside the domain from interacting with a site from outside the domain. This loop model explains all of our data. In the future, we need to do CHIP assay, which would reveal proteins that organize the transcribing regions into such a domain.

Chromosomal domains have significant implications for cell function because they ensure that topological changes in one domain do not affect another domains. Co-regulated expression of a group of genes in a single domain would require domain boundaries. For several decades, researchers have been seeking the barriers that define domain structure. For the first time, our work indicates that high transcription generates a supercoil domain in the bacterial chromosome. The hunt for the structural basis of this transcription-driven domain will be very interesting and challenging.

The lessons learned from bacterial chromosomes can apply to eukaryotic chromosomes. In eukaryotes, whether transcription can generate a domain remains unknown because there are no tools to investigate this possibility. However, recently, Rubin's laboratory (161) showed that there are transcriptional domains in the eukaryotic chromosome. Hundreds of microarray expression profiles for *Drosophila* were analyzed, and the profile for each gene was mapped to the position of genes along the *Drosophila* chromosome. Highly expressed genes were often grouped together. Groups of physically adjacent genes had strikingly similar expression profiles. There are about 200 such groups, which are called transcriptional domains. These authors (161) proposed that local chromatin structure might define chromosomal domains that in turn control the expression of large

groups of genes; perhaps the regulation of large groups reflects an "open" or "closed" chromatin state that is caused by expression of a few genes within the domain. Such transcriptional domains might be akin to the transcription-driven domains we found in the bacterial chromosome. Thus, understanding the mechanism of prokaryotic domains could be important for gaining an increased insight into the mechanism of eukaryotic domain formation and function.

LIST OF GENERAL REFERENCES

1. Holmes, V. F. & Cozzarelli, N. R. (2000) *Proc. Natl. Acad. Sci. USA* **97,** 1322-1324.

2. Pettijohn, D. E. (1996) in *Escherichia coli and Salmonella*, ed. Neidhardt, F. C. (Am. Soc. Microbiol., Washington, D.C.), Vol. 1, pp. 158-166.

3. Drlica, K. & Rouviere-Yaniv, J. (1987) *Microbiol. Rev.* **51,** 301-319.

4. Rahmouni, A. R. & Wells, R. D. (1989) *Science* **246,** 358-363.

5. Sinden, R. R., Carlson, J. O. & Pettijohn, D. E. (1980) *Cell* **21,** 773-783.

6. Higgins, N. P. (1999) in *Organization of the Prokaryotic Genome*, ed. Charlebois, R. L. (Am. Soc. Microbiol., Washington, D.C.), Vol. 1, pp. 189-202.

7. Funnell, B. E., Baker, T. A. & Kornberg, A. (1986) *J. Biol. Chem.* **261,** 5616-5624.

8. Pruss, G. J. & Drlica, K. (1989) *Cell* **56,** 521-523.

9. Drlica, K. (1992) *Mol. Microbiol.* **6,** 425-433.

10. Zechiedrich, E. L., Khodursky, A. B. & Cozzarelli, N. R. (1997) *Genes Dev.* **11,** 2580-2592.

11. Berger, J. M. (1998) *Curr. Opin. Struct. Biol.* **8,** 26-32.

12. Champoux, J. J. (2001) *Annu. Rev. Biochem.* **70,** 369-413.

13. Wang, J. C. (1996) *Annu. Rev. Biochem.* **65,** 635-692.

14. Dean, F., Krasnow, M. A., Otter, R., Matzuk, M. M., Spengler, S. J. & Cozzarelli, N. R. (1983) *Cold Spring Harb. Symp. Quant. Biol.* **47 Pt 2,** 769-777.

15. Gellert, M., Mizuuchi, K., O'Dea, M. H. & Nash, H. A. (1976) *Proc. Natl. Acad. Sci. USA* **73,** 3872-2876.

16. Kato, J., Nishimura, Y., Imamura, R., Niki, H., Hiraga, S. & Suzuki, H. (1990) *Cell* **63,** 393-404.

17. Harmon, F. G., DiGate, R. J. & Kowalczykowski, S. C. (1999) *Mol. Cell* 3, 611-620.

18. Levine, C., Hiasa, H. & Marians, K. J. (1998) *Biochim. Biophys. Acta* 1400, 29-43.

19. Drlica, K. & Zhao, X. (1997) *Microbiol. Mol. Biol. Rev.* **61,** 377-392.

20. Wang, J. C. (1971) *J. Mol. Biol.* **55,** 523-533.

21. Luttinger, A. (1995) *Mol. Microbiol.* **15,** 601-606.

22. Masse, E. & Drolet, M. (1999) *J. Biol. Chem.* **274,** 16654-16658.

23. Drolet, M., Phoenix, P., Menzel, R., Masse, E., Liu, L. F. & Crouch, R. J. (1995) *Proc. Natl. Acad. Sci. USA* **92,** 3526-3530.

24. Cheng, B., Rui, S., Ji, C., Gong, V. W., Van Dyk, T. K., Drolet, M. & Tse-Dinh, Y. C. (2003) *FEMS Microbiol. Lett.* **221,** 237-242.

25. DiGate, R. J. & Marians, K. J. (1988) *J. Biol. Chem.* **263,** 13366-13373.

26. Swanberg, S. L. & Wang, J. C. (1987) *J. Mol. Biol.* **197,** 729-736.

27. Yamagishi, J., Yoshida, H., Yamayoshi, M. & Nakamura, S. (1986) *Mol. Gen. Genet.* **204,** 367-373.

28. Adachi, T., Mizuuchi, M., Robinson, E. A., Appella, E., O'Dea, M. H., Gellert, M. & Mizuuchi, K. (1987) *Nucleic. Acids Res.* **15,** 771-784.

29. DiNardo, S., Voelkel, K. A., Sternglanz, R., Reynolds, A. E. & Wright, A. (1982) *Cell* **31,** 43-51.

30. Pruss, G. J., Manes, S. H. & Drlica, K. (1982) *Cell* **31,** 35-42.

31. McEachern, F. & Fisher, L. M. (1989) *FEBS Lett.* **253,** 67-70.

32. Oram, M. & Fisher, L. M. (1992) *J. Bacteriol.* **174,** 4175-4178.

33. Luttinger, A. L., Springer, A. L. & Schmid, M. B. (1991) *New Biol.* **3,** 687-697.

34. Hojgaard, A., Szerlong, H., Tabor, C. & Kuempel, P. (1999) *Mol. Microbiol.* **33,** 1027-1036.

35. Ullsperger, C. & Cozzarelli, N. R. (1996) *J. Biol. Chem.* **271,** 31549-31555.

36. Zechiedrich, E. L. & Cozzarelli, N. R. (1995) *Genes. Dev.* **9,** 2859-2869.

37. Levine, C. & Marians, K. J. (1998) *J. Bacteriol.* **180,** 1232-1240.

38. Stonington, O. G. & Pettijohn, D. E. (1971) *Proc. Natl. Acad. Sci. USA* **68,** 6-9.

39. Worcel, A. & Burgi, E. (1972) *J. Mol. Biol.* **71,** 127-147.

40. Kavenoff, R. & Bowen, B. C. (1976) *Chromosoma* **59,** 89-101.

41. Kavenoff, R. & Ryder, O. A. (1976) *Chromosoma* **55,** 13-25.

42. Delius, H. & Worcel, A. (1974) *Cold Spring Harb. Symp. Quant. Biol.* **38,** 53-58.

43. Postow, L., Hardy, C. D., Arsuaga, J. & Cozzarelli, N. R. (2004) in preparation.

44. Sinden, R. R. & Pettijohn, D. E. (1981) *Proc. Natl. Acad. Sci. USA* **78,** 224-228.

45. Pettijohn, D. E. & Hecht, R. (1973) *Cold Spring Harb. Symp. Quant. Biol.* **38,** 31-41.

46. Higgins, N. P., Yang, X., Fu, Q. & Roth, J. R. (1996) *J. Bacteriol.* **178,** 2825-2835.

47. Pettijohn, D. E. & Pfenninger, O. (1980) *Proc. Natl. Acad. Sci. USA* **77,** 1331-1335.

48. Snyder, M. & Drlica, K. (1979) *J. Mol. Biol.* **131,** 287-302.

49. Yang, Y. & Ames, G. F. (1988) *Proc. Natl. Acad. Sci. USA* **85,** 8850-8854.

50. Gilson, E., Perrin, D., Clement, J. M., Szmelcman, S., Dassa, E. & Hofnung, M. (1986) *FEBS Lett.* **206,** 323-328.

51. Condemine, G. & Smith, C. L. (1990) *Nucleic. Acids Res.* **18,** 7389-7396.

52. Gamper, H. B. & Hearst, J. E. (1982) *Cell* **29,** 81-90.

53. Liu, L. F. & Wang, J. C. (1987) *Proc. Natl. Acad. Sci. USA* **84,** 7024-7027.

54. Harada, Y., Ohara, O., Takatsuki, A., Itoh, H., Shimamoto, N. & Kinosita, K., Jr. (2001) *Nature* **409,** 113-115.

55. Lynch, A. S. & Wang, J. C. (1993) *J. Bacteriol.* **175,** 1645-1655.

56. Pruss, G. J., Franco, R. J., Chevalier, S. G., Manes, S. H. & Drlica, K. (1986) *J. Bacteriol.* **168,** 276-282.

57. Lin, D. C. & Grossman, A. D. (1998) Cell 92, 675-685.

58. Hiraga, S., Ichinose, C., Niki, H. & Yamazoe, M. (1998) *Mol. Cell* **1,** 381-387.

58. Kim, S. K. & Wang, J. C. (1998) *Proc. Natl. Acad. Sci. USA* **95,** 1523-1527.

59. Hiraga, S. (1992) *Annu. Rev. Biochem.* **61,** 283-306.

60. Lynch, A. S. & Wang, J. C. (1995) *Pro.c Natl. Acad. Sci. USA* **92,** 1896-1900.

61. Menzel, R. & Gellert, M. (1994) *Adv. Pharmacol.* **29A,** 39-69.

62. Wang, J. C., Barkley, M. D. & Bourgeois, S. (1974) *Nature* **251,** 247-249.

63. Malan, T. P., Kolb, A., Buc, H. & McClure, W. R. (1984) *J. Mol. Biol.* **180,** 881-909.

64. McClure, W. R. (1985) *Annu. Rev. Biochem.* **54,** 171-204.

65. Hsieh, T. & Wang, J. C. (1978) *Nucleic Acids Res.* **5,** 3337-3345.

66. Melnikova, A. F., Beabealashvilli, R. & Mirzabekov, A. D. (1978) *Eur. J. Biochem.* **84,** 301-309.

67. Siebenlist, U. (1979) *Nature* **279,** 651-652.

68. Sasse-Dwight, S. & Gralla, J. D. (1989) *J. Biol. Chem.* **264,** 8074-8081.

69. Borowiec, J. A. & Gralla, J. D. (1987) *J. Mol. Biol.* **195,** 89-97.

70. Davidson, N. (1972) *J. Mol. Biol.* **66,** 307-309.

71. Hsieh, T. S. & Wang, J. C. (1975) *Biochemistry* **14,** 527-535.

72. Menzel, R. & Gellert, M. (1987) *Proc. Natl. Acad. Sci. USA* **84,** 4185-4189.

73. Menzel, R. & Gellert, M. (1987) *J. Bacteriol.* **169,** 1272-1278.

74. Krohn, M., Pardon, B. & Wagner, R. (1992) *Mol. Microbiol.* **6,** 581-589.

75. Carty, M. & Menzel, R. (1989) *Proc. Natl. Acad. Sci. USA* **86,** 8882-8886.

76. Dubnau, E. & Margolin, P. (1972) *Mol. Gen. Genet.* **117,** 91-112.

77. Franco, R. J. & Drlica, K. (1989) *J. Bacteriol.* **171,** 6573-6579.

78. Margolin, P., Zumstein, L., Sternglanz, R. & Wang, J. C. (1985) *Proc. Natl. Acad. Sci. USA* **82,** 5437-5441.

79. Trucksis, M., Golub, E. I., Zabel, D. J. & Depew, R. E. (1981) *J. Bacteriol.* **147,** 679-681.

80. Menzel, R. & Gellert, M. (1983) *Cell* **34,** 105-113.

81. Tse-Dinh, Y.-C. (1985) *Nucleic. Acids. Res.* **13.**

82. Higgins, C. F., Dorman, C. J., Stirling, D. A., Waddell, L., Booth, I. R., May, G. & Bremer, E. (1988) *Cell* **52,** 569-84.

83. Dorman, C. J., Barr, G. C., Bhriain, N. N. & Higgins, C. F. (1988) *J. Bacteriol.* **170,** 2816-2826.

84. Karem, K. & Foster, J. W. (1993) *Mo4l. Microbiol.* **10,** 75-86.

85. Balke, V. L. & Gralla, J. D. (1987) *J. Bacteriol.* **169,** 4499-4506.

86. Gemmill, R. M., Jones, J. W., Haughn, G. W. & Calvo, J. M. (1983) *J. Mol. Biol.* **170,** 39-59.

87. Richardson, S. M., Higgins, C. F. & Lilley, D. M. (1988) *EMBO J.* **7,** 1863-1869.

88. Lockshon, D. & Morris, D. R. (1983) *Nucleic Acids Res.* **11,** 2999-3017.

89. Pruss, G. J. (1985) *J. Mol. Biol.* **185,** 51-63.

90. Wu, H. Y., Shyy, S. H., Wang, J. C. & Liu, L. F. (1988) *Cell* **53,** 433-440.

91. Pruss, G. J. & Drlica, K. (1986) *Proc. Natl. Acad. Sci. USA* **83,** 8952-8956.

92. Leng, F. & McMacken, R. (2002) *Proc. Natl. Acad. Sci. USA* **99,** 9139-9144.

93. Figueroa, N. & Bossi, L. (1988) *Proc. Natl. Acad. Sci. USA* **85,** 9416-9420.

94. Chen, D. & Lilley, D. M. (1999) *J. Mol. Biol.* **285,** 443-448.

95. Lilley, D. M. & Higgins, C. F. (1991) *Mol. Microbiol.* **5,** 779-783.

96. El Hanafi, D. & Bossi, L. (2000) *Mol. Microbiol.* **37,** 583-594.

97. Gellert, M. & Nash, H. (1987) *Nature* **325,** 401-404.

98. Bellomy, G. R. & Record, M. T., Jr. (1990) *Prog. Nucleic Acid Res. Mol. Biol.* **39,** 81-128.

99. Schleif, R. (1992) *Annu. Rev. Biochem.* **61,** 199-223.

100. Reed, R. R. (1981) *Cell* **25,** 713-719.

101. Heffron, F. (1983) in *Mobile Genetic Elements*, ed. Shapiro, J. A. (Academic Press, New York), pp. 223-260.

102. Shapiro, J. A. (1979) *Proc. Natl. Acad. Sci. USA* **76,** 1933-1937.

103. Wasserman, S. A. & Cozzarelli, N. R. (1986) *Science* **232,** 951-960.

104. Stark, W. M., Boocock, M. R. & Sherratt, D. J. (1989) *Trends. Genet.* **5,** 304-309.

105. Oram, M., Marko, J. F. & Halford, S. E. (1997) *J. Mol. Biol.* **270,** 396-412.

106. Grindley, N. D., Lauth, M. R., Wells, R. G., Wityk, R. J., Salvo, J. J. & Reed, R. R. (1982) *Cell* **30,** 19-27.

107. Kitts, P. A., Symington, L. S., Dyson, P. & Sherratt, D. J. (1983) *EMBO J.* **2,** 1055-1060.

108. Wells, R. G. & Grindley, N. D. (1984) *J. Mol. Biol.* **179,** 667-687.

109. Reed, R. R. & Grindley, N. D. (1981) *Cell* **25,** 721-728.

110. Boocock, M. R., Brown, J. L. & Sherratt, D. J. (1986) *Biochem. Soc. Trans.* **14,** 214-216.

111. Wasserman, S. A. & Cozzarelli, N. R. (1985) *Proc. Natl. Acad. Sci. USA* **82,** 1079-1083.

112. Parker, C. N. & Halford, S. E. (1991) *Cell* **66,** 781-791.

113. Staczek, P. & Higgins, N. P. (1998) *Mol. Microbiol.* **29,** 1435-1448.

114. Higgins, N. P., Deng, S., Pang, X., Stein, R., Champion, K. & Manna, D. (2004) in *The Bacterial Chromosome*, ed. Higgins, N. P. (Am. Soc. Microbiol. Washington, D.C.), pp. 133-153.

115. Benjamin, H. W. & Cozzarelli, N. R. (1988) *EMBO J.* **7,** 1897-1905.

116. Stark, W. M., Sherratt, D. J. & Boocock, M. R. (1989) *Cell* **58,** 779-790.

117. Bliska, J. B., Benjamin, H. W. & Cozzarelli, N. R. (1991) *J. Biol. Chem.* **266,** 2041-2047.

118. Saldanha, R., Flanagan, P. & Fennewald, M. (1987) *J. Mol. Biol.* **196,** 505-516.

119. Bliska, J. B. & Cozzarelli, N. R. (1987) *J. Mol. Biol.* **194,** 205-218.

120. Castilho, B. A., Olfson, P. & Casadaban, M. J. (1984) *J. Bacteriol.* **158,** 488-495.

121. Way, J. C., Davis, M. A., Morisato, D., Roberts, D. E. & Kleckner, N. (1984) *Gene.* **32,** 369-379.

122. Mizuuchi, K. (1992) *Annu. Rev. Biochem.* **61,** 1011-1151.

123. Craigie, R., Mizuuchi, M. & Mizuuchi, K. (1984) *Cell* **39,** 387-394.

124. Chaconas, G., Giddens, E. B., Miller, J. L. & Gloor, G. (1985) *Cell* **41,** 857-865.

125. Adzuma, K. & Mizuuchi, K. (1988) *Cell* **53,** 257-266.

126. Adzuma, K. & Mizuuchi, K. (1989) *Cell* **57,** 41-47.

127. Manna, D . & Higgins, N. P. (1999) *Mol. Microbiol.* **32,** 595-606.

128. Court, D. L., Sawitzke, J. A. & Thomason, L. C. (2002) *Annu. Rev. Genet.* **36,** 361-388.

129. Copeland, N. G., Jenkins, N. A. & Court, D. L. (2001) *Nat. Rev. Genet.* **2,** 769-779.

130. Ellis, H. M., Yu, D., DiTizio, T. & Court, D. L. (2001) *Proc. Natl. Acad. Sci. USA* **98,** 6742-6746.

131. Yu, D., Ellis, H. M., Lee, E. C., Jenkins, N. A., Copeland, N. G. & Court, D. L. (2000) *Proc. Natl. Acad. Sci. USA* **97,** 5978-5983.

132. Zhang, Y., Buchholz, F., Muyrers, J. P. & Stewart, A. F. (1998) *Nat. Genet.* **20,** 123-128.

133. Muyrers, J. P., Zhang, Y., Testa, G. & Stewart, A. F. (1999) *Nucleic Acids Res.* **27,** 1555-1557.

134. Muyrers, J. P., Zhang, Y., Buchholz, F. & Stewart, A. F. (2000) *Genes. Dev.* **14,** 1971-1982.

135. Datsenko, K. A. & Wanner, B. L. (2000) *Proc. Natl. Acad. Sci. USA* **97,** 6640-6645.

136. Karu, A. E., Sakaki, Y., Echols, H. & Linn, S. (1975) *J. Biol. Chem.* **250,** 7377-7387.

137. Murphy, K. C. (1991) *J. Bacteriol.* **173,** 5808-5821.

138. Karakousis, G., Ye, N., Li, Z., Chiu, S. K., Reddy, G. & Radding, C. M. (1998) *J. Mol. Biol.* **276,** 721-731.

139. Li, Z., Karakousis, G., Chiu, S. K., Reddy, G. & Radding, C. M. (1998) *J. Mol. Biol.* **276,** 733-744.

140. Muniyappa, K. & Radding, C. M. (1986) *J. Biol. Chem.* **261,** 7472-7478.

141. Hill, F., Benes, V., Thomasova, D., Stewart, A. F., Kafatos, F. C. & Ansorge, W. (2000) *Genomics* **64,** 111-113.

142. McClelland, M., Sanderson, K. E., Spieth, J., Clifton, S. W., Latreille, P., Courtney, L., Porwollik, S., Ali, J., Dante, M., Du, F., *et al.* (2001) *Nature* **413,** 852-856.

143. Yu, D., Sawitzke, J. A., Ellis, H. & Court, D. L. (2003) *Proc. Natl. Acad. Sci. USA* **100,** 7207-7212.

144. Wang, J. C. & Lynch, A. S. (1993) *Curr. Opin. Genet. Dev.* **3,** 764-768.

145. Droge, P. (1994) *Bioessays* **16,** 91-99.

146. Chen, C. C. & Wu, H. Y. (2003) *Front Biosci.* **8,** D430-4349.

147. Wei, Y., Lee, J. M., Richmond, C., Blattner, F. R., Rafalski, J. A. & LaRossa, R. A. (2001) *J. Bacteriol.* **183,** 545-556.

148. Bernstein, J. A., Khodursky, A. B., Lin, P. H., Lin-Chao, S. & Cohen, S. N. (2002) *Proc. Natl. Acad. Sci. USA* **99,** 9697-9702.

149. Hillen, W. & Berens, C. (1994) *Annu. Rev. Microbiol.* **48,** 345-369.

150. Drolet, M., Broccoli, S., Rallu, F., Hraiky, C., Fortin, C., Masse, E. & Baaklini, I. (2003) *Front Biosci.* **8,** D210-221.

151. Masse, E. & Drolet, M. (1999) *J. Mol. Biol.* **294,** 321-332.

152. Weitao, T., Dasgupta, S. & Nordstrom, K. (2000) *Mol. Microbiol.* **38,** 392-400.

153. Niki, H., Jaffe, A., Imamura, R., Ogura, T. & Hiraga, S. (1991) *EMBO J.* **10,** 183-193.

154. Cobbe, N. & Heck, M. M. (2000) *J. Struct. Biol.* **129,** 123-143.

155. Hirano, T. (2002) *Genes Dev.* **16,** 399-414.

156. Jessberger, R., Frei, C. & Gasser, S. M. (1998) *Curr. Opin. Genet. Dev.* **8,** 254-259.

157. Hirano, M. & Hirano, T. (1998) *EMBO J.* **17,** 7139-7148.

158. Hirano, M., Anderson, D. E., Erickson, H. P. & Hirano, T. (2001) *EMBO J.* **20,** 3238-3250.

159. Melby, T. E., Ciampaglio, C. N., Briscoe, G. & Erickson, H. P. (1998) *J. Cell Biol.* **142,** 1595-1604.

160. Hagstrom, K. A. & Meyer, B. J. (2003) *Nat. Rev. Genet.* **4,** 520-534.

161. Spellman, P. T. & Rubin, G. M. (2002) *J. Biol.* **1,** 5.

GRADUATE SCHOOL
UNIVERSITY OF ALABAMA AT BIRMINGHAM
DISSERTATION APPROVAL FORM
DOCTOR OF PHILOSOPHY

Name of Candidate Shuang Deng

Graduate Program Biochemistry and Molecular Genetics

Title of Dissertation Effects of Transcription on Chromosome Domain and Characterization of Transcription-Induced Domain Barriers to Supercoiling Diffusion in the *Salmonella Typhimurium* Chromosome

I certify that I have read this document and examined the student regarding its content. In my opinion, this dissertation conforms to acceptable standards of scholarly presentation and is adequate in scope and quality, and the attainments of this student are such that she may be recommended for the degree of Doctor of Philosophy.

Dissertation Committee:

Name	Signature
N. Patrick Higgins, **Chair**	
Thomas R. Broker	
Jamila Horabin	
Susan M. Lobo Ruppert	
Tim M. Townes	

Director of Graduate Program

Dean, UAB Graduate School

Date